ISSN 0021-9673

VOL. 505 NO. 2 MAY 4, 1990

THIS ISSUE COMPLETES VOL. 505

JOURNAL OF CHROMATOGRAPHY

INTERNATIONAL JOURNAL ON CHROMATOGRAPHY, ELECTROPHORESIS AND RELATED METHODS

ELSEVIER

JOURNAL OF CHROMATOGRAPHY

Scope. The *Journal of Chromatography* publishes papers on all aspects of chromatography, electrophoresis and related methods. Contributions consist mainly of research papers dealing with chromatographic theory, instrumental development and their applications. The section *Biomedical Applications*, which is under separate editorship, deals with the following aspects: developments in and applications of chromatographic and electrophoretic techniques related to clinical diagnosis or alterations during medical treatment; screening and profiling of body fluids or tissues with special reference to metabolic disorders; results from basic medical research with direct consequences in clinical practice; drug level monitoring and pharmacokinetic studies; clinical toxicology; analytical studies in occupational medicine.

Submission of Papers. Papers in English, French and German may be submitted, in three copies. Manuscripts should be submitted to: The Editor of *Journal of Chromatography*, P.O. Box 681, 1000 AR Amsterdam, The Netherlands, or to: The Editor of *Journal of Chromatography, Biomedical Applications*, P.O. Box 681, 1000 AR Amsterdam, The Netherlands. Review articles are invited or proposed by letter to the Editors. An outline of the proposed review should first be forwarded to the Editors for preliminary discussion prior to preparation. Submission of an article is understood to imply that the article is original and unpublished and is not being considered for publication elsewhere. For copyright regulations, see below.

Subscription Orders. Subscription orders should be sent to: Elsevier Science Publishers B.V., P.O. Box 211, 1000 AE Amsterdam, The Netherlands, Tel. 5803 911, Telex 18582 ESPA NL. The *Journal of Chromatography* and the *Biomedical Applications* section can be subscribed to separately.

Publication. The *Journal of Chromatography* (incl. *Biomedical Applications*) has 37 volumes in 1990. The subscription prices for 1990 are:

J. Chromatogr. (incl. *Cum. Indexes, Vols. 451–500*) + *Biomed. Appl.* (Vols. 498–534):
Dfl. 6734.00 plus Dfl. 1036.00 (p.p.h.) (total *ca.* US$ 3885.00)

J. Chromatogr. (incl. *Cum. Indexes, Vols. 451–500*) only (Vols. 498–524):
Dfl. 5616.00 plus Dfl. 756.00 (p.p.h.) (total *ca.* US$ 3186.00)

Biomed. Appl. only (Vols. 525–534):
Dfl. 2080.00 plus Dfl. 280.00 (p.p.h.) (total *ca.* US$ 1180.00).

Our p.p.h. (postage, package and handling) charge includes surface delivery of all issues, except to subscribers in Argentina, Australia, Brasil, Canada, China, Hong Kong, India, Israel, Malaysia, Mexico, New Zealand, Pakistan, Singapore, South Africa, South Korea, Taiwan, Thailand and the U.S.A. who receive all issues by air delivery (S.A.L. — Surface Air Lifted) at no extra cost. For Japan, air delivery requires 50% additional charge; for all other countries airmail and S.A.L. charges are available upon request. Back volumes of the *Journal of Chromatography* (Vols. 1–497) are available at Dfl. 195.00 (plus postage). Claims for missing issues will be honoured, free of charge, within three months after publication of the issue. Customers in the U.S.A. and Canada wishing information on this and other Elsevier journals, please contact Journal Information Center, Elsevier Science Publishing Co. Inc., 655 Avenue of the Americas, New York, NY 10010. Tel. (212) 633-3750.

Abstracts/Contents Lists published in Analytical Abstracts, ASCA, Biochemical Abstracts, Biological Abstracts, Chemical Abstracts, Chemical Titles, Chromatography Abstracts, Clinical Chemistry Lookout, Current Contents/Life Sciences, Current Contents/Physical, Chemical & Earth Sciences, Deep-Sea Research/Part B: Oceanographic Literature Review, Excerpta Medica, Index Medicus, Mass Spectrometry Bulletin, PASCAL-CNRS, Pharmaceutical Abstracts, Referativnyi Zhurnal, Science Citation Index and Trends in Biotechnology.

See inside back cover for Publication Schedule, Information for Authors and information on Advertisements.

0021-9673/90/$03.50

CONTENTS

(*Abstracts/Contents Lists published in Analytical Abstracts, ASCA, Biochemical Abstracts, Biological Abstracts, Chemical Abstracts, Chemical Titles, Chromatography Abstracts, Current Contents/Life Sciences, Current Contents/Physical, Chemical & Earth Sciences, Deep-Sea Research/Part B: Oceanographic Literature Review, Excerpta Medica, Index Medicus, Mass Spectrometry Bulletin, PASCAL-CNRS, Referativnyi Zhurnal and Science Citation Index*)

(Continued overleaf)

In articles with more than one author, the name of the author to whom correspondence should be addressed is indicated in the article heading by a 6-pointed asterisk (*)

Also available in a paperback student edition

Contemporary Practice of Chromatography

by **C.F. Poole** *and* **S.A. Schuette,** *Dept. of Chemistry, Wayne State University, Detroit, MI, USA*

"A tremendous amount of work has gone into the writing of this book, and it may be considered to be one of the few volumes of its kind that could be used both as a text by senior students in the field and by analysts in many industries. All academic, research association and appropriate industrial laboratories should buy at least one copy (preferably more, as borrowers will probably wish to keep it on loan for some time)." (The Analyst)

Written for everyone who uses chromatography as an analytical tool, this book covers all areas of gas, liquid, and thin-layer chromatography; **no other book offers the same scope.** The authors have had considerable experience in teaching graduate-level courses and the material presented here has been tried and tested, having formed the basis for short courses taught to groups of industrial chemists. Emphasis is on the practice of chromatographic methods, including "how to" sections and numerous examples of calculation methods. Extensively illustrated, the book contains numerous tables of all useful constants, materials and formulas frequently used by chromatographers. Valuable features are the chapters on sample preparation for chromatographic analysis, on instrumental methods for sample identification, and the comprehensive literature review.

Contents: 1. Fundamental Relationships of Chromatography. 2. The Column in GC. 3. Instrumental Requirements for GC. 4. The Column in LC. 5. Instrumental Requirements for HPLC. 6. Preparative-Scale Chromatography. 7. Sample Preparation for Chromatographic Analysis. 8. Hyphenated Methods for Identification after Chromatographic Separation. 9. High Performance Thin-Layer Chromatography. Subject Index.

1984. 2nd repr. 1986 x + 708 pages

Hardcover edition:	*Paperback edition:*
US$92.00/Dfl.175.00	US$37.50/Dfl.110.00
ISBN 0-444-42410-5	ISBN 0-444-42506-3

ELSEVIER SCIENCE PUBLISHERS

P.O. Box 211, 1000 AE Amsterdam, The Netherlands
P.O. Box 882, Madison Square Station, New York, NY 10159, USA

Journal of Chromatography, 505 (1990) 307–318
Elsevier Science Publishers B.V., Amsterdam — Printed in The Netherlands

CHROM. 22 307

Comparison of octadecyl-bonded alumina and silica for reversed-phase high-performance liquid chromatography

JEROME E. HAKY*and SHOBHA VEMULAPALLI
Department of Chemistry, Florida Atlantic University, Boca Raton, FL 33431 (U.S.A.)
and
LARRY F. WIESERMAN
Surface Technology Division, Alcoa Laboratories, Alcoa Center, PA 15069 (U.S.A.)
(First received August 29th, 1989; revised manuscript received December 8th, 1989)

SUMMARY

Chromatographic properties of an octadecyl-bonded alumina (ODA) high-performance liquid chromatographic stationary phase are described and compared with those of commonly used octadecylsilica (ODS) stationary phases. Under reversed-phase conditions, selectivity of the ODA phase is shown to be similar to that of ODS, resulting in similar elution orders for most compound mixtures. The higher stability of the ODA material to alkaline solvents and the absence of acidic silanol sites on its surface allow a more efficient separation of organic bases with simpler mobile phases than is generally possible with ODS. Comparison of the correlation of the capacity factors of 31 organic compounds on the ODA and ODS stationary phases indicates a higher degree of hydrogen-bonding solute–stationary phase interactions on ODA than on ODS. Multiple-ring aromatic compounds are more strongly adsorbed on the ODA stationary phase than on ODS. Differences in the retention behavior of benzylamine on the ODA and ODS stationary phases with increasing percentages of methanol in the mobile phase are reported. These are interpreted in terms of the differences in solute–stationary phase interactions on the two phases resulting from the chemical properties of their silica and alumina backbones.

INTRODUCTION

The use of chemically modified silicas as stationary phases in high-performance liquid chromatography (HPLC) is well established. Advances in the understanding of the chemical and physical properties of silica have led to the development of silica-based bonded phases with a wide variety of selectivities and efficiencies. In particular, alkyl-bonded silica stationary phases have gained wide popularity for HPLC separations of low-molecular-weight organic molecules using aqueous mobile phases[1]. Recently, these types of stationary phases have been employed for separations of higher-molecular-weight compounds, such as peptides and proteins[2,3].

0021-9673/90/$03.50

Despite their wide utility, the chemical properties of silica often limit the conditions under which separations of compounds can be attempted. Silica and its derivatives are generally stable only between pH 2 and 8, and thus mobile phases used with silica-based stationary phases are limited to this pH range. This complicates the separations of some compounds (*e.g.* weak organic bases) which are ionized over this pH range. In addition to poor separations caused by equilibrium between ionized and unionized forms of basic solutes, residual acidic silanol groups which are present in varying degrees on the surface of alkyl-bonded silicas can interact with organic bases, often resulting in irreproducible retention and poor peak symmetry[4,5]. Limiting these effects in the analysis of basic compounds on silica-based stationary phases requires a very careful choice of column manufacturer, mobile phase pH, mobile phase additives and sample size[6].

To overcome the problems associated with silica-based stationary phases, there have been many efforts to develop alkyl-bonded HPLC stationary phases which are based on materials that are more chemically stable and contain less chromatographically active sites than silica. Most of these efforts have employed derivatives of either polystyrene–divinylbenzene copolymers or alumina, materials which can be fabricated into microspherical particles of usable diameters and porosities for HPLC applications. Benson and coworkers bonded octadecyl functionalities onto a polystyrene–divinylbenzene polymer matrix, producing a stationary phase (MP-1) with remarkable pH stability (pH 2–14) and superior mass-transfer properties to stationary phases consisting of polystyrene–divinylbenzene copolymers alone[7]. However, retention of compounds on these stationary phases is substantially greater than that obtained with octadecylsilane columns using solvents of similar strength, and high column backpressures can result with certain mobile phases (*e.g.* those containing tetrahydrofuran) due to irreversible swelling of the polymeric particles. Bien-Vogelsang *et al.*[8] coated porous alumina (Spherisorb) with a variety of polymeric films, including polybutadiene and polyoctadecylsilane. Only a few applications of these pH stable stationary phases have been reported[9,10]. However, polymer-coated stationary phases have generally been found to exhibit lower chromatographic efficiency than corresponding monomeric alkyl-bonded materials[11].

Recently, Wieserman and co-workers successfully produced a material in which monomeric octadecyl functionalities are covalently bonded to the surface of a highly porous, microspherical alumina developed specifically for chromatographic applications[12]. Preliminary studies of this "octadecylalumina" (ODA) material demonstrated that it retains the pH stability and permeability of its alumina precursor, while exhibiting chromatographic selectivity similar to standard octadecylsilica (ODS) stationary phases[13]. In this paper, we report some chromatographic properties of this unique alumina-based HPLC stationary phase, and compare them with the properties of the more common silica-based ODS material.

EXPERIMENTAL

Materials

All solvents used were glass distilled, obtained from E.M. Science (Cherry Hll, NJ, U.S.A.). Pharmaceutical compounds were obtained from Sigma (St. Louis, MO, U.S.A.). All other compounds were obtained from Aldrich (Milwaukee, WI, U.S.A.).

Apparatus

The HPLC system consisted of a Perkin-Elmer Series 410 solvent-delivery system, a Rheodyne Model 7125 injector (20-μl loop) and a Perkin-Elmer Model LC-135 diode-array UV–visible detector. Unless otherwise specified, the wavelength monitored was 220 nm. Chromatographic data were recorded and processed on a Perkin-Elmer Omega data system.

The ODA column used in these studies was obtained from Biotage (Cambridge, MA, U.S.A.). It was packed with an experimental (not yet available for purchase) Alcoa Unisphere™ monomeric octadecyl-bonded alumina stationary phase, as described by Wieserman and co-workers[12,13]. The Unisphere alumina particle consists of *ca.* 2000-Å thick platelets bonded together to form 8-μm spherical particles with open, readily accessible inner-platelet macroporosity and inter-platelet microporosity. The following physical measurements were obtained on the Unisphere material before bonding of the octadecyl groups:

Mean particle size	8 μm
Surface area	103 m^2/g
Pore volume	0.295 ml/g
Median pore size of microporosity	11 nm

The bonded phase consists of bound monomolecular octadecyl groups on the surface. The preparation conditions insure that only covalently bound octadecyl groups remain on the surface of the Unisphere particles. No capping reagents were used because of the high loading density of the octadecyl groups and excellent chromatographic performance before capping. The loading of the octadecyl groups were 7.35% (w/w) carbon and 3.4 μmol C_{18}/m^2. The dimensions of the ODA column were 250 mm × 4.6 mm I.D. When this column was used, the mobile phase flow-rate was set at 2 ml/min.

A column packed with unbonded Unisphere alumina was also obtained as a gift from Biotage. The material had the same particle size, surface area and pore volume described above. Column dimensions were 250 mm × 4.6 mm I.D., and the mobile phase flow-rate was set at 2 ml/min.

Two ODS columns were used in these studies: (I) Perkin-Elmer C_{18}, 150 mm × 4.6 mm I.D., 5 μm particle size; mobile phase flow-rate 1 ml/min, and (II) Alltech Econosil C_{18}, 250 × 4.6 mm I.D., 10 μm particle size; mobile phase flow-rate 2 ml/min.

Test mixture analyses

The mixture of substituted anilines used to produce the chromatograms shown in Fig. 1 contained 0.5–1.0 mg/ml of each compound in methanol. Analysis of this mixture on the ODA column (Fig. 1A) was performed using a mobile phase consisting of methanol–0.01 *M* aqueous 4-morpholinopropanesulphonate (MOPS) (50:50), adjusted to pH 7.4 by addition of concentrated sodium hydroxide solution. Analysis of the mixture on ODS column I (Fig. 1B) was performed using a mobile phase consisting of methanol–0.05 *M* aqueous ammonium phosphate buffer (70:30) adjusted to pH 7.4. Chromatographic peak asymmetry factors (Table I) were calculated using the method described by Kirkland *et al.*[14].

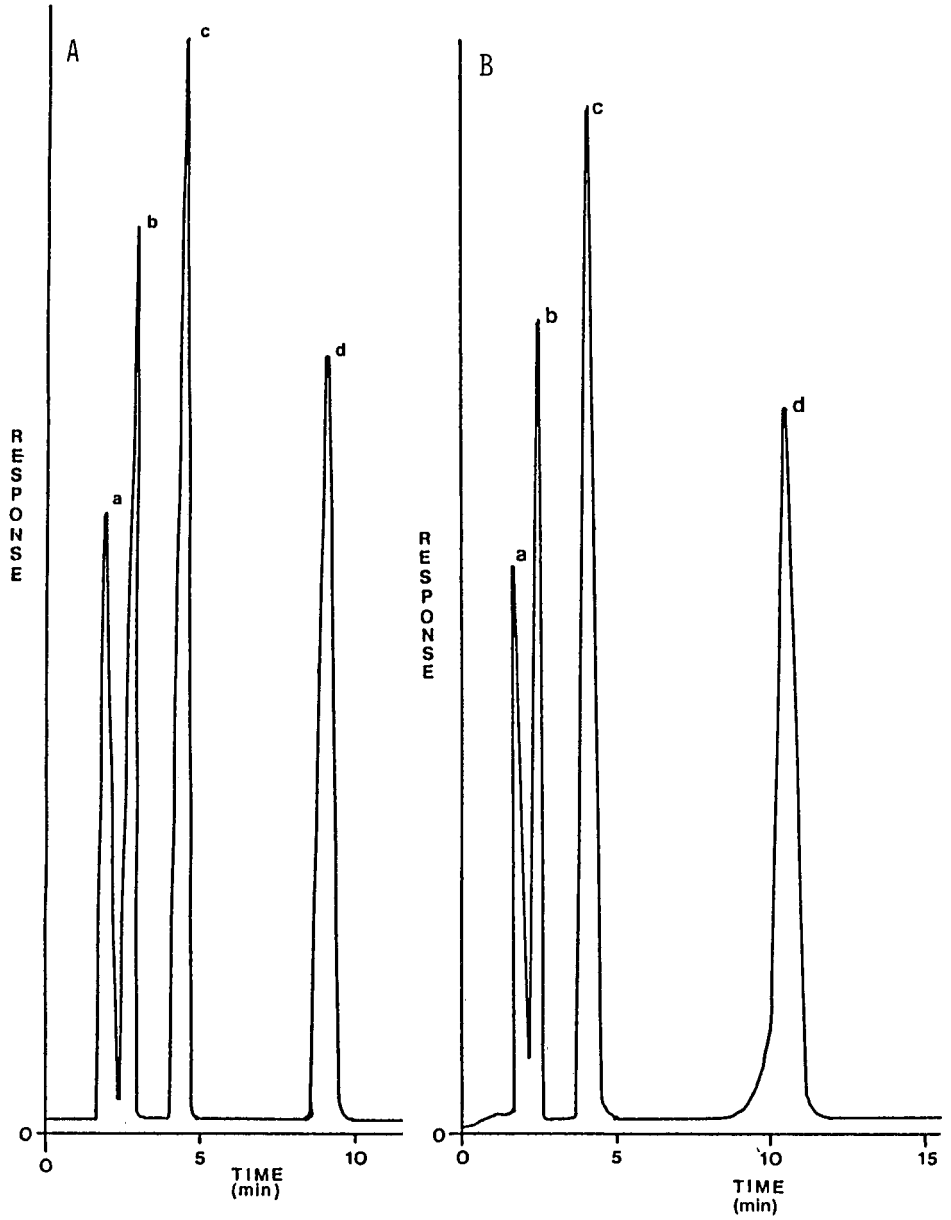

Fig. 1. HPLC chromatograms of aniline derivatives on ODA (A) and ODS (B) stationary phases, using mobile phases buffered at pH 7.4. Detector wavelength = 254 nm. Peaks: a = aniline; b = N-methylaniline; c = N,N-dimethylaniline; d = N,N-diethylaniline.

The mixture of pharmaceutical compounds used to produce the chromatogram shown in Fig. 2 contained 0.2–0.5 mg/ml of each compound in methanol. Analysis of the mixture was performed on the ODA column using a mobile phase consisting of methanol–0.1 *M* aqueous sodium hydroxide (35:65).

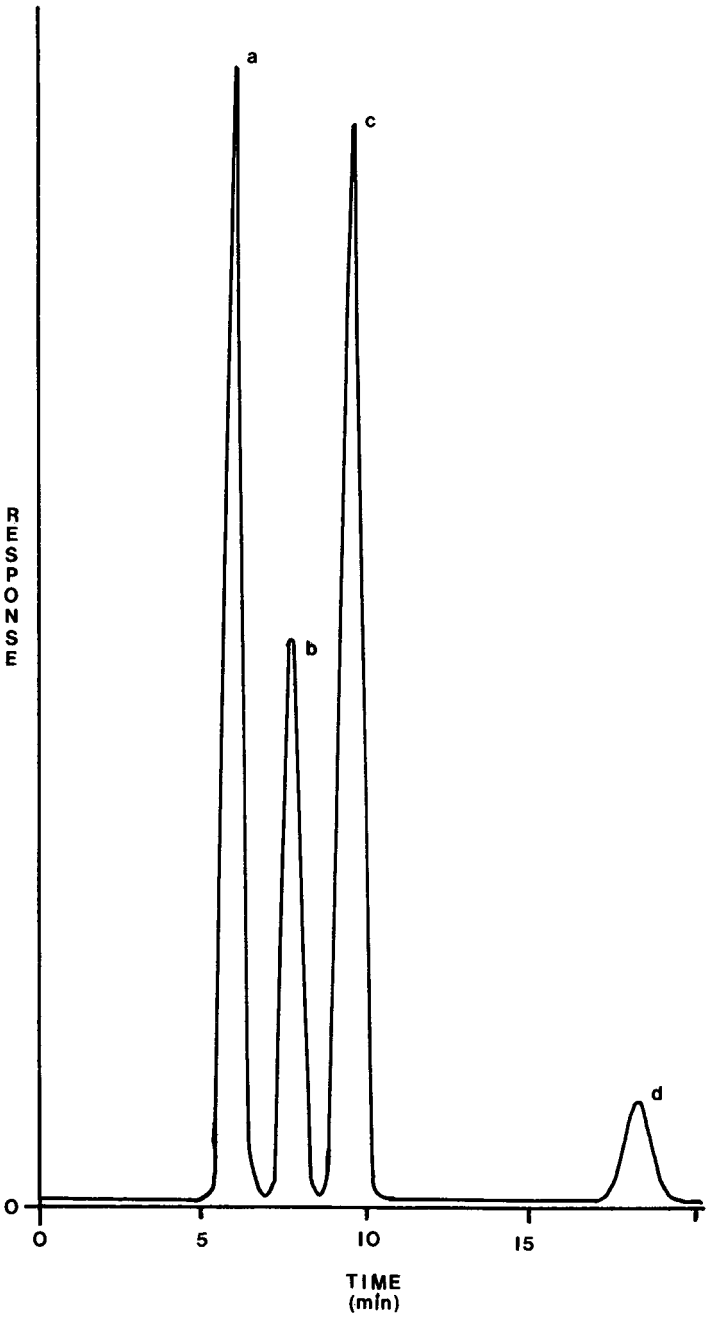

Fig. 2. HPLC chromatogram of a drug mixture on ODA stationary phase using an alkaline mobile phase consisting of methanol–0.10 *M* aqueous sodium hydroxide (35:65). Peaks: a = codeine; b = procaine; c = thebaine; d = cocaine.

TABLE I

CALCULATED ASYMMETRY FACTORS FOR PEAKS IN THE CHROMATOGRAMS OF SUBSTITUTED ANILINE MIXTURE (FIG. 1)

Peak	*Compound*	*Asymmetry Factor (ODS)*	*Asymmetry Factor (ODA)*
a	Aniline	1.00	1.00
b	N-Methylaniline	1.00	1.00
c	N,N-Dimethylaniline	1.25	1.06
d	N,N-Diethylaniline	0.57	0.98

Capacity factor determinations

Retention times for each of the compounds shown in Table II (injected as 1-mg/ml solutions in methanol) were determined on the ODA column using a mobile phase consisting of methanol–0.01 *M* aqueous MOPS (30:70) adjusted to pH 7.4, and on ODS column II using a mobile phase consisting of methanol–0.01 *M* aqueous MOPS (50:50), also adjusted to pH 7.4. The capacity factor, k', of each compound was calculated by the formula $k' = (t - t_0)/t_0$, where t is the compound's retention time and t_0 is the retention time of an unretained substance, determined by injection of a sample of pure methanol.

An attempt was made to evaluate the k' values of anthracene, phenanthrene and biphenyl on the unbonded Unisphere alumina column using the same conditions as that used with the ODA column. However, none of these compounds eluted from the column over a 2-h period.

TABLE II

CHROMATOGRAPHIC CAPACITY FACTORS ON ODS AND ODA COLUMNS

Compound	*Log k' (ODS)*	*Log k' (ODA)*	*Compound*	*Log k' (ODS)*	*Log k' (ODA)*
m-Aminophenol	−0.663	−0.275	Methyl benzoate	0.609	0.861
Benzamide	−0.274	0.044	Trichloroethylene	0.855	1.045
Resorcinol	−0.608	−0.021	Methyl salicylate	0.852	1.252
Aniline	−0.058	0.079	Chlorobenzene	1.071	1.249
Benzyl alcohol	0.088	0.230	Ethyl benzoate	1.007	1.200
Acetanilide	0.031	0.066	1-Naphthol	0.769	1.461
Picoline	0.154	0.016	Toluene	0.946	1.183
Phenol	−0.022	0.373	2-Naphthol	0.705	1.366
Ethyl propionate	0.338	0.230	Bromobenzene	1.142	1.386
Benzonitrile	0.185	0.376	Benzophenone	1.019	1.428
Acetophenone	0.285	0.447	Thymol	1.213	1.625
p-Cresol	0.363	0.729	Naphthalene	1.358	1.641
m-Cresol	0.351	0.692	Biphenyl	1.625	−[a]
Benzene	0.731	0.772	Phenanthrene	1.807	−[a]
Quinoline	0.433	0.655	Anthracene	1.807	−[a]

[a]Did not elute under the chromatographic conditions.

Capacity factor determinations of benzylamine with various percentages of methanol in the mobile phase

The retention times of benzylamine (injected as a 1-mg/ml solution in methanol) were determined on the ODA column and ODS column II using mobile phases ranging from 0–100% methanol and 100–0% aqueous MOPS, adjusted to pH 7.4. Capacity factors were calculated by the equation described above.

RESULTS AND DISCUSSION

General chromatographic properties

Since the monomeric ODA stationary phase is structurally similar to standard octadecylsilane material, the general hydrophobic partitioning mechanisms associated with retention of solutes on ODS stationary phases are also present in ODA. As a result, the selectivity of the alumina-based ODA stationary phase is similar to that of the silica-based ODS. This is demonstrated by the correspondence of elution order in the separation of some substituted anilines obtained on an ODA column (Fig. 1A) and on an ODS column (Fig. 1B).

Despite the relative similarity of the chromatograms of the aniline mixture obtained on the ODS and ODA columns, the following subtle differences in the chromatographic conditions and peak shapes gives an indication of the unique properties of the alumina-based material. Firstly, with this and other separations on the ODA column, it is necessary to avoid the commonly used phosphate buffers in the mobile phase; otherwise, reduced solute retention and unreproducible selectivity can result[15]. This phenomenon, which does not occur with polymer-coated alumina phases, is apparently caused by the displacement of surface octadecyl groups on ODA by phosphate ion, occuring in much the same way as halide ions displace surface hydroxyl groups on underivatized alumina[16]. This problem is easily avoided by substituting for phosphate a popular zwitterionic buffer, MOPS[17]. We have found that the MOPS buffer does not degrade the ODA phase to any measurable extent. Using a mobile phase consisting of this buffer and methanol, the symmetries of the peaks obtained in the chromatogram of the aniline mixture on the ODA column at pH 7.4 were equal or superior to those in the chromatogram of the same mixture on the ODS column, also obtained at pH 7.4 under optimized conditions (see calculated asymmetry factors in Table I).

Despite the incompatibility of the ODA stationary phase with mobile phases containing phosphate buffers at neutral pH values, the material is remarkably resistant to decomposition by hydroxide solutions or other alkaline solvents. This allows the employment of mobile phases at high pH values for suppressing the ionization and thus simplifying conditions for the separation of basic compounds that are ionized over the usable pH range of ODS (*i.e.* pH 2–8). An example of such an application is the separation of some pharmaceutical compounds on ODS using a methanolic mobile phase containing aqueous sodium hydroxide. The chromatogram obtained using this mobile phase (pH $>$ 10) is shown in Fig. 2, and exhibits good separations and peak symmetries. Since the pK_a values of the compounds are all within the range of 7–9 (ref. 18), suppression of ionization using a mobile phase with a pH compatible with an ODS phase is impossible. In fact, the only reported successful separation of these compounds on ODS required a more complicated mobile phase containing ion-pairing reagents[19].

Log k' correlations

Several recent studies have provided definitive evidence that retention of low molecular weight compounds on ODS occurs by a partitioning mechanism. This evidence includes the linear correlation of log k' of organic compounds on ODS with the logarithms of their octanol–water partition coefficients[20] as well as a similar correlations of log k' values with stationary phase carbon densities[21]. However, other studies have demonstrated a small but significant contribution of other types of solute-stationary phase interactions, including those related to hydrogen-bonding[22]. In order to obtain comparative information on the retention mechanisms operating with ODS and ODA stationary phases, the correlation of the k' values of 31 compounds on ODA with those obtained on an ODS column under similar conditions was investigated.

The compounds used for the log k' correlation study and their capacity factors are shown in Table II, and a graph of the data is displayed in Fig. 3. The correlation between log k' values on the two columns is generally good, indicating a general similarity in retention mechanisms for both ODS and ODA. Yet, there are a few differences. The non-elution of biphenyl, anthracene and phenanthrene on ODA under the chromatographic conditions (see Table II) can at least in part be attributed to an adsorption mechanism. These three compounds were also found not to elute from an unbonded Unisphere alumina column using the same mobile phase, which is consistent with the strong adsorption of polycyclic aromatic hydrocarbons (PAHs) on unbonded alumina reported in previous studies[16,23]. This strong adsorption has been attributed to the interaction of electron-rich solutes such as PAHs with electron-deficient aluminum atoms on alumina[16,23,24]. The analogous adsorption effects found with the ODA column suggest a similar accessibility of the PAHs to electron-deficient aluminum atoms in the bonded ODA phase. Surprisingly, the retention of naphthalene is apparently not affected by this adsorption mechanism; it does not have an abnormally high k' value, and it fits well on the overall log k' correlation line (see Table II and Fig. 3). Although the reason for this is not clear, it may be that a greater number of π electrons (as in anthracene) or a greater constitutional flexibility (as in biphenyl) is required before adsorption becomes a significant retention mechanism for solutes on the ODA stationary phase.

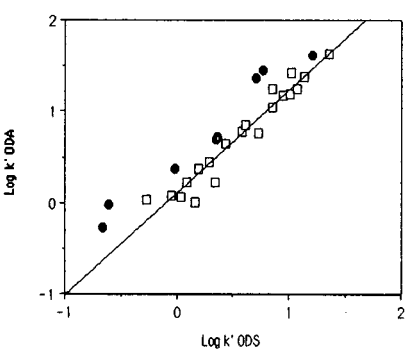

Fig. 3. Plot of the logarithm of the capacity factors (log k') of the compounds shown in Table II on the ODA stationary phase *vs.* the logarithm of their capacity factors on an ODS stationary phase. □ = Non-phenolic compounds; ● = phenolic compounds.

Comparison of log k' correlations obtained for phenolic and non-phenolic compounds on the ODS and ODA columns indicates that the effects of hydrogen bonding and acid–base interactions on retention of compounds on the two types of columns are somewhat different. As shown in Fig. 3, the phenolic compounds exhibit a small but significant deviation from the correlation obtained for other compounds. The data points for the phenols fall above the general ODA–ODS correlation line, indicating that these compounds are retained on ODA to a greater degree than on ODS. Greater relative retention of phenols on unbonded alumina than on silica has been observed previously, and has been atrributed to the greater Brønsted basicity (*i.e.* hydrogen-bond accepting ability) of the alumina's oxygen atoms *vs.* those of silica[16,23,25]. The occurrence a similar difference in the relative retention of phenolic solutes on the ODA vs ODS phases indicates that at least some of these basic oxygen atoms are accessbile to phenolic solutes during their separation on ODA. The data are consistent with an inherently greater basicity of the ODA phase than ODS, corresponding to the previously established greater basicity of unbonded alumina than silica[4,23].

Acid–base interactions and effects of methanol composition in mobile phase

The overt acidity of unbonded silanol groups present in ODS and other silica-based stationary phases can cause interactions between these groups and basic solutes. These interactions are much stronger than those associated with hydrogen bonding discussed earlier, and can interfere with the normal hydrophobic partitioning processes, resulting in loss of chromatographic separation and efficiency[4–6]. As shown in this and earlier studies, acidic sites on alumina have a much lower effect on chromatographic retention than corresponding sites on silica. As a result, interfering interactions with basic compounds are minimal, and separations and chromatographic peak shapes are improved for such compounds at neutral pH values. This is reflected in the greater symmetry (Table I) of the peaks corresponding to the most basic compounds (*i.e.*, N,N-dimethylaniline and N,N-diethylaniline) in the chromatogram of the substituted aniline mixture on the ODA column (Fig. 1A) than of those in the chromatogram of the same mixture on an ODS column (Fig. 1B) using a similare mobile phase.

Comparison of the retention behavior of another weak base, benzylamine, on the ODS and ODA columns also indicates differences in solute–stationary phase interactions occurring on the two materials. Fig. 4 shows a semilogarithmic graph of k' of benzylamine on each column *vs.* the percentage of methanol in the mobile phase. On the ODS column, k' first decreases with methanol composition, reaches a minimum at 50% methanol, and then increases as the percentage of methanol is increased beyond that. Similar relationships between the k' values of weak organic bases and the percentage of methanol in the mobile phase have been reported previously[26,27]. The passage of the k' values of such compounds through a minimum as the fraction of methanol is increased has been attributed to two different effects:

(1) A change in the partitioning mechanism from one dominated by hydrophobic solute expulsion from the aqueous component of the solvent to one dominated by polar solute interactions with the solvent's methanolic component[26,28];

(2) A change in mechanism from one dominated by hydrophobic expulsion to one dominated by interactions of the basic solutes with the acidic silanol sites on the

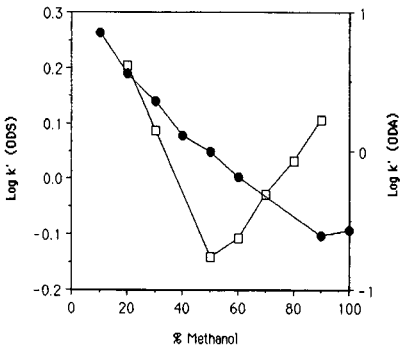

Fig. 4. Plot of the logarithm of the capacity factors of benzylamine on the ODS and ODA columns *vs.* the percentage of methanol in the mobile phase. □ = ODS column; ● = ODA column.

stationary phase[27]. As shown in Fig. 4, the retention behavior of benzylamine on the ODA stationary phase as the percentage of methanol in the solvent is increased is obviously different from that on ODS. Moreover, this difference gives an indication of the dominant mechanisms responsible for the phenomenona observed on both phases. In contrast to that observed on ODS, the k' value of benzylamine continues to decrease as the percentage of methanol in the mobile phase is increased beyond 50%, levelling off only when the compound becomes virtually unretained. The parabolic relationship between capacity factor and methanol composition on the ODS column is not observed on ODA, and therefore it cannot be caused exclusively by a change in the partitioning properties of the solvent alone (effect 1, above), since that would have caused a similar relationship on the ODA column. A change in the partitioning properties of the ODS, or an increase in the relative effect of an interfering retention mechanism on the stationary phase as the methanolic component of the solvent is increased must play a part in establishing the relationship between k' and percentage methanol on ODS. An increasing degree of acid-base interactions between basic solutes and residual silanol sites on the ODS column (or at least a relative increase in their effects on retention) as the amount of methanol in the mobile phase is increased (*i.e.*, effect 2, above) is the most plausible explanation. It accounts for the different retention behavior of benzylamine on the ODA stationary phase, which has no silanol sites and therefore is not subject to this mechanism. Additionally, benzylamine and other weak bases have been previously demonstrated to interact strongly with acidic silanol sites on ODS, especially when methanolic solvents are employed[29]. While this explanation has not been rigorously proven here, the data clearly indicates that the parabolic relationship between k' and methanol percentage for benzylamine and other weak bases found on ODS must at least in part be dependent upon the properties of the stationary phase, and not simply upon those of the mobile phase.

CONCLUSIONS

In this work, the general partitioning mechanisms associated with retention of solutes on a monomeric octadecyl-bonded alumina HPLC stationary phase have been shown to be similar to those of the widely used octadecylsilane phases. The

alumina-based material has a greater stability to alkaline solvents than ODS, and contains no acidic silanol sites which can interfere with hydrophobic partitioning on silica-based phases. All of these features allow the ODA stationary phase to give predictable and efficient separations of some types of compounds (*e.g.* weak bases) using simpler chromatographic conditions than those which are needed to obtain comparable separations on ODS. More research is needed on the chromatographic properties and optimal conditions for separating other compound classes on ODA (*e.g.* phenols and PAHs), which are more strongly retained on the alumina-based phase than on ODS.

Subtle differences in the retention of compounds on ODA and ODS can only be understood in terms of solute interactions with the alumina and silica backbones of these phases (*e.g.* hydrogen bonding). Since neither silica nor alumina are completely inert, it is not likely that such interactions can ever be completely eliminated by modifying chromatographic conditions. Consideration of the nature and extent of these interactions is thus necessary for accurately predicting the retention properties of solutes on either of these types of materials.

ACKNOWLEDGEMENTS

This work was supported in part by a grant from the Florida Atlantic University Division of Sponsored Research. We thank the Biotage Company (Cambridge, MA, U.S.A.) for their generous donation of several HPLC columns.

REFERENCES

1 L. R. Snyder, J. L. Glajch, and J. J. Kirkland, *Practical HPLC Method Development*, Wiley, New York, 1988, pp. 53–84.
2 F. E. Regnier, *LC · GC, Mag. Liq. Gas Chromatogr.*, 5 (1987) 230.
3 R. L. Garnick, N. J. Solli and P. A. Papa, *Anal. Chem.*, 60 (1988) 2546.
4 L. R. Snyder and J. J. Kirkland, *Introduction to Modern Liquid Chromatography*, Wiley, New York, 2nd ed., 1979, Ch. 5, 7 and 11.
5 S. H. Unger and G. H. Chiang, *J. Med. Chem.*, 24 (1981) 262.
6 M. A. Stadalius, J. S. Berus and L. R. Snyder, *LC · GC, Mag. Liq. Gas Chromatogr.*, 6 (1988) 494.
7 J. R. Benson and D. J. Woo, *J. Chromatogr. Sci.*, 22 (1984) 386.
8 U. Bien-Vogelsang, A. Deege, H. Figge, J. Kohler and G. Schomberg, *Chromatographia*, 19 (1984) 170.
9 R. Kaliszan, R. W. Blain and R. A. Hartwick, *Chromatographia*, 25 (1988) 5.
10 R. Kaliszan, J. Petrusewicz, R. W. Blain and R. A. Hartwick, *J. Chromatogr.*, 458 (1988) 395.
11 J. J Kirkland, J. L. Glajch and R. D. Farlee, *Anal. Chem.*, 61 (1989) 2.
12 L. F. Wieserman and E. S. Martin, presented at *39th Pittsburgh Conference on Analytical Chemistry and Applied Spectroscopy, New Orleans, LA, 1988*, paper 391.
13 L. F. Wieserman, R. R. Burr, K. Cross and F. J. Simpson, Jr., presented at *39th Pittsburgh Conference on Analytical Chemistry and Applied Spectroscopy, New Orleans, LA, 1988*, paper 393.
14 J. J. Kirkland, W. W. Yau, H. J. Stoklosa and C. H. Dilks, Jr., *J. Chromatogr. Sci.*, 15 (1977) 303.
15 L. F. Wieserman, unpublished results.
16 C. H. Giles, in E. Heftmann (Editor), *Chromatography*, Reinhold, New York, 1961, Ch. 4, pp. 33–55.
17 T. W. Brimble, *Kontakte (Merck)*, 1 (1981) 319.
18 D. D. Perrin, *Dissociation Constants of Organic Bases in Aqueous Solution*, Butterworths, London, 1965.
19 I. S. Lurie and S. M. Demchuk, *J. Liq. Chromatogr.*, 4 (1981) 357.
20 K. A. Dill, *J. Phys. Chem.*, 91 (1987) 1980.
21 K. B. Sentell and J. G. Dorsey, *Anal. Chem.* 61 (1989) 930.
22 J. E. Haky and A. M. Young, *J. Liq. Chromatogr.*, 7 (1984) 675.

23 L. R. Snyder, *Principles of Adsorption Chromatography*, Marcel Dekker, New York, 1968, Ch. 7, 10, 11.
24 G. S. Nolan, L. J. Saethre, M. R. Siggel, T. D. Thomas and L. Ungier, *J. Am. Chem. Soc.*, 107 (1985) 6563.
25 J. King, Jr. and S. W. Benson, *J. Chem. Phys.*, 44 (1966) 1007.
26 N. El. Tayar, H. Van De Waterbeemd and B. Testa, *J. Chromatogr.*, 320 (1985) 293.
27 K. E. Bij, Cs. Horváth, W. E. Melander and A. Nahum, *J. Chromatogr.* 203 (1981) 65.
28 E. D. Katz, C. H. Lochmuller and R. P. W. Scott, *Anal. Chem.*, 61 (1989) 349.
29 P. C. Sadek and P. W. Carr, *J. Chromatogr. Sci.*, 21 (1983) 314.

Journal of Chromatography, 505 (1990) 319–328
Elsevier Science Publishers B.V., Amsterdam — Printed in The Netherlands

CHROM. 22 297

Design of a photoionization detector for high-performance liquid chromatography using an automated liquid-to-vapor phase interface and application to phenobarbital in an animal feed and to amantadine

JOHN T. SCHMERMUND
Superpharm Corporation, 1769 Fifth Avenue, Bayshore, NY 11706 (U.S.A.)
and
DAVID C. LOCKE*
Chemistry Department, Queens College and The Graduate School, The City University of New York, Flushing, NY 11367 (U.S.A.)
(First received July 25th, 1989; revised manuscript received January 9th, 1990)

SUMMARY

An automated liquid-to-vapor phase interface system forms the basis for a new high-performance liquid chromatography (HPLC)–photoionization detection (PID) system. The system incorporates a six-valve interface enabling peak trapping, solvent switching and thermal desorption of the solute of interest into a vapor phase PID. For reversed-phase HPLC, the eluted solute peak is isolated on a Tenax trap after dilution of the effluent with water; the water is then evaporated, following which the trapped solute is flash-evaporated into the PID system. For normal-phase HPLC, the column effluent is diluted with hexane, the solute peak is concentrated on a short column packed with a propyl-amino/cyano bonded phase and the solvent is evaporated. The solute is then eluted with water onto the Tenax trap, and the above procedure for reversed-phase HPLC followed. All operations are controlled with a microcomputer. The advantages of the new detector system include completely automated operation, fast sample preparation, high sensitivity, and inherent selectivity. The system was applied to phenobarbital, which was extracted with acetonitrile from spiked laboratory animal feed, and to amantadine. The phenobarbital assay used a normal-phase separation with hexane–methyl *tert.*-butyl ether–methanol eluent. The manual sample preparation time was 5 min and the limit of detection was 2 ng phenobarbital injected; a conventional HPLC assay with UV detection required a longer sample preparation time and had a detection limit of 700 ng. Amantadine was assayed using a reversed-phase HPLC system with a water–methanol–triethylamine–orthophosphoric acid mobile phase. The detection limit was 25 ng injected.

0021-9673/90/$03.50

INTRODUCTION

In quest of the sensitive, universal detector for high-performance liquid chromatography (HPLC), we have earlier evaluated two modes of detector based on photoionization. The first[1] involved the continuous flash evaporation of the total HPLC effluent into a conventional vapor-phase photoionization detection (PID) system. The device was sensitive to about 10^{-11} g/s of solutes, with a linear dynamic range of 10^5, but suffered the limitation that it was effectively restricted to normal-phase systems. Driscoll *et al.*[2] improved upon these results somewhat by using a commercial PID system and effluent splitting. Our second design[3] attempted direct measurement of liquid-phase photoionization currents. This mode of operation was also restricted to normal-phase HPLC. Other designs of liquid-phase PID systems using high-power, pulsed-laser sources for two-photon ionization processes have also been described[4–10].

We describe here an improved version of the HPLC effluent-evaporation, vapor-phase PID system, which is amenable to both normal- and reversed-phase HPLC. The deleterious effects of the solvent vapors on PID are circumvented by trapping the peak of interest, evaporating off the solvent and then flash-evaporating the solute peak into a gas-phase PID system in a stream of argon. For quantitative solute trapping efficiency, effluent dilution is usually required. With reversed-phase HPLC, the effluent is diluted with water before the solute is trapped on Tenax. Tenax was selected because it has little affinity for water but adsorbs organic compounds and is commonly used to trap organics from water samples[11]. It is also one of the few adsorbents amenable to repetitive, rapid heating for fast solute desorption, without decomposing itself[12]. The water is then evaporated and the solute flashed into the PID system. With normal-phase HPLC, the effluent is first diluted with hexane, the peak trapped on a short column packed with propyl-amino/cyano (PAC) bonded phase and the solvent evaporated in a stream of nitrogen. The sample component is then displaced with water onto a Tenax trap and the operation completed as above. The entire system is microprocessor-controlled for completely automated operation.

Illustrative applications of the system are given to the determination of phenobarbital [5-ethyl-5-phenyl-2,4,6-(1H,3H,5H)-pyrimidine trione] and of amantadine (tricyclo-3.3.1.1.^{3,7}-decan-1-amine), the former spiked into a complex test matrix, laboratory animal feed. The system is more sensitive and more rapid than currently used procedures and allows avoidance of the extensive manual cleanup procedures used in most established HPLC methods for drug substances in animal feeds[13–18].

The system is another example of the application of valve-switching techniques to HPLC. Various applications of a different type of microprocessor-controlled valve-switching unit for automated sample cleanup and trace component enrichment were described by Little *et al.*[19]. Conley and Benjamin[20] devised an automatic column-switching technique using a pneumatically-operated six-port valve for on-line cleanup and analysis of drugs in topical cream formulations. An automated heteromodal column-switching HPLC system using silica and cyano-bonded columns and fluorescence detection was developed by Cox and Pullen[21] for the determination of E-prostaglandin panacyl ester derivatives.

The present system combines sample cleanup and sensitive PID in a unique interface. The limitations of the system include (a) the complexity and expense of the

apparatus, (b) the requirements that the solute be quantitatively trapped by the Tenax and subsequently quantitatively thermally desorbed from it and that the Tenax be stable over many thermal cycles, and (c) the practical ability to handle only a limited number of peaks. However, in many applications in pharmaceuticals, pesticide residues, food, quality control, clinical and process studies, etc., there is only one component of interest in an otherwise complex matrix.

SYSTEM DESIGN

To isolate a chromatographic peak of interest from reversed- and normal-phase HPLC columns and then to detect it with vapor-phase PID requires the ability to

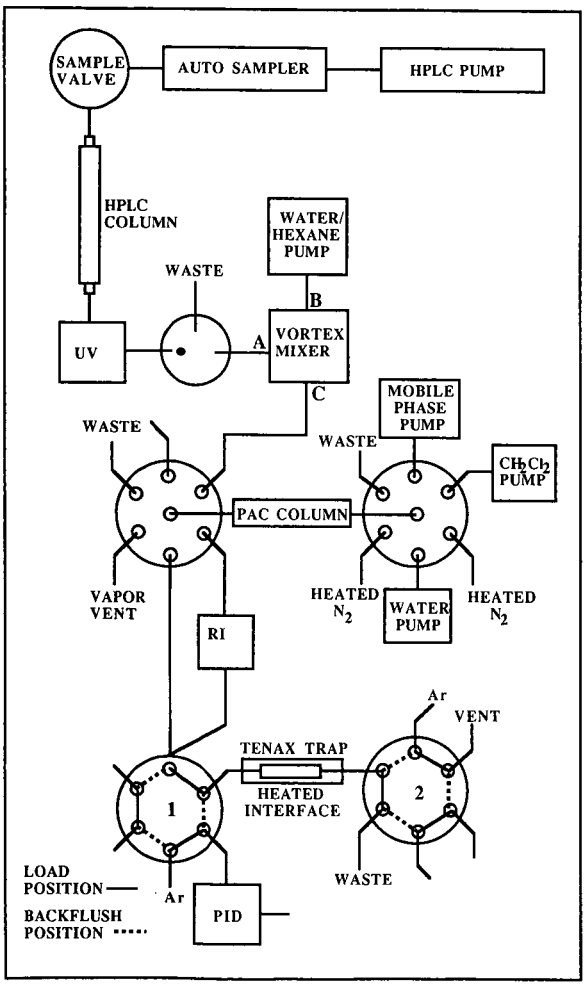

Fig. 1. Diagram of the liquid-to-vapor phase interface for HPLC–PID. Load position refers to trapping of solute peak onto the Tenax trap. Backflush position refers to displacement of solute from Tenax trap to PID system. See text for discussion of the arrangement.

switch columns, change HPLC modes, control liquid flows and thermally desorb the HPLC solvent and the solute in independent steps. We have achieved this capability with a novel interface using up to six valves. The sequencing requires a microprocessor controller, programmed to control the various devices in the system in a fixed timing sequence. A stable and reproducible chromatographic system is therefore required. The hardware is described first, then the controller system and finally applications to two representative systems are given.

HPLC and trapping system

A block diagram of the overall fluid and electrical control systems of the apparatus is shown in Fig. 1. The HPLC pump was a DuPont Model 870. Samples (10 μl) were injected into the HPLC column with a Micromeritics 725 autosampler in which the Micromeritics valve was replaced with a Rheodyne Model 7000 valve. The former valve tended to clog and was not reproducible. The HPLC column was thermostatted in a DuPont column oven. For normal-phase HPLC, a 25 cm × 4.6 mm I.D. column packed with 10-μm Whatman Co:Pell PAC was used at 25°C; for RP-HPLC, the column was a 25 cm × 4 mm I.D. DuPont Zorbax C_8 column at 25°C. The variable-wavelength UV detector used to optimize the chromatographic separation of the phenobarbital was a Kratos Model 773. To facilitate solute peak trapping, the HPLC column effluent was mixed with the diluent, a weak solvent (hexane in the case of normal-phase HPLC; water in reversed-phase HPLC), using an Altex vortex dynamic mixer. The mixer was modified to convert the original cylindrical mixing compartment into a conical shape which provided more efficient mixing. Although the mixer's dead volume was *ca.* 100 μl, peak broadening considerations are generally not as important here as in other HPLC applications, because the peak is trapped prior to detection. Diluent was pumped into port B using a Beckman Model 110A metering pump under the control of the microprocessor and was blended with column effluent entering port A to cause vortexing motion in the conical section of the mixer. The concentration of the stronger solvent in the eluent [methyl *tert.*-butyl ether (MTBE)–methanol in normal-phase HPLC; acetonitrile in reversed-phase HPLC] could be reduced up to 75% using this system.

The trapping or concentrator column which isolated the peak of interest from the effluent was a 3 cm × 4.6 mm I.D. column packed with 30–38-μm Whatman Co:Pell PAC. This trap was used only in the normal-phase HPLC mode. Depending on the chemical nature of the peak of interest, alternative adsorbents could be used. The concentrator column was connected as shown in Fig. 1 to the two tandem, pneumatically operated, actuator-controlled Rheodyne Model 5704 valves. Compressed air at 28–30 p.s.i. drove the valves on command from the microprocessor. This part of the sequence started with the hexane-diluted normal-phase HPLC effluent from the vortex mixer being pumped through the concentrator column to trap out the peak (flow was left-to-right through port 1). The valve was then advanced to allow hexane solvent to be evaporated by a back-flow of warm nitrogen to dry the packing material (flow was now right-to-left, to vent). In the third valve position, the trapped solute was backflushed from the dried PAC concentrator colum to the Tenax trap with water pumped from a second Beckman 110A metering pump. After quantitative transfer, the PAC column was regenerated by successive valve advances. First, heated nitrogen through port 3 drove most of the water from the concentrator col-

umn; dichloromethane was then pumped through port 4 using a third Beckman 110A pump to displace the remaining water. Finally the PAC concentrator column was equilibrated with 6–7 column volumes of the normal-phase eluent in preparation for the next fraction switched from the analytical HPLC column. The Hewlett-Packard refractive index (RI) detector indicated on Fig. 1 was used to determine the time required to purge solvent from the colum with nitrogen and also to optimize the HPLC separation of the UV-transparent amantadine solute.

The Tenax trap now contained the solute band eluted from the PAC concentrator column and was connected as shown in Fig. 1 for load and backflush positions. These valves were Carle Instruments Model 5621 valves housed in a Carle Model 4300 valve oven. The valves and transfer lines had to be maintained at a temperature at least as high as the desorption temperature to prevent condensation of solute vapors. The valves were held in the load position until most of the water was flushed from the valve to waste in the nitrogen stream and were then rotated under control of the microprocessor to the backflush position. The trap was 3 cm × 4.6 mm I.D., dry-packed with 80–100 mesh Tenax-GC (Alltech Assoc.) which had been conditioned in a vacuum oven at 250°C for 24 h to remove any volatiles. The Carle valve oven was mounted onto the front of a Perkin-Elmer Model 3290 gas chromatography (GC) system. The GC system served as a convenient device to connect the trap to the H Nu Model PI-52-02 PID system via a 3 cm × 4.6 mm I.D. glass-lined stainless-steel tube. The PID system was mounted atop the GC system adjacent to the valve oven. The PID discharge tube contained Kr, which produced an intense line of 10.2 eV energy. Signals from the H Nu PID electronics were recorded on a Hewlett-Packard 3390 integrator.

Thermal desorption unit

The Tenax trap was contained in the thermal desorption unit which was constructed of an aluminum block into which holes were drilled for a cartridge heater, a linear thermistor (linistor) and the Tenax trap. The unit was controlled by a contact closure from the microprocessor output board. The cartridge heater was powered with a precise temperature controller using a closed-loop proportional feedback system incorporating the linistor, based on an RCA circuit[22]. The temperature accuracy of this controller was of the order of ± 0.2°C and depended on the input sensitivity of the RCA CA 3059 hybrid integrated circuit, the specific linistor used and the level of temperature being controlled. A range of temperatures up to 300°C could be provided. The microprocessor turned the circuit on and rapidly ramped the temperature up to the preset value. The microprocessor quartz crystal clock monitored the duration of the preset and desorption temperatures before the cool-down process at the programmed time.

Microprocessor controller

The system was controlled using an expanded Systec SLIC-1400 microcomputer. The 8-bit central processing unit was based on a 6502 chip, which regulated all operations of the microcomputer based on the sequence of instructions programmed into memory from a keyboard. Timing by the unit's quartz crystal clock synchronized data transfer. The program was started to run by a contact closure on the Micromeritics autosampler. Both the analog and digital outputs of the SLIC-1400 were utilized.

The analog output provided a continuously variable voltage which was used to control the pumps in Fig. 1. For example, a controlled-voltage ramp allowed the HPLC column pump to reach a specified flow-rate over a designated time interval to avoid a rapid pressure surge that could damage the column. The digital output was cascaded to provide sixteen individual channels. Each channel contained a 10-A relay which provided a contact closure to switch a valve or to start a thermal cycle. Time intervals for the contact closures were programmed from the keyboard.

The system described is amenable to considerable simplification. A personal computer could substitute for the SLIC-1400. An oven simpler than a GC system would suffice to connect the Tenax trap to the PID system. The refractive index detector was a one-time requirement for a UV-transparent solute; similarly, a UV detector need not be dedicated to this system but is used only to optimize chromatographic conditions. If only reversed-phase HPLC is to be done, which is the usual case in pharmaceutical analyses, provision for solvent-switching is obviated, which eliminates the need for two of the Beckman pumps and one valve.

Materials

Phenobarbital was United States Pharmacopoeia (U.S.P.) reference material. Solutions were prepared every 12 h, because solutions of the compound are unstable. Amantadine was also U.S.P. reference grade. All solvents were Burdick & Jackson distilled-in-glass HPLC grade. Animal feed samples were Purina Laboratory Chow (Ralston-Purina, St. Louis, MO, U.S.A.). Spiking was carried out by adding 5.0 ml of a 1-mg/ml solution in acetonitrile–water (1:1) to 10.0 g of ground feed, which was then agitated mechanically in a flask and the solvent evaporated at ambient temperature in a Büchi Rotovap. The internal standard used was 4-hydroxy benzoic acid heptyl ester (heptyl paraben).

RESULTS AND DISCUSSION

Phenobarbital assay

HPLC. Phenobarbital can be determined using either reversed-phase HPLC or normal-phase HPLC. Reversed-phase HPLC was used to study the animal feed extraction solvent. However, the automated PID study was conducted using normal-phase HPLC, because (a) the polar materials coextracted with the phenobarbital were more easily separated using normal-phase HPLC and (b) normal-phase HPLC represented a more difficult challenge for the new PID system. The reversed-phase HPLC eluent composition was established by systematically varying the proportions of water, glacial acetic acid and acetonitrile. The best separation of the phenobarbital and the heptyl paraben internal standard with good peak symmetry was obtained with water–acetonitrile–acetic acid (69:30:1, v/v/v) at 2.0 ml/min. For normal-phase HPLC, a series of solvent optimization experiments led to the choice of a normal-phase eluent containing hexane–MTBE–methanol (79:18:3, v/v/v).

Extraction study. Animal feed samples (10.0 g) spiked with 5.0 mg of phenobarbital were extracted 3 times for 1 h with 100 ml of the solvents below. Extracts were decanted through silanized glass wool. The extract solutions were evaporated to dryness at 35°C using a Büchi Rotovap. To each were then added 5.0 ml of a 0.1-mg/ml solution of heptyl paraben internal standard in acetonitrile–water (1:1) and the resi-

due dissolved with mechanical shaking for 10 min. Solutions were placed into HPLC autosampler vials and analyzed using the reversed-phase HPLC system with a UV detector at 235 nm. Ratios of the areas of phenobarbital to heptyl paraben peaks were compared with a linear calibration plot covering the range of 0.10–10 μg phenobarbital and 0.01–1.0 μg heptyl paraben in the 10μl aliquot injected. The solutions were prepared using dilutions of a solution containing 1 mg phenobarbital plus 0.1 mg heptyl paraben per ml of acetonitrile–water (1:1, v/v). Of the extraction solvents tested, *i.e.* hexane, MTBE, dichloromethane, chloroform, ethyl acetate, acetonitrile, acetone and methanol, acetonitrile gave reasonable recovery [71.9% ± 1.5% relative standard deviation (R.S.D.) ($n=3$)] with minimal extraction of extraneous feed matrix components. Acetone and methanol gave higher recoveries (90%) but extracted lipophilic materials that interfered with the chromatographic determination of the phenobarbital. The other solvents gave poorer recoveries than acetonitrile. The purity of the phenobarbital peak was confirmed by collecting the peaks after repetitive injections, evaporating the solvent and using direct-inlet probe mass spectrometry. The mass spectrum of the combined collected peaks was identical to that of a sample of pure phenobarbital.

Normal-phase HPLC concentrator column. Seven different commercially available HPLC packing materials were tested for use as concentrator column packings. Each was dry-packed into short (3 cm × 4.6 mm I.D.) stainless-steel tubes. Each concentrator column was connected in turn to the effluent end of the vortex mixer, which was itself connected to the normal-phase HPLC column. A 10-μl sample of phenobarbital spiking standard was injected into the HPLC column and eluted with 2.0 ml/min of the normal-phase mobile phase. The polarity of the effluent was reduced by dilution with hexane to facilitate trapping of solute on the concentrator packing; in the vortex mixer, 1.0 ml/min of hexane was pumped into the HPLC effluent stream. The effluent from the concentrator column was monitored with the Kratos UV detector at 235 nm. The retention times of phenobarbital on the concentrator columns tested were: Baker diol, 2.3 min, DuPont Permaphase ETH, 3.5 min, Baker cyano, 5.3 min, Whatman Pre-Col silica gel, 5.7 min, DuPont Zorbax BP-cyano, 6.2 min, Whatman HC Pellosil silica gel, 7.0 min and Whatman Co:Pell PAC, >30 min. Thus, as noted above, the Whatman Co:Pell PAC material was selected because phenobarbital has a retention volume greater than 90 ml, more than adequate for our purposes.

Displacement of phenobarbital onto the Tenax trap. A 10-μg phenobarbital peak was isolated on the PAC concentrator column from the HPLC-resolved feed extract as described above. First, the column was dried for 10 min in a stream of warm nitrogen. To determine the volume of water required to elute the phenobarbital from the concentrator column, the UV detector was connected to the column and water was pumped in at 1.0 ml/min. Phenobarbital eluted as a narrow peak in 10 min.When the Tenax trap was inserted between the UV detector and the PAC concentrator column, phenobarbital did not elute from the latter after 20 min, *i.e.* it was quantitatively trapped on the Tenax column. In practice, water was pumped at 1.0 ml/min for 12.0 min to effect transfer from PAC to Tenax traps.

Thermal desorption from Tenax into the PID system. Samples of phenobarbital (0.5 μg) were transferred from the HPLC column to the Tenax trap installed in the Perkin-Elmer 3290 GC oven between the carrier gas inlet and the PID system accord-

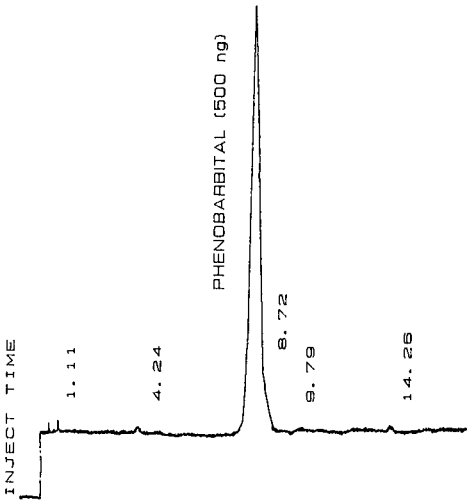

Fig. 2. Optimized desorption of phenobarbital from Tenax. Conditions: Perkin-Elmer 3290 GC oven, temperature raised from 50 to 150°C in 3 min; carrier gas, Ar, 55 ml/min; PID. Values given are retention times in min.

ing to the above operation and the water removed in a stream of warm nitrogen. The temperature was stabilized at 50°C and then programmed to 150°C over 3 min. The PID system detected a single peak corresponding to phenobarbital, as illustrated in Fig. 2.

Comparison with a conventional HPLC method. A published study of the determination of phenobarbital in animal feed[14] used a methanol extraction followed by sequential liquid–liquid extractions at pH 13 and pH 1, a silica gel column cleanup and reversed-phase HPLC (water–methanol, 60:40) with UV detection at 210 nm. We found this method required analyst preparation time of about 15 min/sample, and, on a routine basis, gave a lower limit of detection of 0.14 ppm and an assay precision of 1.4% (R.S.D., $n = 3$).

The automated HPLC–PID method described here required only about 5 min of analyst sample preparation time per sample. The detection limit based on the injected weight of phenobarbital required to produce a peak twice the noise level was 2 ng. This would correspond to a concentration in the feed of 0.06 ppm. However, we should note the lowest level of spiking for which the entire method was tested was 25 ppm; whether extraction recovery is satisfactory at much lower levels will have to be demonstrated. The present work was carried out to evaluate the new detection system and the feasibility of applying it to a complex matrix, rather than to validate a new specific analytical method. The overall precision of the automated HPLC–PID procedure was 2.4% (R.S.D., $n = 3$) at the spiking level of 500 μg/g of animal feed.

Amantadine assay

A brief study of the behavior of amantadine in this system was also conducted to illustrate the application of the automated HPLC–PID method in the reversed-phase mode. The conventional assay for amantadine used packed-column GC with a

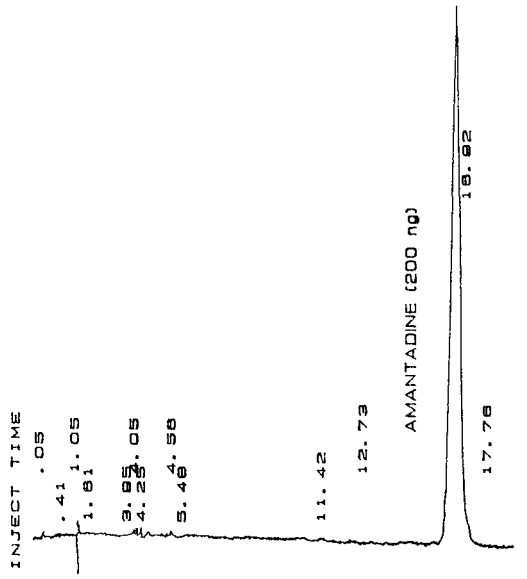

Fig. 3. Optimized desorption of amantadine from Tenax. Conditions: same as Fig. 2 except temperature varied from 50 to 180°C in 4 min and Ar flow at 40 ml/min.

flame ionization detector[23]. Kirschbaum[23] also described briefly an HPLC method requiring derivatization of the amantadine to phthalimido-adamantane followed by reversed-phase HPLC on a C_{18} column with methanol–water–85% orthophosphoric acid (60:40:0.1, v/v/v) and a UV detector operated at 254 nm. Amantadine itself is transparent in the UV.

Reversed-phase HPLC. The mobile phase of Kirschbaum[23] was modified by the addition of 1% (v/v) of triethyl amine. The triethylamine improved symmetry of the underivatized amantadine peak by acting as a competing base and seemed to ameliorate the other problems noted by Kirschbaum[23] in the HPLC of the free base. To set up the automated PID method, the refractive index detector was used.

Trapping on Tenax. With reversed-phase mobile phases, the column effluent need only be diluted with water prior to trapping on the Tenax, thus eliminating the need for a concentrator column and phase-switching. The effluent and water streams were combined in the vortex mixer before passing into the trap. It was found that a 100-μg sample of amantadine was retained in the Tenax trap more than 15 min when 2.0 ml/min of eluent diluted with 1.5 ml/min of water was passed through it.

Thermal desorption of amantadine-PID Amantadine is thermally stable and eluted from the Tenax in the heated interface at 180°C in argon at 40 ml/min into the PID system. A typical chromatogram is shown in Fig. 3.

Sensitivity and precision. The precision of the new assay procedure for amantadine determined by injection into the HPLC of 10-μl aliquots of a 20-μg/ml solution of amantadine in methanol was 1.5% (R.S.D., $n = 3$). Based on the quantity of amantadine required to give a signal twice the noise level, the limit of detection using the automated HPLC–PID method was 25 ng amantadine injected. The limit of

detection of an overall method including extraction from spiked animal feed has yet to be determined.

ACKNOWLEDGEMENTS

We appreciate the assistance of Suresh Tewani in the preparation of the figures. This work was supported in part by a grant from the PSC-CUNY FRAP program.

REFERENCES

1 J. T. Schmermund and D. C. Locke, *Anal. Let.*, 8 (1975) 611.
2 J. N. Driscoll, D. W. Conron, P. Ferioli, I. S. Krull and K.-H. Xie, *J. Chromatogr.*, 302 (1984) 43.
3 D. C. Locke, B. S. Dhingra and A. D. Baker, *Anal. Chem.*, 54 (1982) 447.
4 E. Voightman and J. D. Winefordner, *Anal. Chem.*, 54 (1982) 1834.
5 E. Voightman and J. D. Winefordner, *J. Liq. Chromatogr.*, 5 (1982) 2113.
6 S. Yamada, A. Hino and T. Ogawa, *Anal. Chim. Acta*, 156 (1984) 273.
7 S. Yamada, A. Hino, K. Kano and T. Ogawa, *Anal. Chem.*, 55 (1983) 1914.
8 S. Yamada, C. Sakane and T. Ogawa, *Talanta*, 34 (1987) 4671.
9 J. W. Jorgenson, *J. Chromatogr.*, 411 (1987) 201.
10 K. S. Epler, T. C. O'Haver, G. C. Tuck and W. A. MacCrehan, *Anal. Chem.*, 60 (1988) 2062.
11 V. Leoni, G. Puccetti, R. J. Colombo and A. M. D'Ovidio, *J. Chromatogr.*, 125 (1976) 399.
12 J. F. Pankow, M. P. Ligocki, M. E. Rosen, L. M. Isabelle and K. M. Hunt, *Anal. Chem.*, 60 (1988) 40.
13 M. C. Bowman and C. R. Nony, *J. Chromatogr. Sci.*, 15 (1977) 160.
14 M. C. Bowman and L. G. Rushing, *J. Chromatogr. Sci.*, 16 (1978) 23.
15 H. B. Hucker and S. C. Stauffer, *J. Chromatogr. Sci.*, 15 (1977) 357.
16 M. C. Allred and D. L. Dunmire, *J. Chromatogr. Sci.*, 16 (1978) 533.
17 R. R. Quadrel and F. M. Bogdansky, *J. Chromatogr. Sci.*, 18 (1980) 622.
18 H. S. I. Tan, N. W. Brake, H. J. Keily, K. J. Dalal and H. G. Higson, *J. Pharm. Sci.*, 68 (1979) 1413.
19 C. J. Little, D. J. Tomkins, O. Stahel, R. W. Frei and C. E. Werkhoven-Goewie, *J. Chromatogr.*, 264 (1983) 183.
20 D. L. Conley and E. J. Benjamin, *J. Chromatogr.*, 257 (1983) 337.
21 J. W. Cox and R. H. Pullen, *Anal. Chem.*, 56 (1984) 1866.
22 C. Johnson, *RCA Solid State Power Circuits Manual*, RCA Solid State Division, Somerville, NJ, 1971, pp. 339–408.
23 J. Kirschbaum, in K. Florey, (Editor), *Analytical Profiles of Drug Substances*, Vol. 12, Academic Press, New York, 1983, pp. 1–36.

Journal of Chromatography, 505 (1990) 329–347
Elsevier Science Publishers B.V., Amsterdam — Printed in The Netherlands

CHROM. 22 323

Two-component protein adsorption to the cation exchanger S Sepharose® FF

GRAHAM L. SKIDMORE and HOWARD A. CHASE*
Department of Chemical Engineering, University of Cambridge, Pembroke Street, Cambridge CB2 3RA (U.K.)
(First received September 7th, 1989; revised manuscript received February 2nd, 1990)

SUMMARY

A model system, consisting of bovine serum albumin, lysozyme and the cation exchanger S Sepharose® FF, was used to investigate multicomponent protein adsorption to ion exchangers. Two models, one based on a complete absence of competition between adsorbing molecules and the other a competitive model, based on the assumption that all adsorption sites are available to both proteins, have been compared to experimental results. Evidence for competitive adsorption was seen in experiments in which breakthrough curves and the profiles of adsorbed proteins in packed beds were determined. However, although the results for packed-bed experiments were more closely predicted by the fully competitive model, some discrepancies were found suggesting that when considering multicomponent protein adsorption to ion exchangers it may also be necessary to take account of factors such as the molecular size of the adsorbing proteins and any potential inter-protein interactions, factors which may hinder the development of a general model of multicomponent protein adsorption to ion exchangers.

INTRODUCTION

Capital expenditure on both process equipment and consumable materials can account for significant proportions of the costs of large scale production of pharmaceutical proteins. It is desirable therefore, to design and optimise the purification protocol to keep this expenditure to a minimum. The design of a purification process requires the use of a model which is able to predict the required parameters. Whilst there are many published studies of the adsorption of single proteins to different adsorbents, few studies have been reported using more realistic multicomponent systems which involved more than one adsorbing protein, a fact that has been pointed out by Janson and Hedman[1]. A theoretical discussion of an approach to modelling multicomponent protein adsorption has been published by Velayudhan and Horváth[2], although they did not present any associated experimental data. Experimental results from a non-protein system have been published in an earlier

0021-9673/90/$03.50

paper from the same laboratory[3]. This paper presented two methods for determining competitive adsorption isotherms from the results of frontal analysis chromatography and included a theoretical discussion of the derivation and use of the parameters of the Langmuir isotherm. Results of studies of the adsorption of a mixture of albumin and β-lactamase to encapsulated ion exchangers have been published recently by Nigam *et al.*[4]. They report that competition between the two adsorbing proteins occurred, with albumin displacing the more weakly binding β-lactamase from the ion exchanger.

In order to commence studying multicomponent adsorption, we have examined a model system consisting of two adsorbing species, bovine serum albumin (BSA) and lysozyme, and the strong cation exchanger S Sepharose® FF. We have studied the characteristics of the adsorption of each pure protein to S Sepharose FF and the results of those studies were fully reported in a previous paper[5]. Those studies showed that the Langmuir adsorption isotherm could be used to describe the equilibrium adsorption characteristics of both proteins. In addition, using parameters from the Langmuir isotherm, two different models of the rate of uptake of protein, a kinetic rate constant model and a film and pore diffusion model, were presented. The predictions for the adsorption of lysozyme to S Sepharose FF in both batch, agitated tanks and packed beds were in close agreement with the experimental results. However in the case of BSA, only the film and pore diffusion model was in close agreement with the actual adsorption profile seen in batch, agitated tanks, whilst neither model agreed precisely with the results obtained in column experiments. This was largely due to the fact that the observed breakthrough curves are asymmetric and approach the inlet concentration very slowly. This effect is more pronounced in experiments with BSA, but is observed nevertheless in several different protein–adsorbent systems and makes calculation of the amount of protein adsorbed at equilibrium difficult in these packed-bed experiments.

In this paper we present the results of studies of multicomponent adsorption of BSA and lysozyme to S Sepharose FF and compare these to two models, one based on competitive adsorption to the ion exchanger and the other based on non-competitive adsorption. The choice of proteins for these studies was determined on two grounds. Firstly the high capacity of ion exchangers for proteins meant that gram quantities of pure proteins were required at reasonable cost. Secondly there had to be a method of quantifying the amounts of each protein present in a mixture. The difference in molecular size between BSA and lysozyme enabled the proteins to be separated by molecular-exclusion chromatography and the amounts of the two proteins could be determined by analysis of the resulting chromatogram.

THEORY

Analysis of multicomponent adsorption to ion exchangers benefits from an understanding of the nature of the protein adsorption sites on the adsorbent. Proteins adsorb to ion exchangers as a result of ionic interactions between charged groups on the surface of the protein and oppositely charged groups on the ion exchanger. A protein molecule carries many charged groups and multiple ionic interactions will occur with the adsorbent. Gosling[6] for example, has demonstrated the expulsion of 15–20 chloride counter ions from a diethylaminoethyl-exchanger for each mole of BSA adsorbed. As the three-dimensional distribution of ionic groups on the surface of the

adsorbent is random, the actual protein adsorption site is not a unique entity. Hence the adsorption site on a protein ion exchanger cannot strictly be treated in the same manner as that postulated for affinity adsorption where molecules of the immobilised affinity ligand constitute adsorption sites with identical properties. A Langmuir type isotherm might not be expected to describe the adsorption of single proteins to ion exchangers as fundamental thermodynamic conditions such as the identical nature of adsorption sites and an absence of lateral interaction between adsorbed solute molecules are not obeyed. However, experimental results from systems in which a single protein is adsorbed to an ion exchanger yield equilibrium isotherms which can be described by a Langmuir equation of the form shown below, for example see Leaver[7], Annesini and Lavecchia[8] and Graham *et al.*[9]:

$$q^* = \frac{c^* q_m}{c^* + K_d} \tag{1}$$

where q represents the concentration of protein adsorbed to the ion exchanger, q_m represents the maximum concentration of protein that can be adsorbed to the ion exchanger, c the concentration of protein in the bulk solution and K_d is the dissociation constant of the protein–ion exchanger complex. The superscript * indicates equilibrium values.

In particular, our previous experiments[5] involving the single-component adsorption of BSA and lysozyme to S Sepharose FF show that the equilibrium adsorption isotherms are of the above form and the equilibrium adsorption parameters determined in those studies are presented in Table I. The observation of a Langmuir-type shape can probably be explained by protein adsorption to the ion exchanger continuing until there is no longer room on the surface of the adsorbent for further molecules of adsorbate to bind. Hence further adsorption ceases once monolayer coverage has occurred. This eventual saturation of the adsorbent surface leads to adsorption isotherms of a similar shape to the Langmuir isotherm even though the underlying thermodynamic assumptions are not strictly obeyed, and the Langmuir isotherm therefore is widely used as a simple empirical model of the equilibrium adsorption characteristics of various protein–adsorbent systems.

In addition to uncertainties arising from the undefined nature of the adsorption sites on an ion exchanger for the adsorption of a single, pure protein, the situation is further complicated when the adsorption of two or more proteins is being considered. As a result of the different sizes and distribution of charges on the surfaces of different

TABLE I

VALUES OF K_d AND q_m FOR THE ADSORPTION OF PURE BSA AND LYSOZYME TO S SEPHAROSE FF

The values were determined as described previously[5].

	K_d (mg ml^{-1})	K_d (M)	q_m (mg ml^{-1})	q_m (mol l^{-1})
BSA	0.133	$2.0 \cdot 10^{-6}$	113	$1.7 \cdot 10^{-3}$
Lysozyme	0.019	$1.3 \cdot 10^{-6}$	120	$8.4 \cdot 10^{-3}$

proteins, the number of ionic groups that will participate in the adsorption interaction and the amount of adsorbent surface which interacts with the different proteins will vary. Whilst recognising the complexities of multicomponent adsorption of proteins to ion exchangers, in this paper we have adopted two extreme views to analyse two-component protein adsorption, namely a non-competitive model and a totally competitive model. Both of these models are based on the Langmuir adsorption isotherm, an approach supported by our earlier single-component studies of the adsorption of BSA and lysozyme to S Sepharose FF[5]. It is shown that the totally competitive model more accurately describes the experimental observations.

Non-competitive adsorption model

One extreme view of the adsorption of two proteins to an ion exchanger is to assume that the adsorption sites for the two proteins are mutually independent, that is the adsorption of one type of protein to the ion exchanger in no way affects the adsorption of the other species and there is therefore no competition between the proteins for the adsorption sites. This may be an unlikely situation as the fundamental mechanism for the adsorption of both types of protein molecules involves interaction with the available ionic groups on the surface of the exchanger. If there is no competition between the proteins for adsorption, the adsorption characteristics of each protein will be the same as if the other protein were not present, *i.e.*

$$q_1^* = \frac{c_1^* q_{m1}}{c_1^* + K_{d1}} \quad \text{and} \quad q_2^* = \frac{c_2^* q_{m2}}{c_2^* + K_{d2}} \tag{2}$$

where the subscripts 1 and 2 indicate adsorbate species 1 and 2.

Totally competitive adsorption model

The other extreme approach to the analysis of two-component adsorption is to assume that there is total competition between proteins for adsorption to the ion exchanger. Although the exchanger shows different maximum capacities for the two proteins (q_{m1} and q_{m2}), a competitive model can be developed which involves a fractional occupancy of the adsorption capacity for each type of protein and uses Langmuir parameters derived from single-component experiments. It should always be borne in mind that such an approach violates the Gibbs–Duhem relationship (see ref. 10) and that a thermodynamically rigorous approach would demand the use of parameters determined from two-component experiments. However in the present study it was assumed that at the micromolar concentrations of soluble protein employed in these experiments, the use of parameters determined in single-component studies was a sufficiently accurate approximation.

Let θ represent the fractional occupancy of the adsorbent at equilibrium with a particular protein, such that:

$$\theta_1 = \frac{q_1^*}{q_{m1}}; \qquad \theta_2 = \frac{q_2^*}{q_{m2}} \tag{3}$$

The fraction of unoccupied sites is therefore given by $(1 - \theta_1 - \theta_2)$. At equilibrium

$$K_{d1} = \frac{c_1^*(1 - \theta_1 - \theta_2)}{\theta_1}; \qquad K_{d2} = \frac{c_2^*(1 - \theta_1 - \theta_2)}{\theta_2} \tag{4}$$

giving

$$c_1^* = \theta_1(K_{d1} + c_1^*) + c_1^*\theta_2; \qquad c_2^* = \theta_2(K_{d2} + c_2^*) + c_2^*\theta_1 \tag{5}$$

and

$$(1 - \theta_1 - \theta_2) = \frac{K_{d1}\theta_1}{c_1^*} = \frac{K_{d2}\theta_2}{c_2^*} \tag{6}$$

From eqn. 6:

$$c_1^*\theta_2 = \frac{K_{d1}}{K_{d2}} c_2^*\theta_1 \tag{7}$$

So substituting into eqn. 5 for $c_1^*\theta_2$ from eqn. 7 and for θ_1 from eqn. 3 gives:

$$q_1^* = \frac{q_{m1}c_1^*}{K_{d1} + c_1^* + \dfrac{K_{d1}}{K_{d2}}c_2^*} \tag{8}$$

and similarly

$$q_2^* = \frac{q_{m2}c_2^*}{K_{d2} + c_2^* + \dfrac{K_{d2}}{K_{d1}}c_1^*} \tag{9}$$

The equilibrium position of a batch system can be determined by solving eqns. 8 and 9 simultaneously with the mass balance equations:

$$Vc_{01} = Vc_1^* + vq_1^* \tag{10}$$

$$Vc_{02} = Vc_2^* + vq_2^* \tag{11}$$

where V is the volume of the liquid phase and v is the settled volume of adsorbent in the system. c_{01} and c_{02} are the initial concentrations of the two proteins. A program was written in BASIC to solve eqns. 8, 9, 10 and 11 for values of c_i^* and q_i^* for a particular set of initial conditions V, v and c_{0i} by an iterative method using the values of K_{di} and q_{mi} determined in single-component adsorption isotherm measurements.

EXPERIMENTAL

Materials

BSA and lysozyme (EC 3.2.1.17) were obtained from Sigma (Poole, U.K.), catalogue Nos. A-3912 and L-6876 respectively. BSA has a relative molecular mass of 66 300 daltons[11] and an isoelectric point (p*I*) of 4.7 (ref. 12), whilst lysozyme has a relative molecular mass of 14 500 daltons[13] and a p*I* of 11.1 (ref. 14).

All solutions were buffered with 0.1 *M* sodium acetate–acetic acid, pH 5. Sodium acetate, acetic acid and sodium chloride were all laboratory-grade reagents. S Sepharose FF was a gift from Pharmacia-LKB (Uppsala, Sweden). Known volumes of ion exchanger were obtained by allowing a suspension of the ion exchanger to settle in a measuring cylinder overnight and then adjusting the liquid volume to equal that of the settled ion exchanger. Aliquots of a known volume of a 50:50 (v/v) suspension were then obtained by the use of a Gilson Pipettman automatic pipette.

Determination of protein concentration in the liquid phase

In experiments in which only one protein was present in solution, it was possible to determine protein concentration by measuring the optical density at 280 nm which could be converted to concentration by reference to calibration data. In experiments in which both BSA and lysozyme were present in solution together, quantitation of the concentrations of the individual proteins was achieved by analytical separation of the proteins by molecular-exclusion chromatography using a Fast Protein Liquid Chromatography system (FPLC™) (Pharmacia-LKB). All samples and buffer solutions for FPLC were filtered through 0.22-μm low protein binding Durapore® filters (Millipore, Harrow, U.K.). Protein samples of 200 μl were applied to an HR10/30 column of Superose™ 12 equilibrated with 0.1 *M* sodium acetate–acetic acid, pH 5. The column was eluted with this buffer at a flow-rate of 1 ml/min. This flow-rate, higher than usually recommended for good performance using this column, still resulted in resolution of the two proteins due to the large difference in molecular weight between BSA and lysozyme and allowed a sample to be analysed in 25 min. Integration of the peaks on the resultant chromatogram was performed by the LCC-500 chromatography controller unit of the FPLC system. The concentrations of each protein were then determined from the areas of their peaks by reference to calibration data.

The FPLC method for determining protein concentration was validated by comparing the protein concentration in the outlet stream from packed beds loaded with a single pure protein, determined directly from optical density measurements at 280 nm, with the concentrations determined using the FPLC method. The results of the two determinations were in close agreement and it was decided that the concentration of each protein in samples from the two-component experiments could be accurately determined solely from FPLC analysis. It was also established that the presence of salt had no effect on the separation by FPLC of the two proteins, nor on the quantitation of the integrated areas, thus samples eluted from S Sepharose FF in 1 *M* sodium chloride could be analysed for protein composition with no pretreatment.

Batch equilibrium adsorption studies

A number of experiments were performed in which samples of S Sepharose FF

were equilibrated with different mixtures of BSA and lysozyme. The experiments were performed in flasks prepared according to the protocol for determining adsorption isotherms described previously[5], with the difference that each flask contained not one protein but a mixture of the two proteins. The total mass of protein present in each flask was varied whilst the volume of solution and S Sepharose FF was kept constant. The amounts of BSA and lysozyme used in each flask were always equal on a mass basis. The flasks were incubated overnight in a shaking water bath at 25°C to allow equilibrium to be established. At equilibrium the amount of each protein present in the liquid phase was determined by FPLC as described above, allowing the amounts of each protein that were adsorbed to the ion exchanger to be calculated by mass balance.

Packed-bed experiments

All column experiments were performed with 2 ml (settled volume) of S Sepharose FF packed in a chromatography column, 1 cm diameter (0.785 cm^2 cross-sectional area), mounted vertically. It was found that the volume of ion exchanger used gave a bed height of 2.2–2.3 cm, equivalent to a packed volume of approximately 1.75 ml. All experiments were performed at a volumetric flow-rate of 1 ml/min (superficial velocity 1.27 cm/min) and flow was always in an upward direction. Optical density at 280 nm of the outlet stream was recorded and fractions of 2 ml were collected at the column exit as required for FPLC analysis as described above.

Determination of adsorbed protein profiles in packed beds

A series of packed-bed experiments, in which the bed was loaded with a two-component protein mixture for 50, 100, 150, 200, 250 and 400 min, was performed. At the end of the loading period liquid was removed from the bed by passing 5 ml of air through the bed with a syringe in the reverse direction to that of the original liquid flow. The column was then clamped and the upper endpiece removed. The ion-exchange bed was then extracted from the column by pushing the lower endpiece upwards with a threaded rod. As the adsorbent emerged from the column, slices of approximately 2–3 mm (giving 9–12 slices in total from each bed) were removed with a scalpel and placed into weighed bijou bottles. The bottles were sealed and reweighed. The amount of ion exchanger present in each slice was calculated from these weights. The adsorbed proteins were eluted from the ion exchanger in each sample with 5 ml of 1 *M* sodium chloride. The bottles were agitated for approximately 15 min, at which point the S Sepharose FF was allowed to settle under gravity and 4 ml of supernatant removed. The concentrations of BSA and lysozyme present in this solution were then determined by FPLC. The amount of each protein that had been adsorbed on each slice of S Sepharose FF could then be calculated.

Consecutive application of single-protein solutions to packed beds

Packed-bed experiments, in which a feed solution containing only one of the proteins was applied, were performed. When the protein concentration of the outlet stream (c), as determined from optical density measurements equaled, or was approaching, that of the inlet stream (c_0), the incoming feed stream was switched to a solution containing only the other protein. Fractions were collected at the column exit for analysis by FPLC.

RESULTS

Batch equilibrium adsorption studies

The results of the batch equilibrium adsorption experiments are plotted in Fig. 1. From each adsorption experiment a pair of equilibrium adsorption results was obtained, one for each of the proteins present. Each result represents the concentration of protein in solution that was in equilibrium with an adsorbed amount of the same protein. When studying Fig. 1 it is important to remember that from each flask a result was obtained for each protein, therefore each point for BSA, in the order of increasing soluble protein concentration, pairs with a corresponding lysozyme point, also in order of increasing soluble protein concentration.

The experimental data are compared to the results predicted by the two models of two-component adsorption. The values of q_{mi} and K_{di} used in the predictions were those determined previously[5] in single-component experiments and presented in Table I. The non-competitive model (Fig. 1a) gave a fairly accurate prediction of the lysozyme adsorption results but greatly overpredicted the amount of BSA that would be adsorbed to the ion exchanger. Conversely the totally competitive model (Fig. 1b) gave a good prediction of the amount of BSA adsorbed but underpredicted the amount of lysozyme adsorbed.

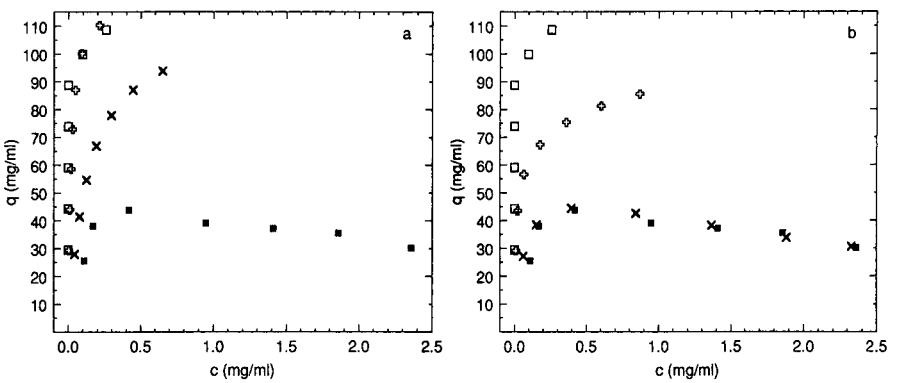

Fig. 1. Batch adsorption of a mixture of lysozyme and BSA to S Sepharose FF in 0.1 *M* acetate buffer, pH 5 at 25°C. The boxes represent experimental results for lysozyme (□) and BSA (■). The crosses represent the predicted values for lysozyme (+) and BSA (×). The data are plotted as mg protein adsorbed per ml S Sepharose FF (q) against mg/ml protein in solution (c). Each BSA point in the order of increasing soluble protein concentration pairs with a lysozyme point also in the order of increasing soluble protein concentration. (a) The experimental results are plotted with the results calculated by the non-competitive model. (b) The experimental results are plotted with the results calculated by the fully competitive model.

Frontal analysis

The development of the breakthrough profiles for BSA and lysozyme when a solution containing a mixture of each protein at a concentration of 1 mg/ml was passed through a bed of S Sepharose FF are shown in Fig. 2a. This figure shows that the breakthrough of BSA occurs before that of lysozyme, with the breakthrough profiles of both proteins having similar slopes. The concentration of BSA is seen to rise above that of the inlet concentration ($c/c_0 > 1$) before it falls back towards it. This

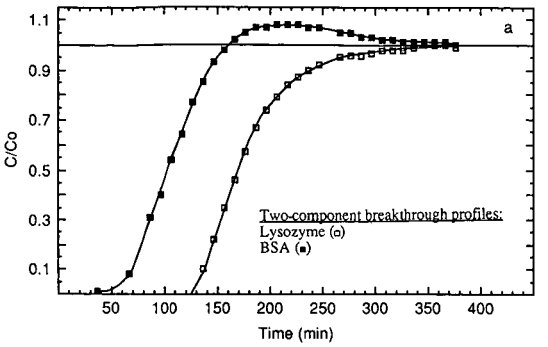

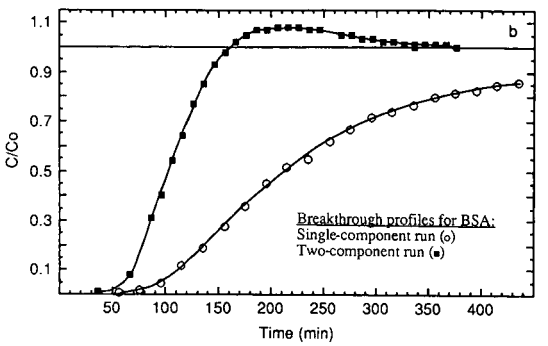

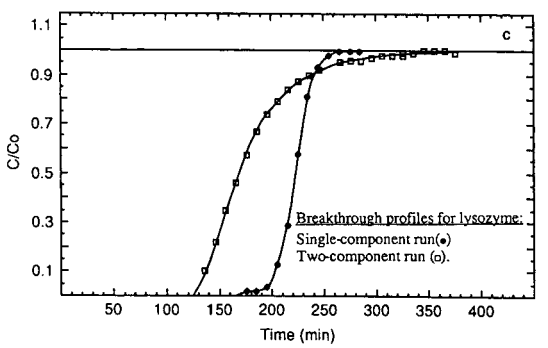

Fig. 2. Breakthrough profiles for the adsorption of lysozyme and BSA to S Sepharose FF in packed beds. The beds used were 1 cm diameter and 2.2 cm high and were loaded at a flow-rate of 1 ml/min in an upward direction. (a) The breakthrough profiles of lysozyme (□) and BSA (■) when a solution containing both proteins, each present at a concentration of 1 mg/ml, was passed through the bed. (b) Breakthrough curves for BSA from experiments in which pure BSA, at a concentration of 1 mg/ml, was applied to a bed (○) and when the mixture of BSA and lysozyme was applied (■). (c) Breakthrough curves for lysozyme from experiments in which pure lysozyme, at a concentration of 1 mg/ml, was applied to a bed (●) and when a mixture of BSA and lysozyme was applied (□).

profile indicates that lysozyme is able to displace, and thereby elute, a certain amount of adsorbed BSA. The amounts of each protein that had bound to the beds were determined by mass balance from the breakthrough profiles. This was performed by integrating the areas above the breakthrough curves for each component taking any area above the $c/c_0 = 1$ line as negative as this represents material eluted from the bed by the more strongly adsorbing component. Allowance was made during these calculations for the void volume of liquid within the bed. It is also possible to use the two models of multicomponent adsorption to calculate the amounts of protein that would be expected to adsorb to the ion exchanger, since at equilibrium the values of c_{01} and c_{02} may be substituted for c_1^* and c_2^* in eqns. 2, 8 and 9. The amounts of each protein bound to the packed bed from experiments and the calculated values from the two models of adsorption are shown in Table II. It can be seen that the experimentally determined figure of 46 mg of BSA adsorbed per ml S Sepharose FF was not accurately predicted by either model but is closer to the value predicted by the fully competitive approach. In the case of lysozyme the experimentally determined figure of 100 mg/ml is almost completely consistent with the fully competitive model.

In order to compare more easily the two-component breakthrough profiles with those obtained from the single-component experiments for each protein, the profiles of multicomponent and single-component experiments have been plotted in the same figures, those for BSA in Fig. 2b and those for lysozyme in Fig. 2c. The single-component breakthrough curves are those determined previously in beds of the same size, under identical conditions and presented in our earlier paper[5]. Fig. 2b clearly shows that the breakthrough profile of BSA in the presence of lysozyme is shifted considerably towards the origin compared to the position of the breakthrough curve when pure BSA is applied to the column. This is a reflection of the fact that significantly more BSA was able to bind to the packed bed in the absence of lysozyme than in the multicomponent experiment. The amount of BSA that was calculated to have adsorbed in the single-component experiment was 130 mg of BSA per ml of S Sepharose FF compared to the 46 mg BSA per ml S Sepharose FF that was bound in the two-component experiment. The slope of the two-component BSA breakthrough profile is seen to be much sharper than that observed in the single-component experiment.

The breakthrough profile of lysozyme obtained in the two-component experiments is shifted towards the origin by a much smaller amount than was the case for

TABLE II

AMOUNTS OF BSA AND LYSOZYME BOUND TO A PACKED BED OF S SEPHAROSE FF AT EQUILIBRIUM

Experimental values were determined using a mixture containing each of the proteins at a concentration of 1 mg mg^{-1} and corresponding figures were calculated from the non-competitive and fully competitive models of adsorption described in the text. All figures are quoted as mg protein adsorbed per ml of S Sepharose FF.

	Experimental (*mg* ml^{-1})	*Non-competitive model* (*mg* ml^{-1})	*Fully competitive model* (*mg* ml^{-1})
BSA	46	100	14
Lysozyme	100	118	103

BSA (Fig. 2c). The position of the two-component curve indicates that although less lysozyme bound to S Sepharose FF in the presence of BSA than was the case when lysozyme alone was present, the difference between the two-component and single-component experiments is not as great as that for BSA, 100 mg of lysozyme per ml S Sepharose FF having been bound in the two-component experiment compared to an adsorbed lysozyme concentration of 125 mg/ml in the single-component experiment. Also in contrast to the result for BSA, the gradient of the two-component lysozyme breakthrough curve is shallower than that obtained in the respective single-component experiment.

The adsorbed protein profile in packed beds

The development of the adsorbed protein profiles of BSA and lysozyme actually within the packed beds is shown in Fig. 3. The diagrams shows the concentration of

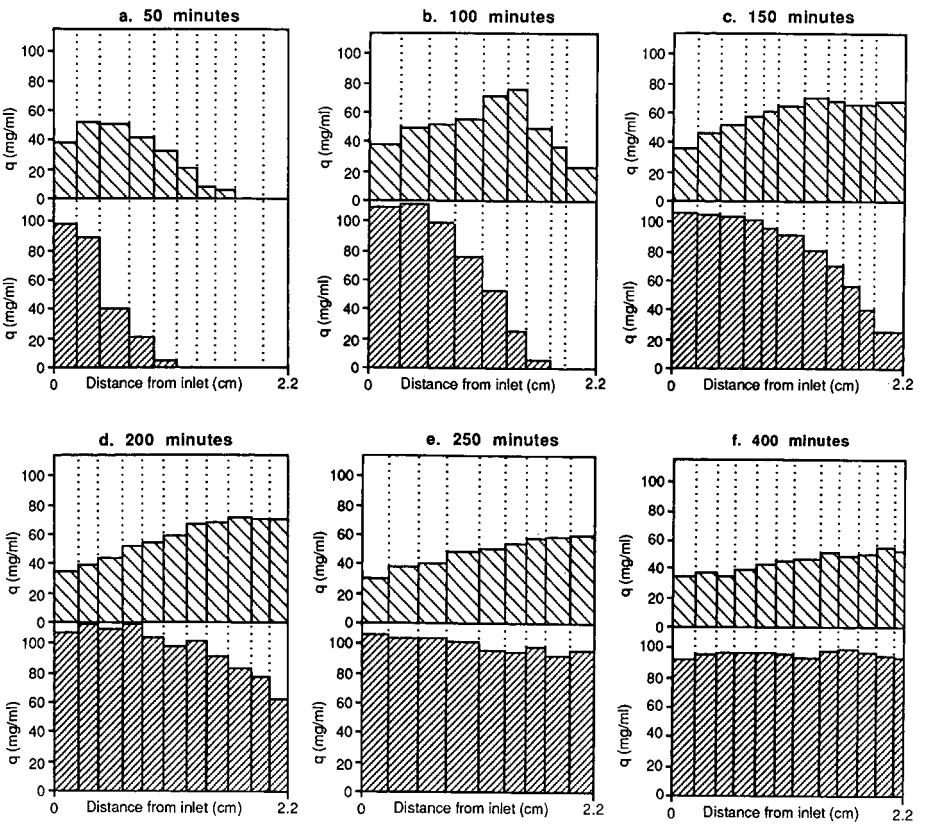

Fig. 3. Adsorbed protein profiles for BSA and lysozyme within packed beds. The beds used were 1 cm diameter and 2.2 cm high and were loaded at 1 ml/min with a solution containing both proteins at a concentration of 1 mg/ml. The BSA profiles are shown in the upper section of each figure in light shading. The lysozyme profiles are shown in the lower section of each figure in dark shading. The results are plotted as the amount of protein adsorbed per ml of S Sepharose FF in each slice against the distance of each slice from the column inlet. The amount of S Sepharose FF in each slice is represented by the different widths of each slice plotted. Each figure shows the profile observed after loading the beds for the following times: (a) 50 min; (b) 100 min; (c) 150 min; (d) 200 min; (e) 250 min; (f) 400 min.

BSA and lysozyme adsorbed on each slice of S Sepharose FF that was taken from a packed bed. The width of each bar in the diagram is proportional to the width of the slices taken from the beds. BSA can be seen to have penetrated further into the bed than lysozyme in the experiments where the column was loaded for 50 and 100 min. This was the expected profile as the breakthrough curves show that BSA appeared in the outlet stream before lysozyme was detected. The adsorbed BSA profile developed a peak which was observed at a maximum in the 100-min experiment. The adsorbed concentration of BSA at this point was 75 mg/ml, far in excess of any previously observed adsorbed BSA concentration in the presence of lysozyme. After this time the peak broadened and developed into a plateau, the concentration of BSA adsorbed on the bed falling as the system approached equilibrium, with the slices closest to the column entry nearing equilibrium first. In the final experiment, in which the column was loaded for 400 min, the amounts of lysozyme and BSA adsorbed, when averaged over the whole bed, were entirely consistent with the values obtained from analysis of the breakthrough curves. The adsorbed concentration of BSA, averaged across the whole bed was 45 mg/ml and the value for lysozyme 96 mg/ml. The figures determined from breakthrough profiles were 46 and 100 mg/ml respectively.

Consecutive application of single-protein solutions to packed beds of S Sepharose FF

Two experiments were performed in which a packed bed of S Sepharose FF was loaded with one protein and then the inlet stream switched to a pure feed of the other protein. The results of these experiments are shown in Fig. 4. The protein profiles are plotted from the point at which the second feed solution first entered the bed. The amounts of protein bound or eluted after the feed was switched were determined from the concentration profiles shown in Fig. 4. In the case of loading a bed with BSA and switching the feed to lysozyme, (Fig. 4a), the concentration of BSA in the exit stream rapidly fell to a low level which during the subsequent FPLC analysis resulted in a peak height that was below the detection limit when the integrator was set at the sensitivity required for lysozyme quantitation. From Fig. 4a it was calculated that approximately 130 mg of lysozyme, equivalent to 74 mg lysozyme per ml S Sepharose FF, bound to a bed which initially contained over 220 mg of adsorbed BSA (125 mg/ml) and of which only 50 mg (29 mg/ml) of BSA was eluted from the column. The result of the complementary experiment in which a bed was loaded with lysozyme and then the feed was switched to BSA is shown in Fig. 4b. In this case the amount of BSA that was adsorbed to the ion exchanger, 29 mg, equivalent to only 17 mg BSA per ml S Sepharose FF, was less than the amount of lysozyme eluted, 40 mg (23 mg/ml).

DISCUSSION

The equilibrium adsorption characteristics of the two proteins, BSA and lysozyme, adsorbing to S Sepharose FF were determined from the single-component adsorption isotherms described previously[5]. The Langmuir isotherm parameters determined are presented in Table I. The equilibrium capacity (q_m) of S Sepharose FF for each protein was found to be similar on a mass basis although due to the greater relative molecular mass of BSA this protein has a smaller q_m value than lysozyme in molar terms. The dissociation constant, K_d, is a measure of the strength of the interaction between the protein and the ion exchanger. In the case of BSA and

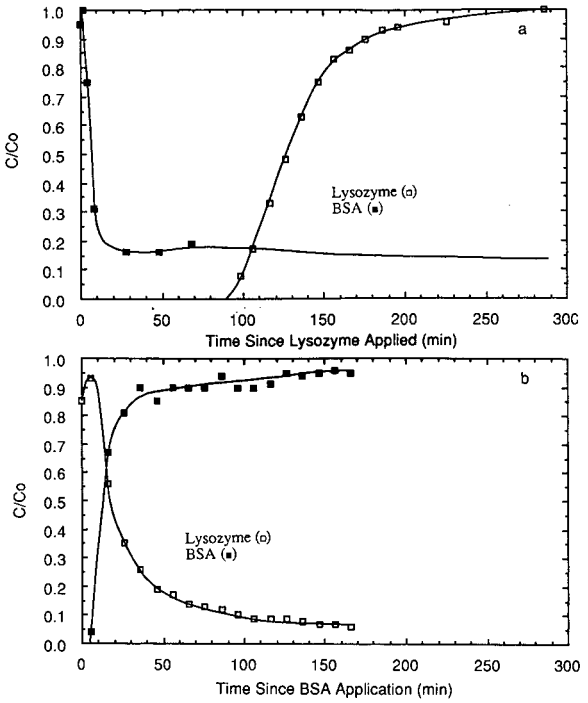

Fig. 4. Adsorption of proteins to packed beds already loaded with another protein. In each experiment the bed was initially loaded with a solution of one protein at a concentration of 1 mg/ml until near to equilibrium with the feed stream. The feed stream was then switched to a solution containing the other protein at a concentration of 1 mg/ml. Concentrations of the two proteins in the exit stream were determined by FPLC analysis and are plotted from the time the feed stream was switched. (a) The profile of BSA (■) and lysozyme (□) in the exit stream of a bed initially loaded with BSA and subsequently loaded with lysozyme. (b) The profile of BSA (■) and lysozyme (□) in the exit stream of a bed initially loaded with lysozyme and subsequently loaded with BSA.

lysozyme adsorbing as single components to S Sepharose FF, lysozyme has a smaller dissociation constant than BSA on both a mass basis and, although the difference is less pronounced, in molar terms. This is probably a reflection of the greater positive charge density found on the lysozyme molecule at pH 5.0. From a consideration of the Langmuir isotherm parameters and the molar concentrations of lysozyme and BSA used in these studies, it was expected that if competitive adsorption occurred, lysozyme would act as the more strongly binding component, with more lysozyme than BSA adsorbing to S Sepharose FF and possibly lysozyme eluting some adsorbed BSA. Such an analysis is supported by predictions from the fully competitive model, using the values of K_{di} and q_{mi} from the single-component studies.

The results of both the two-component batch adsorption and packed-bed experiments did show that greater amounts of lysozyme bound than BSA. However, neither of the models of multicomponent adsorption which were considered correctly predicted the amounts of each protein that bound in either agitated-tank or packed-bed experiments. Since the nature of the adsorption mechanisms of different proteins to an ion exchanger is considered to be based on interactions with the same

charged groups on the ion exchanger surface, it was expected that the experimental results would be in close agreement with the fully competitive model. The major reasons for discrepancies between the observed results and those predicted by the fully competitive Langmuir adsorption model are summarised in Table III and discussed in greater detail below.

In the batch adsorption studies, only the adsorption of BSA was similar to the results of the fully competitive model, with this model greatly underpredicting the amounts of lysozyme that were bound. In contrast, the non-competitive model gave predictions which agreed closely with the amounts of lysozyme that were bound in these batch adsorption experiments, whilst overpredicting the amount of bound BSA. It should be remembered that the experimental results presented in this paper do not constitute a set of competitive adsorption isotherms but rather a collection of paired lysozyme and BSA points, each point lying on a different isotherm. In order to produce a competitive isotherm it is necessary to hold the soluble concentration of one component constant whilst that of the other is varied. Such conditions are impossible to develop in a closed batch adsorption system such as that employed in these studies but can be successfully used in column experiments in which the adsorbent is continually presented with fresh adsorbate solution[3]. Experiments of this kind were not performed in this study due to the length of time (over 5 h) required to allow equilibrium to be established in each column run and in order to construct a set of isotherms many of these experiments are required. Such an approach is therefore

TABLE III

POSSIBLE REASONS FOR THE DIFFERENCES BETWEEN THE OBSERVED EXPERIMENTAL RESULTS AND THOSE PREDICTED BY THE FULLY COMPETITIVE LANGMUIR ADSORPTION ISOTHERM MODEL FOR THE MULTICOMPONENT ADSORPTION OF BSA AND LYSOZYME TO S SEPHAROSE FF

Reason	*Explanation*
Protein size	A large size difference between adsorbing molecules may be reflected in different proportions of the adsorbent surface being available for adsorption with each protein. The fully competitive model assumes that all adsorption sites are available for the adsorption of each molecule.
Protein–protein interactions	If protein–protein interactions occur within the packed beds which are different to those in batch systems as a result of different concentration/time histories of these two systems, more protein may adsorb within the packed bed than is predicted by a Langmuir adsorption model.
Non-equilibrium	The low values of the Langmuir dissociation constants for protein adsorption to ion exchangers suggest that the desorption reactions occur much slower than the adsorption reactions. This may be a reflection of the fact that although protein adsorption occurs via multivalent attachment, only one, or a small number of bonds, may be required to initiate adsorption of a protein whilst all (possibly 10–15) bonds may be required to be broken to desorb a molecule. Consequently it is possible that whilst it was not possible to detect any changes in the soluble protein concentration, protein desorption was still occurring slowly and the results presented do not therefore represent the equilibrium state predicted by the fully competitive model.
Thermodynamics	It is well established that protein adsorption to ion exchangers does not strictly adhere to the thermodynamic assumptions of the single component Langmuir adsorption isotherm. In addition, in the case of multicomponent protein adsorption, violation of the Gibbs–Duhem relationship should also be considered.

better suited to a medium- or high-pressure system such as the non-protein HPLC system used by Jacobson *et al.*[3].

The two extreme models of multicomponent adsorption were also used to calculate the amounts of each protein that would be expected to bind to a packed bed of ion exchanger at equilibrium. In this case the results of the fully competitive model gave a good correlation with the amounts of lysozyme that were bound but the amount of BSA bound was underestimated. These results however, were closer to the fully competitive model than the predictions of the non-competitive model, which overpredicted the amounts of both proteins which should bind, with the discrepancy between predicted and observed results being greatest in the case of BSA.

Despite the lack of exact agreement between the experimental results and those calculated from the fully competitive model, the results of the packed-bed experiments provided substantial evidence, in the form of breakthrough profiles, that some degree of competitive adsorption was occurring. The breakthrough profile of lysozyme was noticeably less sharp in experiments in which a mixture of the two proteins was applied to a packed bed than was the case in single-component experiments. This suggests that the adsorption of lysozyme was hindered by the presence of BSA. In contrast the breakthrough profile of BSA from two-component experiments was sharper than that observed when pure BSA was applied to a bed of S Sepharose FF. The two-component BSA profile was seen to rise above a c/c_0 value of 1, that is the concentration of BSA in the exit stream was greater than that in the inlet stream. This type of profile is caused by a proportion of the more weakly binding component, in this case BSA, being eluted from the adsorbent by the more strongly binding component, in this case lysozyme. Elution of BSA by lysozyme also results in the sharper BSA breakthrough profile observed in the two-component experiments. This effect is analogous to the sharp peak front observed during gradient elution of adsorbates from packed beds. The two-component breakthrough profiles observed are similar to those seen in studies of the multicomponent adsorption of smaller molecules in which competition between adsorbate molecules was occurring[15].

Elution of BSA by lysozyme was also observed in the experiments in which partially loaded beds of S Sepharose FF were extracted and the profile of adsorbed protein determined. In those experiments the amount of BSA adsorbed to the ion-exchange bed passed through a maximum of approximately 80 mg per ml S Sepharose FF after 100 min of loading. At later time points the profile developed into a plateau and after 400 min the amount of BSA on each slice was approximately 40 mg per ml S Sepharose FF. During the experiments lysozyme was seen to penetrate along the length of the bed at a slower rate than BSA, the expected profile as the point of lysozyme breakthrough in the column exit stream is after that of BSA. It is apparent from this profile that the nature of the adsorption process varies along the length of the bed and with time, since in the early stages, at the regions of the bed furthest from the column inlet there is no lysozyme present in the soluble phase and BSA is absorbing as a single component and hence would be able to bind at all sites with no competition occurring. At the column inlet and, as time progresses, over a greater length of the column, adsorption of both proteins occurs simultaneously.

In order to investigate the characteristics of adsorption of protein to ion exchanger which is already loaded with another protein, the experiments in which packed beds of S Sepharose FF were first loaded with one protein and then the feed

solution switched to a solution of the other protein were performed. From consideration of a competitive model of adsorption, supported by the evidence of the breakthrough profiles, it was expected that lysozyme would elute and replace a proportion of the adsorbed BSA. Conversely it was expected that BSA, the less strongly binding component, would be less effective at replacing adsorbed lysozyme. Similar experiments of protein adsorption/displacement in a reversed-phase liquid chromatography system[16] showed just such behaviour. However in this study, the results of applying lysozyme to a bed near to saturation with BSA were found not to correspond to this expectation. The amount of BSA which was eluted from the bed was approximately 30 mg per ml S Sepharose FF, with the final adsorbed concentration of BSA being just under 100 mg per ml S Sepharose FF, whilst an additional 75 mg lysozyme was bound per ml S Sepharose FF. These results are in contrast to those reported by Di Bussolo and Gant[16], who demonstrated complete elution of more weakly binding proteins by more strongly adsorbing proteins. However it should be noted that in that system, significant concentrations of the reversed-phase liquid chromatographic elution agent, 20% acetonitrile, were present in the equilibration buffer. A comparable experiment in the ion-exchange system used in this study would therefore include the presence of salt in the buffers (which in this case had a relatively low ionic strength), in order to weaken the strengths of interaction of both proteins. In the complementary experiment, in which BSA was applied to a bed saturated with lysozyme, as expected the more weakly binding BSA was found to be less effective at eluting and replacing adsorbed lysozyme.

The results of the experiments described have clearly shown that the adsorption of BSA and lysozyme to the ion exchanger S Sepharose FF is, to some extent, competitive in nature. However, the discrepancies between the experimental results and those predicted by either model of multicomponent adsorption indicate that the adsorption process is more complex than the models described. One of the primary assumptions of the fully competitive model is that all adsorption sites are equally accessible to all adsorbate molecules. However it is likely that due to the smaller size of lysozyme in comparison to BSA, lysozyme is able to penetrate regions of the ion exchanger particles which are too restricted for BSA to enter. Such differential access of proteins of different molecular sizes to adsorbent particles is the principle on which molecular-exclusion chromatography is based and underivatised Sepharose is marketed as a gel filtration material. Any lysozyme adsorption which occurred at sites which are inaccessible to BSA would be non-competitive and would result in the amount of adsorbed lysozyme being underpredicted by the fully competitive model. The presence of large quantities of BSA adsorbed within the particles might be expected to hinder the access of lysozyme to these sites.

It should be remembered that predictions from the fully competitive model refer to the amounts of protein that would be bound to the ion exchanger at equilibrium with the liquid phase. It is possible that equilibrium may not have been achieved in some of the adsorption experiments described here and this may be a further reason for the discrepancies between the predictions and the experimental results. Although the lack of variation of the concentrations of proteins in the liquid phase as measured by FPLC appeared to suggest that the systems were at equilibrium, adsorption/desorption may have been still occurring at slow rates. The mechanism for the displacement of an adsorbed molecule by another is unknown but it is possible that an adsorbed

molecule may have to desorb from the ion exchanger as a result of the reversible nature of the interaction before another molecule can be bound. Since it is likely that proteins adsorb to ion exchangers by multivalent attachment[2] then desorption of a protein molecule requires that many bonds be broken before a protein molecule becomes detached from an adsorbent surface. In the case of BSA and lysozyme, the dissociation constants of the protein–adsorbent interaction are small, suggesting that the desorption rates may indeed be slow.

A further adsorption mechanism could be due to protein–protein interactions within the ion exchanger particles. Electrostatic interactions between lysozyme and BSA in free solution have been reported previously[17,18]. Although such interactions were not reported at pH 5, the pH used in these adsorption studies, the large amounts of protein adsorbed within the ion exchanger particles and the possibility that they are adsorbed in specific orientations, may promote such interactions, with the result that protein is adsorbed within the ion exchanger but to other protein molecules rather than ion exchanger functional groups. The BSA molecule has an ellipsoidal shape and the charge distribution along the major axis is known to be asymmetric, such that one end of the molecule carries predominantly positively charged groups and the other end negatively charged groups. Studies of BSA adsorption to a silica-based ion exchanger in which the available surface area was known have indicated that BSA molecules were adsorbed in an "end-on" orientation, that is with the major axes perpendicular to the adsorbent surface[19]. Adsorption of BSA to lysozyme in such an orientation with the positively charged region of the molecule interacting with the negatively charged sulphonic groups on the surface of the ion exchanger, would present the negatively charged region of the BSA molecule pointing out towards the bulk liquid. This may have provided sites with which the strongly positively charged lysozyme molecules could have interacted electrostatically, resulting in adsorption. Any lysozyme adsorbed in this manner would be to sites which would not be available to BSA and would be in addition to those available during single-component adsorption of lysozyme. Under these circumstances the amount of lysozyme predicted to adsorb by the fully competitive model would indeed be an underestimate of the experimental results. It should be emphasised that we are not postulating that such an adsorption mechanism is a general phenomenon but one that may be pertinent to the system under study in this paper. However it should always be borne in mind that at the high protein concentrations found within packed beds and the likelihood of adsorption imposing some kind of order on the orientation of adsorbed protein molecules, then interactions which are not normally seen in free solution may occur within a packed bed.

CONCLUSIONS

The studies presented here have demonstrated some of the experimental techniques and a possible theoretical approach that can be used to investigate multicomponent protein adsorption. In this study multicomponent adsorption isotherms were not determined experimentally and in future studies it would be instructive to determine such isotherms by performing frontal analysis experiments using solutions containing mixtures of varying compositions[3].

Two extreme models of multicomponent protein adsorption have been considered and neither of these accurately predicted the adsorption characteristics of BSA

and lysozyme in either batch adsorption or packed-bed experiments. Clear evidence that a competitive model is the better approach to modelling multicomponent protein adsorption to ion exchangers was provided by the breakthrough curves and the profiles of protein adsorbed along the length of packed beds. Competitive adsorption was demonstrated in those experiments by the observation that lysozyme could elute adsorbed BSA from the ion exchanger. However the discrepancies between the observed and predicted results suggest that in studies of the multicomponent adsorption of proteins of different sizes, it may be necessary to include in the model contributions from non-competitive adsorption in order to allow for the adsorption of small proteins in regions of particles inaccessible to larger molecules. In the particular case of BSA and lysozyme, the development of such a multicomponent adsorption model is yet further complicated by the possibility that lysozyme may become bound to adsorbed BSA molecules as a result of electrostatic interactions. In addition, the suitability of BSA generally as a model protein should be seriously questioned, as its behaviour as a single component can be complicated by interactions with itself and the consequent formation of dimers in the packed bed[5].

In conclusion, the results presented here suggest that the theoretical modelling of multicomponent protein adsorption is a complicated task and that an accurate model may require contributions from the theories of molecular-exclusion chromatography and protein–protein interaction in addition to adsorption chromatography.

ACKNOWLEDGEMENTS

The authors would like to thank the Science and Engineering Research Council for financial support. They are also grateful to Pharmacia LKB Biotechnology (Uppsala, Sweden) for the provision of experimental materials and equipment and to Brenda Horstmann for constructive comments on the text.

SYMBOLS

c liquid phase concentration of protein
c_0 initial or inlet liquid phase protein concentration
K_d dissociation constant for the protein–ion exchanger complex
q concentration of protein adsorbed to the ion exchanger
q_m maximum protein capacity of the ion exchanger
v volume of ion exchanger
V volume of liquid
θ fractional occupancy of adsorption sites with protein at equilibrium
$*$ value when system is at equilibrium

REFERENCES

1 J. C. Janson and P. Hedman, *Biotechnol. Prog.*, 3 (1987) 9.
2 A. Velayudhan and Cs. Horváth, *J. Chromatogr.*, 443 (1988) 13.
3 J. M. Jacobson, J. H. Frenz and Cs. Horváth, *Ind. Eng. Chem. Res. Des.*, 26 (1987) 43.
4 S. C. Nigam, A. Sakoda and H. Y. Wang, *Biotechnol. Prog.*, 4 (1988) 166.
5 G. L. Skidmore, B. J. Horstmann and H. A. Chase, *J. Chromatogr.*, 498 (1990) 113.
6 I. S. Gosling, *Ph.D. Thesis*, University College, University of Wales, Swansea, 1985.
7 G. Leaver, *Ph.D. Thesis*, University College, University of Wales, Swansea, 1984.

8 M. C. Annesini and R. Lavecchia, *Chem. Biochem. Eng. Q.*, 1 (1987) 89.
9 E. E. Graham, A. Pucciani and N. G. Pinto, *Biotechnol. Prog.*, 3 (1987) 141.
10 D. G. Broughton, *Ind. Eng. Chem.*, 40 (1948) 1506.
11 T. Peters and R. G. Reed, in T. Peters and I. Sjöholm (Editors), *FEBS 11th Meeting, Vol. 50, Colloquium B9, Albumin: Structure, Biosynthesis, Function*, 1978, p. 11.
12 R. M. C. Dawson, D. C. Elliot, W. H. Elliot and K. M. Jones, *Data for Biochemical Research*, Oxford University Press, Oxford, 1974.
13 A. Fersht, *Enzyme Structure and Mechanism*, Freeman, Reading, 1977, p. 330.
14 T. Imoto, L. N. Johnson, A. C. T. North, D. C. Phillips and J. A. Rupley, in P. D. Boyer (Editor), *The Enzymes*, Academic Press, New York, 2nd ed., 1972, 7, p. 665.
15 A. Mansour, D. U. von Rosenberg and N. D. Sylvester, *AIChE J.*, 28 (1982) 765.
16 J. M. Di Bussolo and J. R. Gant, *J. Chromatogr.*, 327 (1985) 67.
17 R. F. Steiner, *Arch. Biochem. Biophys.*, 46 (1953) 291.
18 R. F. Steiner, *Arch. Biochem. Biophys.*, 47 (1953) 56.
19 J. P. van der Wiel and J. A. Wesselingh, presented at *NATO Advanced Study Institute, Vimeiro, Portugal, July 17–29, 1988.*

Journal of Chromatography, 505 (1990) 349–356
Elsevier Science Publishers B.V., Amsterdam — Printed in The Netherlands

CHROM. 22 293

Determination of tebufelone (a new anti-inflammatory drug) strength and stability in bulk drug, dosage formulations and feed admixtures by reversed-phase high-performance liquid chromatography

ROSE M. KAFFENBERGER, THOMAS H. EICHHOLD and MATTHEW J. DOYLE*
The Procter & Gamble Company, Miami Valley Laboratories, P.O. Box 398707, Cincinnati, OH 45239-8707 (U.S.A.)
(First received June 27th, 1989; revised manuscript received January 22nd, 1990)

SUMMARY

A rugged reversed-phase high-performance liquid chromatographic method suitable for the quantitative determination of tebufelone, a new anti-inflammatory drug, in bulk drug, various pharmaceutical formulations and animal feed admixtures is described. Tebufelone was easily separated from synthetic by-products and detected by ultraviolet absorption (280 nm). Standard curves were linear ($r^2 > 0.999$) over 2 orders of magnitude with a detection limit of 0.1 μg/ml at a signal-to-noise ratio of 2 (0.05 ml injected). Recovery of tebufelone from bulk drug and dosage formulataions was > 99% with a coefficient of variation of 1.8% throughout the range of the standard curve. Recovery of tebufelone from feed admixtures was 96–102% with a < 5% relative standard deviation at the levels assayed.

INTRODUCTION

Tebufelone {NE-11740: 1-[3,5-bis(1,1-dimethylethyl)-4-hydroxyphenyl]-5-hexyn-1-one} is a new, highly potent anti-inflammatory drug which has exhibited efficacy in a variety of animal models[1]. The compound (Fig. 1) is a member of the di-*tert.*-butylphenol (DTBP) class of non-steroidal anti-inflammatory drugs (NSAIDs). Unlike conventional NSAIDs (*e.g.* indomethacin), which only block cyclooxygenase (CO) activity, tebufelone is an inhibitor of both CO and 5-lipoxygenase (LO) enzymes[2,3]. Some products of CO and LO activity, prostaglandin E_2 (PGE_2) and leukotriene B_4 (LTB_4) in particular, have been shown to mediate the pain, edema and tissue destruction associated with inflammatory processes[4,5].

Several DTBP anti-inflammatory agents[6–9] have been developed in recent years and it is hoped this new class of dual CO/LO inhibitory NSAIDs will prove advantageous for the treatment of arthritic, psoriatic or asthmatic conditions. Clinical evaluation of the therapeutic potential of drug candidates requires the development of

0021-9673/90/$03.50

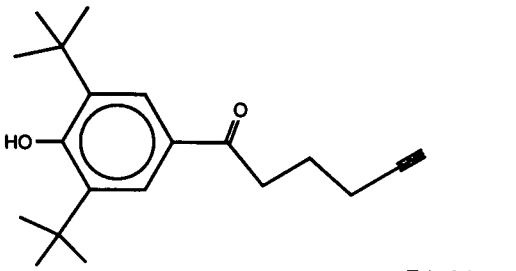

Tebufelone

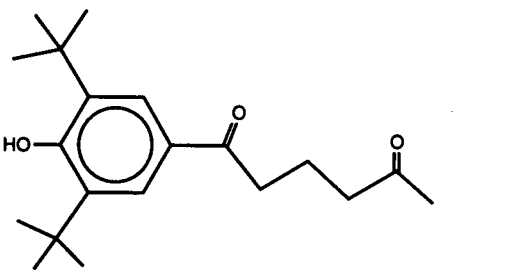

Diketone

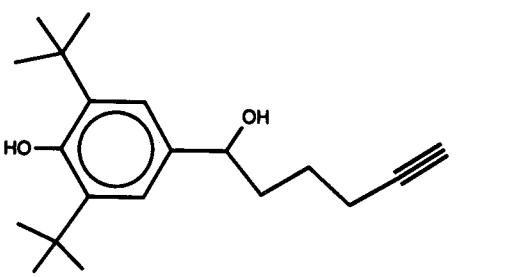

IS

Fig. 1. Chemical structure of tebufelone, the diketone synthetic by-product and the internal standard (IS).

analytical methods suitable for the measurement of active strength, purity and stability in bulk drug, dosage formulations and animal feed admixtures. Reversed-phase (RP) high-performance liquid chromatographic (HPLC) techniques have been successfully employed for the separation and quantification of a variety of phenolic analytes[10,11]. Verhagen *et al.*[12] have recently reported the development of a RP-HPLC procedure for the determination of butylated hydroxytoluene in bovine plasma. In addition, the effect of phenolic ring substitution on column (C_{18}) selectivity has also been investigated[13].

When performing chronic drug safety testing in animals, the preferred method of drug administration is via the diet *ad libitum* primarily for convenience sake. Consistently obtaining homogeneous drug-feed blends is a major concern during the

conduct of these types of studies[14]. The complex nature of animal feed matrices has necessitated the development of a chromatographic procedure utilizing an internal standard (IS). Butylated hydroxytoluene (BHT = 2,6-di-*tert.*-butyl-4-methylphenol) is structurally similar to tebufelone and normally would represent an ideal choice as an internal standard for quantitative purposes. Further, chromatographic methods for the determination of BHT in poultry premix and mixed feeds have recently appeared in the literature[15,16]. However, BHT is commonly added to animal feed as an antioxidant which precludes its use as a universal internal standard for animal feed analyses. For this reason, we chose to use a structural analogue of tebufelone (Fig. 1), in which the aliphatic carbonyl group has been reduced to a hydroxyl moeity, as an IS. The molar extinction coefficient (at 280 nm) for the IS is approximately 10 times less than that for tebufelone.

We report here the development of a facile RP-HPLC method for the determination of tebufelone in bulk drug preparations as well as dosage formulations. In addition, the method was modified to include an internal standard and methanolic extraction step for the determination of tebufelone in rodent chow. Separation is achieved isocratically using an octadecyl stationary phase and the drug is quantified via ultraviolet detection (280 nm).

EXPERIMENTAL

Reagents and chemicals

tebufelone reference standards, IS and ^{14}C-labeled tebufelone (48.2 μCi/mg) were synhesized at Miami Valley Labs. Reference standards were shown to be >99.9% pure by thermogravimetric and titrimetric methods of analysis. tebufelone drug product (tebufelone–pluronic F-108–polyethylene glycol 3350 in No. 00 hard gelatin capsules) was also manufactured at Miami Valley Labs. Capsules were prepared containing between 50 and 200 mg of drug active. Certified rodent chow meal No. 5002 from Ralston Purina (St. Louis, MO, U.S.A.) was formulated with tebufelone (1%) by the wet granulation method (ethanol slurry). Acetonitrile (HPLC grade) and potassium phosphate (ACS grade) were obtained from Fisher Scientific (Cincinnati, OH, U.S.A.). Phosphoric acid was purchased from EM Science (Hawthorne, NY, U.S.A.) and water was Milli-Q Reagent water (> 17 Ω resistivity) from Millipore (Bedford, MA, U.S.A.).

Procedure

Mobile phase preparation. A ternary mobile phase comprised of acetonitrile–water–potasium phosphate (70:30:0.01%) was prepared by adding 100 mg of potassium phosphate to *ca.* 250 ml of Milli-Q water. The pH of this solution was adjusted to 3.5 using phosphoric acid. This buffer solution was diluted to 300 ml with deionized water, added to 700 ml acetonitrile and degassed by aspiration for 10 min.

Standard and sample preparation for bulk drug and dosage formulations. Typically, four tebufelone standard solutions (20, 10, 4 and 2 μg/ml) were prepared in mobile phase. Bulk drug (usually 10 mg of raw material) was placed in a 100-ml volumetric flask and diluted to volume with mobile phase. A 1.0-ml aliquot of this stock solution was further diluted to 25 ml with mobile phase. Drug product was prepared by emptying contents of the capsules into a 250-ml volumetric flask through

a funnel. An accurate weight was obtained and sample was diluted to volume with mobile phase. A 1.0-ml aliquot of this stock solution was further diluted to 100 ml with mobile phase. Standard and sample diluent was injected directly (50 μl) onto the chromatograph. All analyses were performed in duplicate.

Standard preparation for IS-based method. Stock solutions of tebufelone and IS were prepared in mobile phase. Calibration standards, containing both components, were pepared in mobile phase from the stock solutions to yield final concentrations of: 1, 5, 10, 20, 35, 50 μg/ml tebufelone with 50 μg/ml IS in each. Also, an IS stock solution in ethanol was prepared at a concentration of 5 mg/ml.

Sample preparation for animal feed admixtures. Internal standard (100 μl of 5 mg/ml stock solution) was added to a 100-mg portion of the chow admixture in a 120 $\times$ 15 mm glass centrifuge tube (Fisher Scientific) followed by 10 ml of methanol as an extractant phase. This sample was mixed well for *ca.* 10 min to ensure complete extraction of tebufelone and IS. Centrifugation (2000 *g* for 10 min) was used to separate the solids from the organic phase, then 50 μl of the methanol phase was directly injected into the chromatograph.

Equipment and assay conditions

A modular system was employed which consisted of a Constametric III solvent delivery system (LDC/Milton Roy, Riviera Beach, FL, U.S.A.), a Wisp autosampler (Waters, Milford, MA, U.S.A.), and a Spectromonitor III variable-wavelength UV detector (LDC/Milton Roy). A 5-μm 25 cm $\times$ 4.6 mm I.D., Zorbax ODS analytical column (DuPont, Wilmington, DE, U.S.A.) was coupled with a 5-μm 30 mm $\times$ 4.6 mm I.D., RP-18 Brownlee pre-column (Rainin, Woburn, MA, U.S.A.). The analytes were eluted from the column isocratically using a mobile phase flow-rate of 2.0 ml/min and detection was achieved by monitoring the effluent at 280 nm.

Data were collected using version 4.1 of a chromatographic software package (Beckman, Fullerton, CA, U.S.A.) and a Mark 5 digimitry unit (Beckman) to digitize the signal from the detector. Data were then stored on an HP1000E data system (Hewlett-Packard, Avondale, PA, U.S.A.). A Model DU-50 spectrophotometer (Beckman) was used to obtain the UV–VIS spectum. Radioactive fractions were counted using a Packard Model 2000CA Scintillation counter (Downers Grove, IL, U.S.A.).

RESULTS AND DISCUSSION

Spectroscopic characterization of analyte

The UV–VIS absorption spectrum (200–400 nm) of tebufelone appears in Fig. 2. The spectrum is generally characteristic of phenolic compounds with a major band centered at 280 nm and high absorbance occurring below 240 nm[10]. The molar extinction coefficient (at 280 nm) was determined to be 5250 au/$M \cdot$ cm for tebufelone dissolved in acetonitrile–water–potassium phosphate (70:30:0.01). All excipients (pluronic F-108, polyethylene glycol 3350) used to formulate tebufelone drug product exhibited minimal absorption (essentially transparent in mobile phase) at 280 nm. Hence, the chromatographic effluent was monitored at 280 nm for tebufelone quantitative purposes.

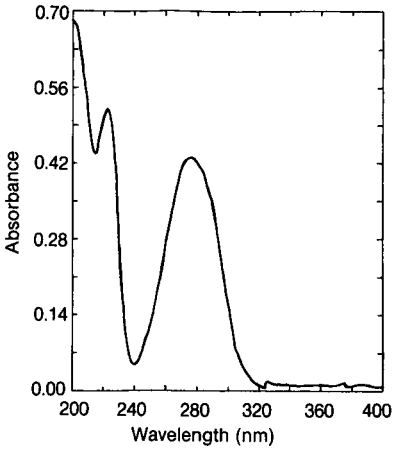

Fig. 2. UV–VIS absorption spectrum (200–400 nm) of a 10 μg/ml tebufelone in acetonitrile–water–potassium phosphate (70:30:0.01) solution.

Determination of tebufelone in bulk drug and dosage formulations

Chromatographically, tebufelone elutes with a retention time (t_R) of 5.6 min [capacity factor (k') = 3.5] under the assay conditions described above. As shown in Fig. 3, tebufelone is well resolved [resolution (R_s) > 2.0] from the diketone analogue which represents the primary synthesis by-product. This by-product is easily separated from active drug as a consequence of the synthetic purification sequence and not normally observed in final bulk drug preparations. During the course of routine analyses, no other potentially interfering peaks have been observed. Column efficiency (N) exceeded 12 000 plates and sample throughput can be maximized by employing shorter columns containing the 5-μm Zorbax C_{18} stationary phase without sacrificing resolution.

tebufelone standard curves (peak area) were linear between 0.2 and 20 μg/ml with a detection limit [signal-to-noise ratio (S/N) = 2] of 0.10 μg/ml. When standard

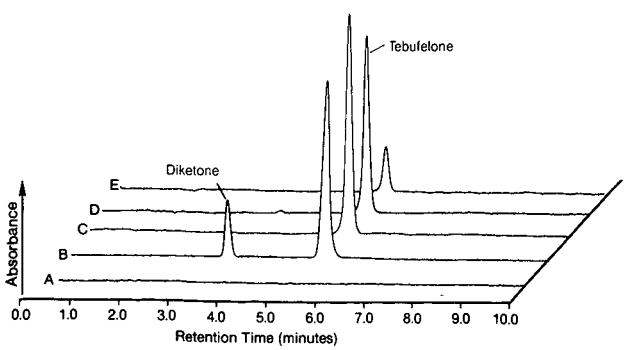

Fig. 3. Stacked plot of chromatograms including: (A) placebo capsule, (B) 4:1 mixture of tebufelone and diketone analogue, (C) 10 μg/ml tebufelone standard, (D) contents of a 200-mg capsule diluted to 8 μg/ml with mobile phase and (E) 2.0 μg/ml tebufelone standard. Detection was by UV absorption at 280 nm (50 μl injected).

data points are fitted using a first order linear regression algorithm, an intercept of 6.53 and slope of 150 was calculated. The correlation coefficient (r^2) for the analytical curve was always > 0.999. The change in response factor (R_f), for successive injections ($n = 10$) of a given analytical sample (Table I) was ± 1.8% relative standard deviation (R.S.D.) and retention times were precise to within ± 0.4% R.S.D. Recovery of [^{14}C]tebufelone injected on column, at concentrations bracketing the standard curve, was quantitative (100%). The accuracy of the method was confirmed by measuring recovery of tebufelone from spiked samples (Table II). Recovery of tebufelone added to excipient mixtures at the 1.9 and 11 μg/mg level was 101 ± 0.1% and 99 ± 0.7%, respectively. These measurements were precise to within 1% of the mean tebufelone concentration for each mixture.

Also, we have employed this methodology to monitor the stability of tebufelone bulk drug and tebufelone drug product (50- and 200-mg capsules). There has been no evidence of tebufelone degradation in samples stored under thermally accelerated conditions (23, 37, 49°C) with an atmospheric headspace over a one-year period. It is anticipated that pharmaceutical products containing tebufelone will be highly shelf-stable.

Determination of tebufelone in animal feed admixtures

As shown in Fig. 4, tebufelone is well resolved (R_s > 2.0) from the internal standard (IS, t_R = 3.5 min). There was no evidence of interfering chow matrix components within the tebufelone or IS retention windows. Calibration curves were linear over 1.5 orders of magnitude with a correlation coefficient (r^2) of 0.999. The limit of detection (S/N = 2) was determined to be 10 μg/g (5 ng on column) without preconcentration of the organic phase. The limit of detection for the method is restricted by the UV (280 nm) properties of the IS.

Instrumental precision was determined by calculating the variance in response factor (R_f = peak area ratio/tebufelone concentration) for a series (n = 10) of

TABLE I

HPLC SYSTEM PRECISION

The contents of a 200 mg tebufelone capsule were diluted in mobile phase and the resulting solution was analyzed repetitively (n = 10) to determine retention times (t_R) and response factor (R_f) reproducibility.

t_R (min)	R_f
5.45	19.79
5.46	19.41
5.46	19.89
5.47	19.62
5.47	19.51
5.47	19.61
5.43	20.30
5.43	20.44
5.43	19.62
5.41	19.49
Mean 5.45 ± 0.02	19.77 ± 0.35
R.S.D. 0.4%	1.8%

TABLE II

RECOVERY OF TEBUFELONE FROM SPIKED SAMPLES

Known quantities of tebufelone were added to pluronic F-108–polyethylene glycol 3350 (50:50) mixtures and analyzed by isocratic reversed-phase HPLC.

Sample No.	*Estimated concentration (μg/mg)*	*Determined concentration (μg/mg)*		*Recovery (%)*
1	1.93	1.95		101.2
2	1.93	1.95		101.2
3	1.93	1.96		101.4
			Mean	101.3 ± 0.1
			R.S.D.	0.1%
4	11.03	10.85		98.3
5	11.03	10.96		99.3
6	11.03	10.99		99.7
			Mean	99.1 ± 0.7
			R.S.D.	0.6%

calibration standards ranging in tebufelone concentration between 100 μg/g and 5 mg/g. Precision of tebufelone and IS measurements was 2.1% R.S.D. of the mean R_f (2.0 ± 0.04). Retention time reproducibility was quite acceptable at less than 0.4% coefficient of variation (C.V.) for both tebufelone (average t_R = 5.66 ± 0.02) and IS (average t_R = 3.52 ± 0.01).

Absolute recovery of tebufelone from rodent chow was determined to be 96–99% (0.08 to 2.7 mg/g range) using [^{14}C]tebufelone as a tracer. The use of a structural analogue of tebufelone as an internal standard precludes the need to correct for analyte losses subsequent to sample handling. The accuracy of the method was demonstrated by analyzing blank chow samples spiked with 0.1 mg/g (n=5) and 5.0 mg/g (n=3) tebufelone. Mean recoveries were 96.2% and 101.9%, respectively with an assay precision of between 1.5% and 5.0%. This methodology is rugged and

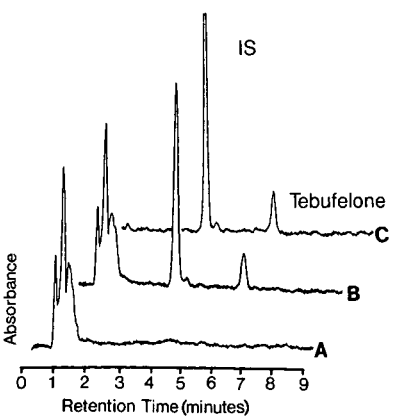

Fig. 4. Reversed-phase HPLC chromatograms of: (A) extract of 100 mg rodent chow, (B) extract of 100 mg rodent chow containing tebufelone (10 μg) and (C) a tebufelone–IS (1:50 ratio) calibration standard.

presently being employed to monitor the stability of tebufelone in rodent feed admixtures. It also may be broadly applicable for the determination of anti-inflammatory di-*tert.*-butylphenol analogues of pharmaceutical interest.

ACKNOWLEDGEMENTS

The authors wish to acknowledge the efforts of Ms. Susanne Menkedick and Mr. Edmund M. Blanken related to the conduct of the drug stability studies. Also the efforts of Messrs. Douglas J. Dobrozsi, Gary R. Kelm and Clarence Dixon, relating to the preparation of the drug-chow admixtures, are greatly appreciated.

REFERENCES

1 M. E. Loomans, J. A. Miller, R. S. Matthews, R. W. Farmer, D. A. Lade, R. A. Underwood, K. L. Skare and H. H. Tai, *Fourth Int. Conf. Inflamm. Res. Assoc., White Haven, PA, October 23–27, 1988*, Abstract No. 51.
2 S. M. Weisman, B. A. Hynd, M. J. Doyle, C. W. Coggeshall, R. M. Kaffenberger, T. H. Eichhold, D. L. Holloway and K. R. Wehmeyer, *Fourth Int. Conf. Inflam. Res. Assoc., White Haven, PA, October 23–27, 1988*, Abstract No. 66.
3 M. J. Doyle, T. H. Eichhold, B. A. Hynd and S. M. Weisman, *J. Pharm. Biomed. Anal.*, (1990) in press.
4 J. Vane and R. Botting, *FASEB J.*, 1 (1987) 89.
5 M. A. Bray, *Agents Actions*, 19 (1/2), (1986) 87.
6 E. S. Lazer, H. C. Wong, G. J. Possanza, A. G. Graham and P. R. Farina, *J. Med. Chem.*, 32 (1989) 100.
7 G. G. I. Moore and K. F. Swingle, *Agents Actions*, 12 (1982) 674.
8 H. Ikuta, H. Shirota, Y. Kobayashi, K. Yamagishi, I. Yamanda, I. Yamatsu and K. Katayama, *J. Med. Chem.*, 30 (1987) 1955.
9 T. Hidaka, K. Hosoe, Y. Ariki, K. Takeo, T. Yamashiti, I. Katsumi, H. Kondo, K. Yamashiti and K. Watanabe, *Jpn. J. Pharmacol*, 36 (1984) 77.
10 E. Tesarova and V. Pacakova, *Chromatographia*, 17 (1983) 269.
11 K. Robards and S. Dilli, *Analyst (London)*, 112 (1987) 933.
12 H. Verhagen, H. H. W. Thijssen and J. C. S. Kleinjans, *J. Chromatogr.*, 422 (1987) 288.
13 E. Burtscher, H. Binder, R. Concin and O. Bobleter, *J. Chromatogr.*, 252 (1982) 167.
14 G. O. Kuhn, J. J. Rollheiser, B. A. Schworer and C. W. Jameson, in D. B. Walters and C. W. Jameson, (Editors), *Chemistry for Toxicity Testing*, Butterworth, Boston, MA, 1984, Ch. 5, p. 59.
15 D. Beker and V. Lovrec, *J. Chromatogr.*, 393 (1987) 459.
16 R. Frankel and I. Slad, *Fresenius' Z. Anal. Chem.*, 331 (7) (1988) 760.

Journal of Chromatography, 505 (1990) 357–364
Elsevier Science Publishers B.V., Amsterdam — Printed in The Netherlands

CHROM. 22 319

Counter-current chromatography of black tea infusions

B. L. WEDZICHA* and M. F. LO
Procter Department of Food Science, University of Leeds, Leeds LS2 9JT (U.K.)
and
T. J. DONOVAN
Lyons Tetley Ltd., 325/347 Oldfield Lane, Middlesex UB6 0AZ (U.K.)
(First received October 18th, 1989; revised manuscript received January 30th, 1990)

SUMMARY

Counter-current chromatography using a multilayer coil planet centrifuge, with solvent system ethyl acetate–butanol–water, permits the separation of black tea infusions into fractions which include pure S_{II} and a mixture of S_I and S_{Ia} thearubigins. Good resolution of several components of the infusion may be achieved in elution times of 1 to 2 h. The appearance of chromatograms is altered on decaffeinating the infusion. The effect of stationary phase composition is considered. Resolution of the peaks improves with butanol content.

INTRODUCTION

Black tea infusions consist of a complex mixture of polyphenols, caffeine, amino acids, proteins, carbohydrates and other components which form minor constituents. The phenolic fraction is regarded as providing most of the characteristics of tea infusions[1–3] and is derived mainly by the oxidation and coupling of naturally occurring flavanols and their gallate esters. Simple products, such as those arising from the combination of two flavanol molecules (*e.g.* bisflavanols, theaflavins) are well characterised but the most abundant polyphenolic fraction, thearubigins, is thought to consist of a complex mixture of polymeric species which has so far proved relatively intractable.

Separation of thearubigins from other components of black tea infusions may be carried out by solvent extraction and precipitation[4,5]. A broad classification of these compounds[4] is those extractable into ethyl acetate, the S_I thearubigins, and those remaining in the aqueous phase, the S_{Ia} and S_{II} thearubigins with the S_{Ia} being more soluble in diethyl ether. A commonly[4] used method for preparation of S_I thearubigins involves exhaustive extraction, with ethyl acetate, of decaffeinated infusions, evaporation of the extract followed by successive steps in which the product is dissolved in acetone and precipitated either with chloroform or diethyl ether. Apart from being lengthy, this procedure does not give rise to a product which is unequivocally that

0021-9673/90/$03.50

present in the original infusion; it is reasonable to expect the polymeric polyphenols, which are also partially oxidised, to be chemically reactive and continuing polymerisation is likely, particularly at the high concentrations present at the time of precipitation. Generally, all that may be guaranteed is that the product is free of low-molecular-weight phenols.

Chromatographic separations of thearubigins have been attempted using, for example, cellulose column chromatography[6], ion-exchange chromatography, paper electrophoresis[7], reversed-phase high-performance liquid chromatography[8] and gel filtration (*e.g.* Pharmacia LH-20)[9]. However, none has proved entirely satisfactory. The main problem is that polyphenolic components of black tea generally have high affinities for the stationary phases and become strongly adsorbed.

One solution to the problem of adsorption in a given mobile–stationary phase combination is to use liquid stationary phases permitting recovery of the components, which had not been eluted, for further separation. This may be achieved by means of counter-current chromatography (CCC); some of the earliest separations of black tea components involved the use of the Craig counter-current apparatus[4], but this technique was limited by the resolution which was possible. A new development in high-speed CCC is the multilayer coil planet centrifuge the principles of which have now been reviewed extensively[10,11].

The purpose of this work was to explore the possibility of the use of CCC for the separation of black tea infusions into polyphenolic fractions and was stimulated by the known tendency of the polymeric fractions to partition into solvents such as ethyl acetate. The use of CCC for the separation of tannins has also been documented[12].

EXPERIMENTAL

Tea infusion

Boiling water (400 ml) was added to a sample of "Lyons Red Label" tea bag tea (4 g) in a Dewar flask and the contents mixed by inverting the flask 10 times after which the mixture was left to stand for 6 min. The spent tea leaves were removed by filtering through a No. 1 sintered-glass funnel and the filtrate analysed after cooling, without delay.

Extraction of caffeine

Methanol (50 ml) was added to the hot tea infusion (200 ml) to prevent formation of "cream" and reduce the tendency for emulsion formation during subsequent extraction. The mixture was extracted with successive amounts (100 ml) of chloroform, each extract being dried (Na_2SO_4) and its absorbance measured at 276 nm (Cecil 292 UV spctrophotometer, Cecil Instruments, U.K.). Extraction was considered complete when the absorbance of the extract was <0.1. The residual chloroform and methanol were removed under reduced pressure (40°C).

Determination of partition coefficient of caffeine

An aqueous solution of caffeine was extracted twice with ethyl acetate (50 ml) in a separating funnel. The absorbance of each extract was measured at 280 nm. The procedure was repeated using a solution of caffeine in ethyl acetate and extracting with water.

Counter-current chromatography

The CCC column was a PTFE tube (*ca.* 130 m × 1.6 mm) with a total volume of *ca.* 310 ml, in an Ito multilayer coil separator–extractor (P.C. Inc., Potomac, MD, U.S.A.) running at 800 rpm. Solvent flow was metered by means of an ACS Series 750 LC pump (Applied Chromatography Services, U.K.) and column effluent monitored at 280 nm using a Cecil 292 UV monitor with an 80-μl, 1-cm path length cell.

Before use the two phases were saturated with each other and their densities measured by weight in a 100-ml volumetric flask. These were used to calculate the mass of the coil from the phase volume ratios to provide an accurate counter-balance for the centrifuge.

Prior to a chromatographic run, the column was filled with stationary phase and the mobile phase eluted from the "head" towards the "tail" of the column if the mobile phase was the more dense or *vice versa* for a less dense mobile phase. The head–tail relationship is referred to an Archimedan screw force which drives all objects in the rotating coil competitively towards the head of the coil. The column was considered to be at equilibrium when droplets of stationary phase no longer appeared in the column effluent and judged by negligible noise on the baseline of the chromatogram.

The column was regularly cleaned by passing methanol followed by aqueous NaOH (1–2%, w/w) and finally washing with water.

Two-dimensional thin-layer chromatography (TLC)

In order to identify the components in each chromatographic peak, fractions corresponding to each peak were combined and concentrated *in vacuo* (40°C). The components were separated on cellulose thin-layer plates (Polygram Cel 300, 20 cm × 20 cm, Macherey-Nagel, F.R.G.) by two-dimensional TLC with butanol–acetic acid–water (4:1:2.2) in the first direction and aqueous acetic acid (2%, v/v) in the second[4]. Phenolic components were revealed by spraying dry plates with ferric chloride (0.15%, w/w) + potassium ferricyanide (0.15%, w/w) in water. The plate was then fixed in 0.1 *M* HCl and excess reagent removed by washing in water.

RESULTS AND DISCUSSION

The distribution of a pure solute component i between two phases α and β is given by the partition (or distribution) coefficient, K, as

$$K = c_i^{\alpha}/c_i^{\beta} \tag{1}$$

where c_i^{α} and c_i^{β} denote the concentrations of that component in each of the phases, respectively. In CCC, the retention volume, V_R, of a solute is related[13] to the partition coefficient by,

$$V_R = V_s/K + V_m \tag{2}$$

where V_m and V_s are, respectively, volumes of the mobile and stationary phases and K is the ratio of solute concentration in the mobile phase to that in the stationary phase (phases α and β, respectively).

If a pure solute is dissolved in one of the phases (volume V^{α}) and solution

extracted twice with a solvent comprising the second phase (volume V^{β}), the partition coefficient may simply be calculated from the concentration of solute in each of the extracts, c_1^{β} and c_2^{β}, respectively, using,

$$K = V^{\alpha}(c_1^{\beta} - c_2^{\beta})/V^{\beta}c_2^{\beta} \tag{3}$$

The concentrations can, of course, be replaced by an appropriate measurable property of the solute, *e.g.* absorbance.

In the first instance water-saturated ethyl acetate was chosen as the stationary phase and ethyl acetate-saturated water as the mobile phase. In order to check the performance of the CCC column, a sample of caffeine (1 ml) was injected onto the column (V_s = 205 ml; V_m = 105 ml) and the position of the peak was found to correspond to K = 1.30. When a caffeine solution in water was extracted twice with ethyl acetate at 20°C, absorbances of the ethyl acetate layers at 280 nm gave K = 1.25. On the other hand, if a solution of caffeine in ethyl acetate was similarly extracted with water the value of K calculated is 0.81, the reciprocal of which, 1.23 corresponds to the values given above. The CCC experiment was, therefore, performing correctly and, in subsequent CCC runs on tea infusions containing caffeine, the position of the caffeine peak was used as a check on performance. The use of caffeine for this purpose was particularly attractive because components with K = 1 run at a retention volume equal to the column volume and caffeine in an ethyl acetate–water system would run with a similar retention volume which ever was the stationary phase.

A typical chromatogram of Lyons Red Label tea bag tea is shown in Fig. 1, component 1 being coloured (yellow) whilst component 2 was caffeine. Further resolution of the peaks was attempted by the addition of butanol to the stationary phase because this solvent has been used in the past for the selective extraction of

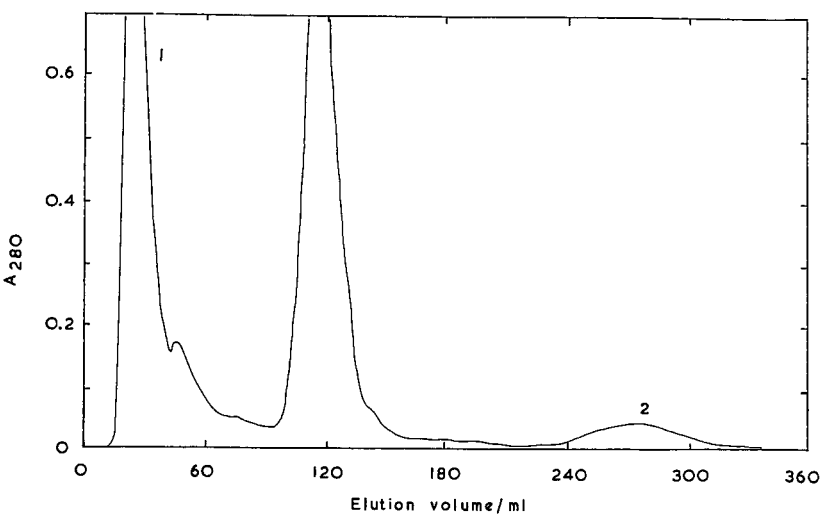

Fig. 1. Counter-current chromatogram of 1% (w/v) infusion of Lyons Red Label tea bag tea. Stationary phase: ethyl acetate-saturated water, 205 ml. Mobile phase: water-saturated ethyl acetate, 105 ml. Flow-rate: 3 ml/min.

TABLE I

EFFECT OF STATIONARY PHASE COMPOSITION ON THE VOLUMES OF MOBILE PHASE (V_m), STATIONARY PHASE (V_s), RETENTION VOLUME (V_R) OF CAFFEINE IN THE CHROMATOGRAM OF A TEA INFUSION AND THE PARTITION COEFFICIENT (K) OF CAFFEINE BETWEEN STATIONARY PHASE AND MOBILE PHASE

Chromatograms were run at 3 ml/min.

Solvent system: butanol–ethyl acetate–water (v/v/v)	V_m *(ml)*	V_s *(ml)*	V_R *(ml)*	K
0:100:100	110	200	270	1.26
10:90:100	98	212	300	1.05
20:80:100	102	208	354	0.83
30:70:100	102	208	398	0.77
40:60:100	130	180	420	0.62
50:50:100	142	168	432	0.56
80:20:100	150	160	434	0.56
100:0:100	180	130	396	0.62

individual thearubigin fractions[4,5]. The main problem with the separation illustrated in Fig. 1 is that the components tended to have too great a bias towards the mobile phase; addition of butanol to stationary phase was expected to increase its polarity and increase its affinity for the polyphenols. The effect of solvent composition of the

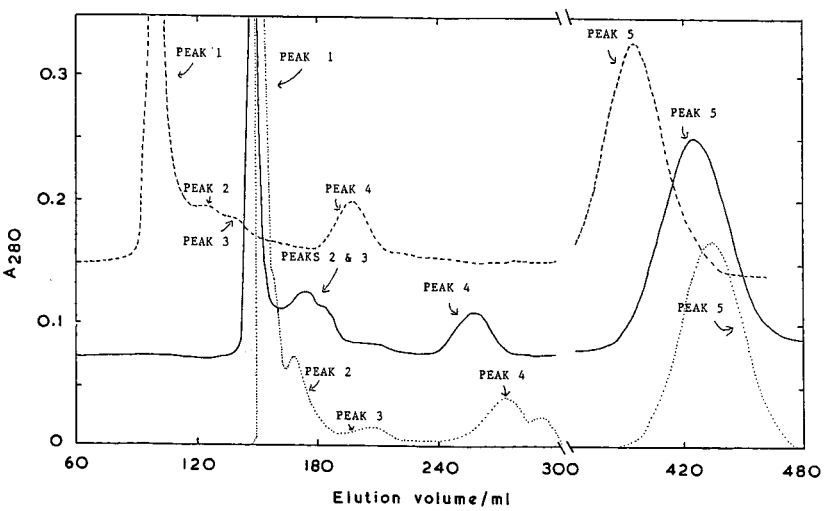

Fig. 2. Counter-current chromatogram of 1% (w/v) infusion of Lyons Red Label tea bag tea. Flow-rate: 3 ml/min. Phase compositions were as follows:

	Mobile (upper phase)	*Stationary (lower phase)*	*System composition: butanol–ethyl acetate–water (v/v/v)*
---------	102 ml	208 ml	30:70:100
———	142 ml	168 ml	50:50:100
.....	150 ml	160 ml	80:20:100

stationary phase on the performance of the CCC experiment and the calculated K values for caffeine are summarised in Table I. The tendency for the value of partition coefficient to decrease with increasing butanol content, and consequent increase of retention volume is consistent with the qualitative prediction of the polarity of the solvent mixtures but the effect is seen up to compositions, butanol–ethyl acetate–water (40:60:100, v/v/v). At higher butanol contents the K value is approximately constant. However, the mobile phase volume continues to increase; it is seen that an approximately 1:2 ratio of mobile:stationary phase for water–ethyl acetate becomes 1.4:1 for water–butanol. Chromatograms obtained at butanol–ethyl acetate–water (30:70:100, v/v/v), (50:50:100, v/v/v) and (80:20:100, v/v/v) are illustrated in Fig. 2 from which it is clear that increase in butanol content improves the resolution of the separation. The identification of the relative positions of specific peaks from one chromatogram to another shown in Fig. 2 was made with the help of chromatograms run at intermediate solvent compositions.

All phase volumes reported here correspond to those measured as the amount of stationary phase displaced by the mobile phase when the system apparently reaches equilibrium at the start of a chromatographic run. The solvent combinations used showed no obvious problems with leakage of stationary phase causing interference to the spectrophotometric measurements, but it was clear that the volume of stationary phase decreased with time during a run. Practical experience has shown that a second chromatogram obtained from the same column filling appears different from the first. It is thought that this may be due to changes in ambient temperature causing desaturation of the mobile phase with respect to stationary phase and dissolution of the latter.

It is well known that polyphenolic components of black tea infusions and particularly thearubigins form complexes with caffeine[14–16]. This binding is known to affect the distribution of caffeine between organic solvents (*e.g.* chloroform) and water and it is possible that complex formation may also affect the CCC running characteristics of the polyphenols themselves. A chromatogram of decaffeinated Lyons Red Label tea bag tea is shown in Fig. 3 which, on comparison with those in Fig. 2, shows the importance of caffeine and the potential consequences of reversible interactions on CCC data.

Identification of the components of individual fractions was carried out by means of two-dimensional TLC[4]. Peak 1 (Fig. 3) gave rise to a streak (R_F 0–0.2) in the butanol–acetic acid–water solvent and showed no mobility in acetic acid. This behaviour is characteristic of S_{II} thearubigins and no components which showed mobility in both solvents could be detected. When the stationary phase was evaporated and the product subjected to TLC, this also was mobile only in the first solvent (R_F 0.6–0.95) indicative of S_I or S_{Ia} thearubigins. Similarly, no components which ran in both solvents could be detected. It is suggested, therefore, that these two fractions consist of thearubigins. Other chromatographic peaks each contained several components which showed mobility in both solvents.

In order to explore the homogeneity of the S_I and S_{Ia} fraction it was decided to analyse the infusion by CCC using the water-rich phase as the stationary phase. Thus components which show a strong bias for the organic phase will be eluted early and it was hoped to see the S_I and S_{Ia} thearubigins close to the solvent front. Fig. 4 shows such a chromatogram with water-saturated organic phase as the mobile phase. Peak 1 was

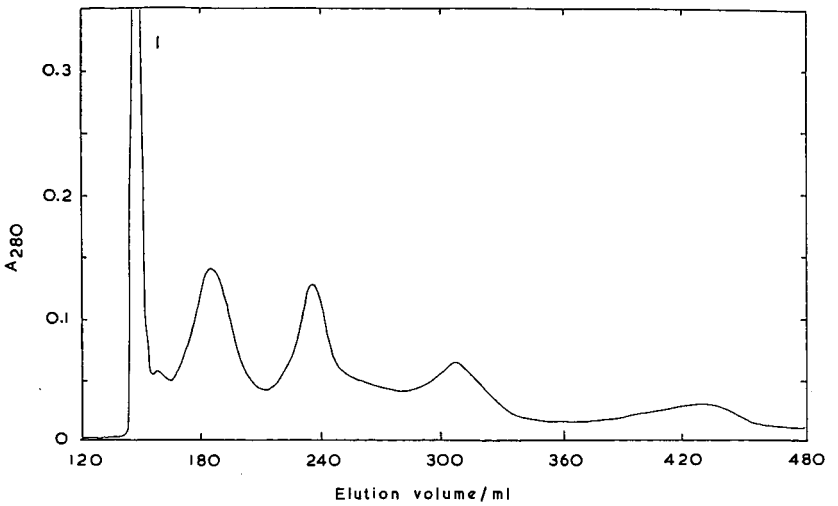

Fig. 3. Counter-current chromatogram of decaffeinated 3% (w/v) infusion of Lyons Red Label tea bag tea. Solvent system: butanol–ethyl acetate–water (50:50:100, v/v/v). Stationary phase: lower phase, 170 ml. Mobile phase: upper phase, 140 ml. Flow-rate: 3 ml/min.

identified as the thearubigin component composed of both types of S_I species whilst peak 2 was due to caffeine. It is significant that in this mode the mobile phase volume is relatively small (90 ml) which implies that components are eluted quickly and that the solvent requirement is small. It is seen that S_I and S_{Ia} thearubigins, or S_{II} thearubigins may be prepared by a single CCC run directly from black tea infusions.

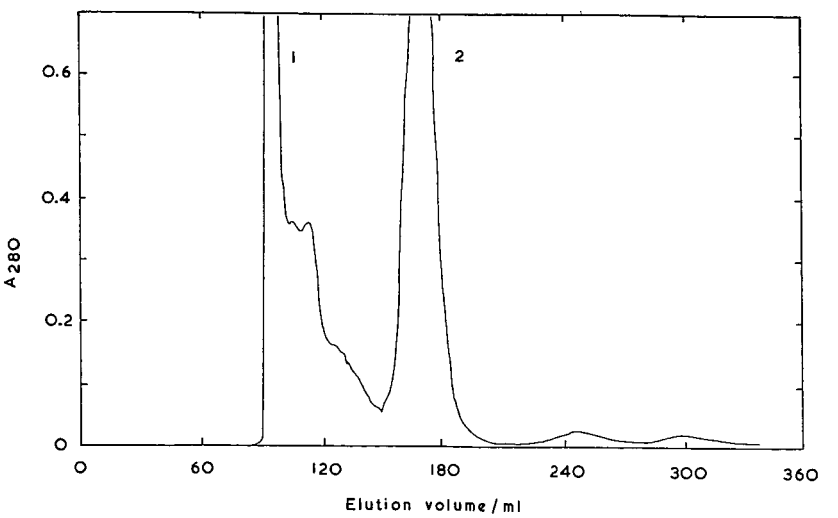

Fig. 4. Counter-current chromatogram of a 1% (w/v) infusion of Lyons Red Label tea bag tea. Solvent system: butanol–ethyl acetate–water (50:50:100, v/v/v). Stationary phase: upper phase, 220 ml. Mobile phase: lower phase, 90 ml. Flow-rate: 3 ml/min.

REFERENCES

1 E. A. H. Roberts, *J. Sci. Food Agric.*, 9 (1958) 212.
2 E. A. H. Roberts, in T. A. Geissman (Editor), *The Chemistry of Flavanoid Compounds*, Pergamon Press, Oxford, 1962, p. 468.
3 W. H. Stahl, *Adv. Food Res.*, 11 (1962) 201.
4 E. A. H. Roberts, R. A. Cartwright and M. Oldschool, *J. Sci. Food Agric.*, 8 (1957) 72.
5 A. G. Brown, W. B. Eyton, A. Holmes and W. D. Ollis, *Phytochemistry*, 8 (1969) 2333.
6 L. Vuataz and H. Brandenberger, *J. Chromatogr.*, 5 (1961) 17.
7 S. I. Ratnaike, *Ph.D. Thesis*, University of Leeds, Leeds, 1980.
8 A. Robertson and D. S. Bendall, *Phytochemistry*, 22 (1983) 883.
9 D. J. Cattell, *Ph.D. Thesis*, University of Leeds, Leeds, 1972.
10 I. A. Sutherland, D. Heywood Waddington and Y. Ito, *J. Chromatogr.*, 384 (1987) 197.
11 Y. Ito, *Trends Anal. Chem.*, 5 (1986) 142.
12 T. Okuda, T. Yoshida, T. Hatano, K. Yazaki, R. Kira and Y. Ikeda, *J. Chromatogr.*, 362 (1986) 375.
13 I. Sutherland, *Lab. Pract.*, 36 (1987) 37.
14 E. A. H. Roberts, *J. Sci. Food Agric.*, 14 (1963) 700.
15 R. F. Smith, *J. Sci. Food Agric.*, 19 (1968) 530.
16 R. L. Wickremasinghe and K. P. Perera, *Tea Quart.*, 37 (1966) 131.

Journal of Chromatography, 505 (1990) 365–374
Elsevier Science Publishers B.V., Amsterdam — Printed in The Netherlands

CHROM. 22 296

Separation and quantitation of phenolic compounds in mainstream cigarette smoke by capillary gas chromatography with mass spectrometry in the selected-ion mode

E. J. NANNI*, M. E. LOVETTE, R. D. HICKS, K. W. FOWLER and M. F. BORGERDING
R. J. Reynolds Tobacco Company, Bowman Gray Technical Center, Winston-Salem, NC 27102 (U.S.A.)
(First received April 14th, 1989; revised manuscript received January 9th, 1990)

SUMMARY

Cigarette smoke condensate is a complex chemical matrix and determination of phenolic compounds in it frequently requires extensive and laborious sample preparation. By utilizing derivatization techniques and capillary column gas chromatography with mass spectrometry in the selected-ion mode, separation and quantitation of selected phenolic compounds found in mainstream cigarette smoke can be accomplished with minimal sample preparation.

This method has been used to determine concentrations of phenol, *o*-cresol, *m*-cresol, *p*-cresol, catechol, resorcinol and hydroquinone in cigarette smoke condensate from a number of commercially available cigarettes and a new cigarette which heats, but does not burn, tobacco. Unlike tobacco-burning cigarettes, levels of the phenolic compounds in the new cigarette smoke are at or below the detection limits for most of the compounds. This result is attributed to the unique design of the new cigarette.

INTRODUCTION

Phenol, cresols and dihydroxybenzenes are well known components of cigarette smoke condensate (CSC). They are formed from pyrolysis of tobacco during the smoking process and contribute to the flavor and aroma of tobacco smoke[1].

Phenolic compounds in tobacco smoke have been determined by a number of techniques[2–15]; however, quantitation of these compounds is often difficult because of the complex chemical matrix in which they occur and the very low concentrations at which they are present. Gas chromatography (GC) has been widely applied to the determination of phenolic compounds but even capillary column GC separations often require preliminary ancillary chromatographic separations or purifications such as solvent partitioning, column chromatography, and/or acid–base extraction. These ancillary purification steps often lead to losses of phenolic constituents, artifactual

0021-9673/90/$03.50

formation of phenols, and the inevitable increase in analytical imprecision. Therefore, an ideal analytical method for these compounds should minimize sample handling and preparation.

A simple, reliable, and accurate method has been developed to determine seven phenolic compounds in CSC with minimal sample preparation. The seven compounds that can be easily separated and quantified by the method are phenol, *o*-cresol, *m*-cresol, *p*-cresol, catechol, resorcinol and hydroquinone.

In short, sample preparation involves collection of CSC by electrostatic precipitation followed by derivatization of the CSC with neat bis-N,O-trimethylsilyl-trifluoroacetamide (BSTFA), which reacts with the phenolic compounds to form their respective mono- and bis-trimethylsilyl (TMS) ethers. The reaction mixture is separated by GC and the TMS ethers are detected using selected-ion mass spectrometry (SIMS). With at least ten-fold excess of BSTFA, silylation (reaction 1) reaches completion within 15 min.

$$\begin{matrix} C_6H_5OH \\ \text{and} \\ C_6H_4(OH)_2 \end{matrix} + CF_3C{=}NTMS \xrightarrow{80°C} \begin{matrix} C_6H_5(OTMS) \\ \text{and} \\ C_6H_4(OTMS)_2 \end{matrix} + CF_3CNH_2 \qquad (1)$$

Moreover, the method cleanly separates *m*- and *p*-cresols, a separation which, heretofore, has not been easily achieved and thus allows for their accurate quantitation during a single analysis.

The method has been applied to determination of seven phenolic compounds in CSC from various commercial cigarettes, 1R4F Kentucky Reference cigarettes, and several prototypes of a new cigarette that heats, but does not burn, tobacco. Unlike the tobacco-burning cigarettes, levels of the phenolic compounds in the CSC from the new cigarette are at or below the detection limits for most of the compounds.

EXPERIMENTAL

Instrumentation and apparatus

A Heinreich Borgwaldt smoking machine (RM 20/CS), central electrostatic smoke trap, and high-tension generator (Model 251) were used to generate and trap CSC for analysis. A Hewlett-Packard (HP) 5890 GC system and HP 5970 mass spectrometry (MS) system with a direct interface were employed to separate and detect components with samples being introduced to the gas chromatograph by an HP 7673 automatic sampler. Control of the gas chromatograph, mass selective detector, and automatic sampler was accomplished using an HP 59770 MS ChemStation. The compounds of interest were separated on a 30 m, narrow bore (0.23 mm I.D.), 5% phenylmethylsilicone capillary column (DB5-30N) available from J & W Scientific. Conditions employed to carry out the GC–MS analyses are found in Table I. The mass spectral ions (*m*/*z*) used for quantitation were 151 and 166 for phenol; 91, 165 and 180 for *o*-, *m*- and *p*-cresol; 149, 185 and 200 for *o*-chlorophenol (internal standard); and 73, 239 and 254 for catechol, resorcinol and hydroquinone.

TABLE I

GC–MS CONDITIONS

GC capillary column:	DB5-30N (30 m × 0.23 mm I.D., 0.25-μm film)
GC oven program:	
Initial temperature:	50°C
Initial time:	3 m
Program rate:	5°C/min
Final temperature:	230°C
Total run time:	55 min
Injector temperature:	225°C
Transfer line temperature:	250°C
Injection mode:	Splitless, 1 μl, 30 s purge
Mass spectra acquisition:	Selected-ion monitoring, 4 groups
Column head pressure:	*Ca.* 15–20 p.s.i.g. (to maintain a flow of *ca.* 30–35 ml/min through the split vent)

Reagents and chemicals

All chemicals were reagent grade quality or better and were used as received without further purification. Phenol (99 + %), *o*-chlorophenol (98 + %) (CAS registry No. 106-48-9), *o*-cresol (99 + %) (95-48-7), *m*-cresol (99%) (108-39-4), *p*-cresol (99 + %) (106-44-5), catechol (99 + %) (120-80-9), resorcinol (98 + %) (106-46-3) and hydroquinone (99 + %) (123-31-9) were all obtained from Aldrich; methyl *tert.*-butyl ether and methylene chloride were purchased from Burdick & Jackson Labs.; and BSTFA (74785-85-6) with 1% trimethylchlorosilane (TMCS) was purchased from either Pierce or Regis.

Preparation of stock solutions and standards

A stock solution (*ca.* 1000 μg/ml) of the phenolic analytes was prepared by accurately weighing approximately 100 mg each of phenol, *o*-cresol, *m*-cresol, *p*-cresol, catechol, resorcinol, and hydroquinone into a 100-ml volumetric flask. The mixture was diluted to the mark with methyl *tert.*-butyl ether. Approximately 100 mg of *o*-chlorophenol were accurately weighed into another 100-ml volumetric flask and diluted to the mark with methyl *tert.*-butyl ether; this solution was the internal standard stock solution. Utilizing both stock solutions calibration standards were prepared as follows. To each of six 5-ml reaction vials 2.5 ml of BSTFA was added. Each vial was sealed with a septum cap and 12 μl of *o*-chlorophenol internal standard stock solution were added by syringe. Appropriate amounts of the analyte stock standard solutions were added by syringe such that concentrations in the reaction vials were 0.1, 0.5, 1.0, 5.0 and 10.0 μg/ml, respectively. The vials were heated overnight at 80°C in a LabLine multi-heating block to ensure completion of the silylation reaction; although as will be discussed in the Results and Discussion section, the reaction is complete within 15 min. After cooling, aliquots from each reaction vial were transferred by syringe to autosampler vials and were used to calibrate the GC–MS system.

Sample preparation

For each cigarette sample, CSC was obtained by smoking twenty cigarettes on

a Heinreich Borgwaldt (HB) 20-port smoking machine. The mainstream smoke particulate phase was condensed by electrostatic precipitation with a HB high-tension generator, a HB electrostatic precipitation (EP) trap, and glass EP tubes. For all samples the Federal Trade Commission (FTC) puffing regimen, *i.e.*, a 35-ml puff of 2 s duration every 60 s, was employed. EP tubes and endcaps were tared prior to smoking and weighed after smoking in order to determine the amount of CSC or wet total particulate matter yielded by the twenty cigarettes. Samples for GC–MS were then otained by accurately weighing *ca.* 25 mg CSC into 5-ml reaction vials, adding 2.5 ml BSTFA and 12 μl *o*-chlorophenol internal standard stock solution to the reaction vials, and heating the reaction vials at 80°C on a LabLine multi-heating block. The reaction vials were heated at least 15 min to ensure completion of the reaction. Aliquots from the reaction vials were then transferred to autosampler GC vials for analysis.

RESULTS AND DISCUSSION

Method validation studies

A number of method validation experiments were conducted prior to the determination of the selected phenolic compounds in CSC. The dynamic range of the method, the ability to separate and detect the compounds of interest, the method precision, and the method accuracy were each assessed to validate the procedure for application to the analysis of CSC. As with any procedure involving reaction chemistry, an accurate measurement of each analyte is possible only if the derivatization process yields quantitative results. Therefore, studies were also conducted to determine the optimum reaction time and the optimum CSC sample size. These studies were conducted both with CSC from a cigarette which burns tobacco and with CSC from a cigarette which only heats tobacco because of the potential for different types of sample matrix effects.

Evaluation of dynamic range and chromatographic resolution of all analytes. Dynamic range of the method was investigated using thirteen cigarettes which yield a wide range of wet total particulate matter. The cigarettes also yield a wide concentration range of phenolic compounds. When samples representative of this range were prepared and analyzed by GC–SIMS, two different MS electron multiplier dynode voltages were employed in order to obtain maximum sensitivity and linear response for the entire range of interest. Hence, two sets of standards were required to construct calibration curves. All calibration curves were linear with r^2 values of 0.998 or better for the seven phenolic compounds in the concentration ranges of 0.1 to 5.0 μg/ml and 1.0 to 50 μg/ml, respectively. The dynode voltage was lowered 400 V relative to the autotune set voltage to record chromatograms of standards in the higher concentration range as compared to those in the lower concentration range. The voltage was set appropriately depending upon the type of sample to be analyzed. Fig. 1 illustrates a typical GC–MS chromatogram of a *ca.* 5 μg/ml standard solution using the higher concentration range settings.

Tables II and III list results for at least six replicate determinations of the seven phenolic compounds in the CSC from thirteen different cigarettes. For all cigarettes studied, except an ultra-low-"tar" tobacco-burning cigarette and the new cigarette that heats, but does not burn, tobacco, calibration curves constructed from

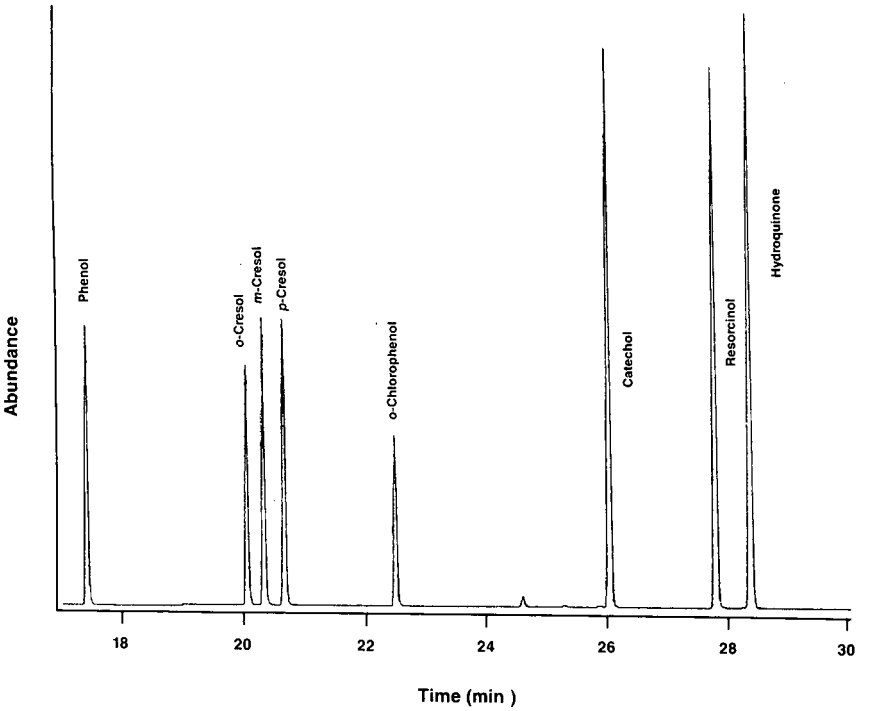

Fig. 1. Chromatogram of set No. 2 standards. Concentration of all standards is 5 μg/ml.

TABLE II

CONCENTRATIONS OF PHENOL AND CRESOLS IN VARIOUS PRODUCTS BY GC–MS

n.d. = None detected. Values in parentheses are the detection limits for the respective compound.

Product	*Concentration (μg/cigarette) ± S.D. (n ⩾ 6)*			
	Phenol	*o-Cresol*	*m-Cresol*	*p-Cresol*
1R4F	7 ± 1	1.8 ± 0.4	1.6 ± 0.4	4.1 ± 0.6
Brand A	12.0 ± 0.7	4.1 ± 0.1	3.92 ± 0.07	7.4 ± 0.3
Brand B	6.1 ± 0.2	1.8 ± 0.3	1.9 ± 0.2	4.0 ± 0.1
Brand C	7.7 ± 0.7	0.33 ± 0.07	1.8 ± 0.1	3.5 ± 0.2
Brand D	17 ± 2	2.0 ± 0.5	3.2 ± 0.3	8 ± 1
Brand E	8.7 ± 0.5	0.9 ± 0.2	1.9 ± 0.1	4.3 ± 0.3
Brand F	7 ± 1	1.8 ± 0.2	2.1 ± 0.1	4.8 ± 0.2
Brand G	3.6 ± 0.1	1.70 ± 0.04	2.01 ± 0.05	3.3 ± 0.1
Brand H[a]	0.26 ± 0.02	n.d. (0.2)	n.d. (0.2)	0.24 ± 0.03
NC-1	0.29 ± 0.05	n.d. (0.2)	n.d. (0.2)	n.d. (0.2)
NC-2	0.25 ± 0.01	n.d. (0.2)	n.d. (0.2)	n.d. (0.2)
NC-3	n.d. (0.1)	n.d. (0.2)	n.d. (0.2)	n.d. (0.2)
NC-4	n.d. (0.1)	n.d. (0.2)	n.d. (0.2)	n.d. (0.2)

[a] Brand H is an ultra-low-"tar" cigarette.

TABLE III

CONCENTRATIONS OF DIHYDROXYBENZENES IN VARIOUS PRODUCTS BY GC–MS

n.d. = None detected. Values in parentheses are the detection limits for the respective compound.

Product	*Concentration (μg/cigarette) ± S.D. (n ⩾ 6)*		
	Catechol	*Resorcinol*	*Hydroquinone*
1R4F	38 ± 5	3.0 ± 0.7	37 ± 5
Brand A	50 ± 1	7.7 ± 0.3	56 ± 2
Brand B	37 ± 2	4,7 ± 0.3	41 ± 1
Brand C	42 ± 4	1.2 ± 0.1	48 ± 7
Brand D	58 ± 3	1.8 ± 0.2	50 ± 4
Brand E	38 ± 1	1.3 ± 0.2	40 ± 1
Brand F	43 ± 2	6 ± 1	40 ± 5
Brand G	45 ± 2	6.3 ± 0.4	46 ± 2
Brand H[a]	3.4 ± 1.7	0.58 ± 0.08	n.d. (0.4)
NC-1	2.1 ± 0.9	0.8 ± 0.6	1.3 ± 0.6
NC-2	1.2 ± 0.4	n.d. (0.4)	n.d. (0.4)
NC-3	0.42 ± 0.06	n.d. (0.4)	n.d. (0.4)
NC-4	0.5 ± 0.1	n.d. (0.4)	n.d. (0.4)

[a] Brand H is an ultra-low-"tar" cigarette.

high-concentration-range standards were used to calculate the amounts of the seven phenolic compounds in the particulate phases. Results for the ultra-low-"tar" and the new cigarette prototypes were determined using the lower-concentration-range standards. The new cigarette prototypes yielded substantially lower amounts of all seven analytes when compared to most tobacco-burning cigarettes. Some new cigarette prototypes, although generally lower, yielded amounts similar to those from the ultra-low-"tar" cigarette. However, the NC-4 new cigarette prototype, which is the culmination of product development efforts to date, yielded substantially less of each analyte detected than did the ultra-low-"tar" cigarette.

Estimation of detection limits. Using the low-range standards and the procedure outlined above, detection limits for the seven phenolic compounds by GC–SIMS were calculated and are listed in Table IV. The detection limit for a particular compound

TABLE IV

DETECTION LIMITS FOR ANALYSIS OF PHENOLIC COMPOUNDS BY GC–MS

Compound	*Amounts (μg/cigarette)*
Phenol	0.1
o-Cresol	0.2
m-Cresol	0.2
p-Cresol	0.2
Catechol	0.3
Resorcinol	0.4
Hydroquinone	0.4

according to the procedure of Miller and Miller[16] is defined as the analyte concentration giving a signal equal to the blank signal plus three standard deviations of the blank. The *y*-intercept and associated standard deviation calculated from regression analysis of the standard calibration curve are used as an estimate of the blank signal and the standard deviation of the blank. Note that many compounds in the CSC from the new cigarette prototypes were not detected according to these parameters (see Table II).

Method precision. The precision of the method was estimated using CSC from 1R4F Kentucky Reference cigarettes. These cigarettes are standard reference cigarettes which can be purchased from the University of Kentucky. In this study, ten aliquots of 1R4F CSC were derivatized and analyzed for the seven compounds. Results are shown in Table V. For all compounds good precision was obtained with relative standard deviation ranging from *ca.* 1 to 5%.

CSC sample size and optimum reaction time. The amount of BSTFA employed to derivatize CSC was chosen after first considering the expected hydroxyl content of CSC and a need to minimize sample dilution which in turn maximizes sensitivity. In preparation of CSC samples 2.5 ml of neat BSTFA was employed. This amount of BSTFA was chosen based on estimates of the number of hydroxyl substituents expected in new-cigarette CSC. Because of the unique cigarette design, the new-cigarette CSC is very different from that of other cigarettes. New-cigarette CSC is composed of *ca.* 80–90% water and glycerol[17,20] and, as such, is much richer in hydroxyl functionality than is CSC from cigarettes which burn tobacco. Thus, for a *ca.* 25 mg sample of new-cigarette CSC it was calculated that 2.5 ml BSTFA should provide at least 10 × as much reagent as would be required to react with all hydroxyl substituents in the samples. In order to maximize sensitivity, the reaction is performed in neat BSTFA without addition of any other solvent.

To corroborate these estimates and to ensure that sufficient BSTFA was utilized in the method, a series of samples containing *ca.* 25, 50, 75, and 100 mg of new cigarette and 1R4F CSC, respectively, were reacted with 2.5 ml BSTFA. Figs. 2 and 3 illustrate, on a per-cigarette basis, the effects of increasing the amounts of either new cigarette or 1R4F CSC on the determination of the phenolic compounds. As the figures show, no or very little effect was found; however, we did discover that with 1R4F smoke aerosols 2.5 ml BSTFA was insufficient to derivatize all of the catechol and hydroquinone in samples greater than 25 mg. The reason for this is that aliquots of 1R4F aerosol greater

TABLE V

PRECISION STUDY

Compound	*Relative standard deviation (%)*
Phenol	3.8
o-Cresol	4.9
m-Cresol	2.4
p-Cresol	3.8
Catechol	4.6
Resorcinol	5.4
Hydroquinone	1.4

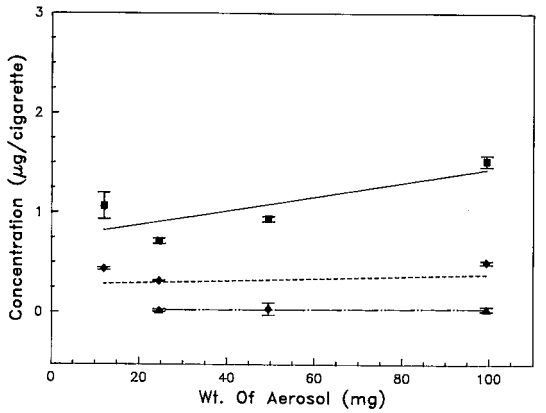

Fig. 2. Effect of varying new-cigarette smoke condensate upon yield of resorcinol (▲), hydroquinone (◆) and catechol (■). Error bars depict 95% confidence intervals.

than 25 mg are not soluble in 2.5 ml BSTFA and catechol and hydroquinone are not extracted sufficiently into this solvent. With a 25-mg aerosol sample 2.5 ml BSTFA are sufficient to consume all the phenolic hydroxyl functions and to drive the reaction to completion.

Since this method involves reaction chemistry, experiments were performed in order to understand the time required for the reaction to reach completion. For these experiments the new cigarette and 1R4F cigarettes were employed and *ca.* 25 mg of mainstream smoke aerosols from the cigarettes were reacted with 2.5 ml BSTFA at 80°C for various lengths of time. Fig. 4 is a representative plot of the amounts of dihydroxybenzenes found in 1R4F aerosols *versus* reaction time. The figure reveals that the reaction is complete within 15 min and that carrying out the derivatization for as long as 18 h has no ill-effects on the analyses. As one might suspect, the TMS ethers of the phenolic compounds are stable, even at temperatures as high as 80°C for 24 to 48 h.

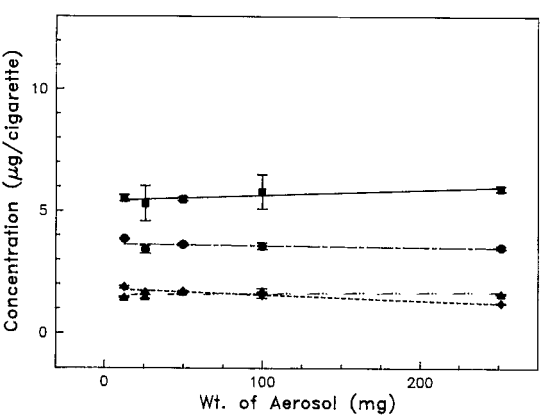

Fig. 3. Effect of varying 1R4F Kentucky Reference cigarette smoke condensate upon yield of *m*-cresol (●), *p* -cresol (▲), *o*-cresol (◆) and phenol (■). Error bars depict 95% confidence intervals.

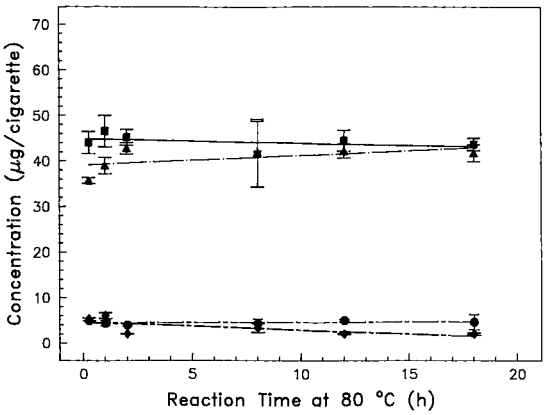

Fig. 4. Effect of varying reaction time of 1R4F Kentucky Reference cigarette smoke condensate with excess BSTFA upon yield of hydroquinone (▲), resorcinol (◆), phenol (●) and catechol (■). Error bars depict 95% confidence intervals.

Comparison of results using different methods

In order to probe the accuracy of the present GC–MS method, results were compared with those obtained by two other methods used at the R. J. Reynolds Tobacco Co.: a liquid chromatography–fluorescence (LC–F) method[18] and a GC method[19]. Fig. 5 compares results obtained by the GC–MS method with the LC–F method. Unlike the GC–MS method the LC–F method cannot separate *m*-cresol from *p*-cresol. Because the GC–MS and LC–F methods yield comparable results, we believe that the GC–MS method yields an accurate measure of phenolic compound concentrations in the mainstream particulate matter. Note there are small differences in amounts of the seven compounds found by each technique: the LC–F method results in slightly higher concentrations of phenolic compounds in the CSCs as compared to the GC–MS method. For the determination of phenol only, both the

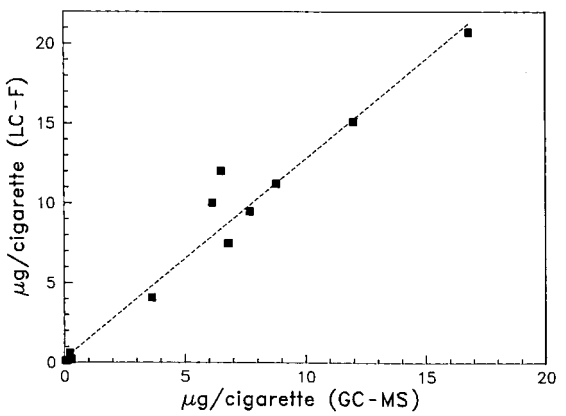

Fig. 5. Comparison of yields of phenol from thirteen cigarette samples by a liquid chromatography–fluorescence detection method (LC–F) with the method that uses BSTFA derivatization followed by gas chromatography–mass spectrometry (GC–MS).

GC–MS and LC–F methods were compared with another GC method used at the R. J. Reynolds Tobacco Co.[19] and good agreement was found among the three methods for amounts of phenol found in the CSCs.

CONCLUSIONS

An accurate and reliable method for analysis of seven phenolic compounds in CSC has been developed. This method involves BSTFA derivatization followed by capillary GC and MS of the TMS ethers. Although the method includes derivatizations, sample preparation is minimal. The method has been successfully applied to determination of seven phenolic compounds in CSC from thirteen different cigarettes. Amounts of the seven phenolic compounds in CSC from all of the tobacco-burning cigarettes in this investigation correlated to FTC "tar" values. Although the amounts of CSC from new cigarettes that heat, but do not burn, tobacco are comparable to those of low-"tar" cigarettes, the concentrations of the seven phenolic compounds in the new cigarette smoke aerosols are 10 to 100 × less than that from tobacco-burning cigarettes.

ACKNOWLEDGEMENTS

We would like to thank Dr. R. A. Lloyd and Mr. J. A. Giles for many helpful suggestions in the development of this method and in the preparation of this manuscript. We would also like to thank Mr. C. H. Risner and Analytical Services at the R. J. Reynolds Tobacco Co. for sharing results obtained by their methods, liquid chromatography–fluorescence and gas chromatography for phenol, respectively.

REFERENCES

1 A. G. Kallianos, *Recent Adv. Tob. Sci.*, 2 (1976) 61.
2 M. E. Snook and P. J. Fortson, *Anal. Chem.*, 15 (1979) 1814.
3 M. E. Snook, P. J. Fortson and O. T. Chortyk, *Tob. Sci.*, 24 (1980) 30.
4 W. J. Chamberlain, M. E. Snook and J. L. Baker, *Anal. Chim. Acta*, 111 (1979) 235.
5 W. A. Court, *J. Chromatogr.*, 130 (1977) 287.
6 G. A. Smith and D. A. King, *Chem. Ind.*, (1964) 540.
7 K. D. Brunnemann, H. C. Lee and D. Hoffmann, *Anal. Lett.*, 9 (1976) 939.
8 M. R. Guerin and G. Olerich, *Tob. Sci.*, 20 (1976) 44.
9 S. Ishiguro, S. Cato, S. Sugawara and Y. Kajuraki, *Agr. Biol. Chem.*, 40 (1976) 977.
10 M. Legtonen, *J. Chromatogr.*, 202 (1980) 413.
11 R. W. Souter and R. H. Bishara, *J. Chromatogr.*, 140 (1977) 245.
12 A. DiCorcia, *J. Chromatogr.*, 80 (1973) 69.
13 P. Buryan, J. Macak and V. M. Nabivach, *J. Chromatogr.*, 148 (1978) 203.
14 J. Hrivnak and J. Macak, *Anal. Chem.*, 43 (1971) 1039.
15 J. Hoshika, *J. Chromatogr.*, 157 (1978) 277.
16 J. C. Miller and J. N. Miller, *Statistics for Analytical Chemistry*, Wiley, New York, 1984.
17 M. F. Borgerding, R. D. Hicks, J. E. Bodnar, D. M. Riggs, E. J. Nanni, G. W. Fulp, Jr., W. C. Hamlin and J. A. Giles, *J. Assoc. Off. Anal. Chem.*, submitted for publication.
18 C. H. Risner and S. Cash, R. J. Reynolds Tobacco Company, personal communication.
19 J. M. Martin and H. L. Gilleland, R. J. Reynolds Tobacco Company, personal communication.
20 *Chemical and Biological Studies On New Cigarette Prototypes That Heat Instead Of Burn Tobacco*, R. J. Reynolds Tobacco Company, Winston-Salem, NC, 1988.

Journal of Chromatography, 505 (1990) 375–384
Elsevier Science Publishers B.V., Amsterdam — Printed in The Netherlands

CHROM. 22 268

Pyrolytic analysis of complex stabilizers in polypropylene

M. ALEXANDRA ROBERSON
Amoco Fabrics and Fibers, 260 The Bluffs, Austell, GA 30001 (U.S.A.)
and
GABOR PATONAY*
Department of Chemistry, Georgia State University, Atlanta, GA 30303 (U.S.A.)
(Received October 31st, 1989)

SUMMARY

Pyrolysis gas chromatography was used to determine high-molecular-weight stabilizers in polypropylene. Chimassorb 944®, Tinuvin 622® and Sandostab P-EPQ® were pyrolyzed and characteristic fragments were separated on a non-polar capillary column. After the retention times of characteristic fragments had been determined, polypropylene extract was analyzed to identify the limitations of using a single characteristic peak and retention time data for quantitative determination of stabilizers. The use of nitrogen–phosphorus detection decreases interference from fragments that do not contain nitrogen or phosphorus. There is no significant interference from the extraction solvent or the polymer matrix.

INTRODUCTION

Quantitative and qualitative determination of complex stabilizers in polypropylene has been the focus of interest[1–22]. Successful separation of complex stabilizers requires a well balanced compromise between resolution, separation temperature and analysis time. Thus, a large amount of effort has gone into the characterization of each of these variables.

Stabilizers are added to polymers to protect the resin from a variety of degradation processes. Antioxidants are used to prevent degradation caused by atmospheric oxygen[3]. UV absorbers are added to polymers to decrease photodegradation induced by sunlight or other UV-rich light source[4]. A large number of antioxidants and UV absorbers of different chemical compositions are available to meet these special requirements. Since these additives are present in the polymer matrix at low concentrations, the analysis of polymer extracts has been used commonly[5].

Polymer additives may be classified by their functional group. Accordingly, hindered amines, phosphites, quenchers, hindered phenols, benzotriazoles and benzophenones[3–8] may be mentioned. The typical molecular weight for these stabilizers may be in the range of 200–2000 and >2000 for polymeric additives. In most cases high-molecular-weight stabilizers produce longer outdoor life for most polymers[4].

0021-9673/90/$03.50

The qualitative and quantitative analysis of additives can be achieved by chromatographic methods. Supercritical fluid chromatography (SFC)[2], gas chromatography (GC) or liquid chromatography are frequently used. SFC is a sensitive method, however, it is limited by the high molecular weight. A high-resolution SFC technique was reported recently[2] for the analysis of additives of molecular mass up to 1178. Universal or sensitive selective detect ion methods, *e.g.* flame ionization detection (FID) or nitrogen–phosphorus detection (NPD) make GC techniques particularly attractive. However, thermal instability may limit the analysis of high-molecular-weight stabilizers. Typically, GC techniques are not feasible for molecules with a molecular weight larger than 800. Although high-performance liquid chromatography (HPLC) does not have the molecular weight limitation, it lacks a detection system comparable to that of GC techniques[2,19–21]. Nevertheless, GC is a frequently used method, in spite of its limitations by the high molecular weight and thermal instability of many complex stabilizers[6]. This thermal instability may be utilized when pyrolysis (Py) is employed to generate characteristic fragments.

Unfortunately, to date, such applications have been substantially hindered by the lack of suitable analytical methodology. The concentration of characteristic fragments is too low at lower pyrolytic temperature, while at higher temperature, the fragmentation would produce too many peaks for a universal detection method. The application of selective GC detectors can improve pyrolytic determination of polymeric stabilizers. We have recently begun to apply Py–GC techniques for the analysis of complex stabilizers in polypropylene. The pyrolysis is performed at relatively low temperature to achieve characteristic fragmentation.

Characteristic fragments containing nitrogen and phosphorus are detected by NPD. Chimassorb 944®, Tinuvin 622® and Sandostab P-EPQ® were chosen for the development of this method. To illustrate typical chemical structures of polymeric stabilizers, two structures are depicted in Fig. 1.

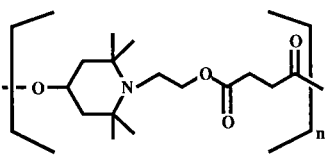

TINUVIN 622

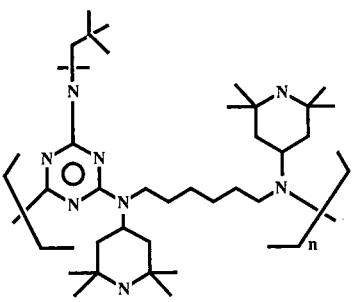

CHIMASSORB 944

Fig. 1. Typical chemical structures of complex stabilizers[6].

Determination of these stabilizers is especially difficult because of their polymeric structure. Sandostab P-EPQ was analyzed by SFC–Fourier transform infrared spectroscopy (FT-IR) using microscopic accessories and solvent eliminator interface[2]. However, this method may not be feasible for Tinuvin 622 and Chimassorb 944. Examples in which Py–GC has been used to achieve analysis of complex stabilizers in polymers are limited in the literature. A Py–GC method using packed columns was described previously[1] for the analysis of Tinuvin 622 and Chimassorb 944. Complicated sample preparation, high retention times, overlapping characteristic peaks and low recovery (72–94%) limited the practicality of this method.

Presently, we wish to report the results of our research in which the sample preparation consists of only a one-step extraction and the recovery rate was 89.9–99.4%. The pyrolysis temperature was optimized to produce nitrogen- or phosphorus-containing characteristic fragments, which were separated on a capillary column and detected by NPD.

EXPERIMENTAL

Chemicals

The antioxidant Sandostab P-EPQ was manufactured by Sandostab and the UV stabilizers Chimassorb 944 and Tinuvin 622 were obtained from Ciba-Geigy. Polypropylene was used as a polymeric matrix. The solvents toluene and methylene chloride were purchased from Fisher Scientific in analytical grade.

Apparatus

The chromatographic system consisted of a Hewlett-Packard Model 5890A with FID and NPD while a Quadrex capillary aluminum clad column was used for separation (25 m × 1.7 μm I.D.). The pyrolysis unit was a Scientific Glass Engineering Pyrojector. The operation conditions of GC were: detector temperature 260°C, oven temperature, initial 70°C, rate 5°C/min, final 130°C, splitless injector temperature 240°C. The pyrojector temperature was set at 800°C. Helium was used as the carrier gas for the pyrojector. The flow-rates were set as follows: column 2.43 ml/min, injector purge 6 ml/min, pyrojector purge 1.5 ml/min. Data were analyzed using Turbochrom software. Data were stored on hard disk and were recalled for data analysis.

Sample preparation

An appropriate sample size (0.2–2.0 g) was obtained from the polymer and was then transferred into 50 ml of toluene. The solvent was refluxed for 5 min and the polymer was then precipitated by adding methylene chloride. The solution was filtered to remove the precipitated polymer. Most of the solvent was then evaporated to concentrate the stabilizer solution using dry nitrogen purging.

Calibration solutions

Several dilutions of Tinuvin 622, Chimassorb 944 and Sandostan P-EPQ solutions were prepared in toluene. These solutions were injected in the same way as the polymer extracts into the pyrojector-GC system.

TABLE I

RETENTION TIME OF CHARACTERISTIC STABILIZER PEAKS

Stabilizer	*Retention time (min)*
Chimassorb 944	1.26 ± 0.02
Tinuvin 622	1.10 ± 0.02
Sandostab P-EPQ	2.36 ± 0.02

RESULTS AND DISCUSSION

Initially, toluene solutions of the additives in Table I were injected into the pyrojector to determine the retention times of the fragments. As mentioned previously, NPD and FID were used to detect the separated fragments. The FID chromatograms obtained showed very complex fragmentation (Fig. 2). The fragments were not well resolved and different additives had fragments of similar retention times. The large solvent peak also limited the usefulness of the chromatogram. Using NPD, on the other hand, decreased the number of peaks considerably. Typical pyrograms of Tinuvin 622, Chimassorb 944 and Sandostab P-EPQ are shown in Figs. 3, 4 and 5, respectively. All the fragments are well resolved and demonstrate the capability of capillary Py–GC–NPD for analysis of complex polymer additives within a few minutes. Peak retention times were found to be very reproducible for identification purposes. This may be attributed to proper temperature control of the pyrojector and column. No cross interference was found when all three additives were injected simultaneously.

After careful examination of the chromatograms, one characteristic peak was chosen for each stabilizer (Table I). The area of these peaks was found to be proportional to the amount of stabilizers. Calibration curves were obtained for each stabilizer by using the peak with 1.28 ± 0.02 min retention time for Chimassorb 944, 1.10 ±

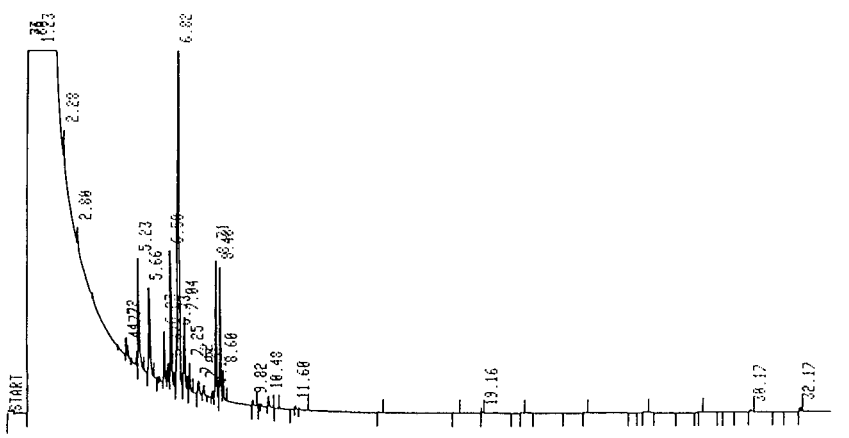

Fig. 2. Typical chromatogram of complex fragmentation of Chimassorb 944 detected by FID. 800°C.

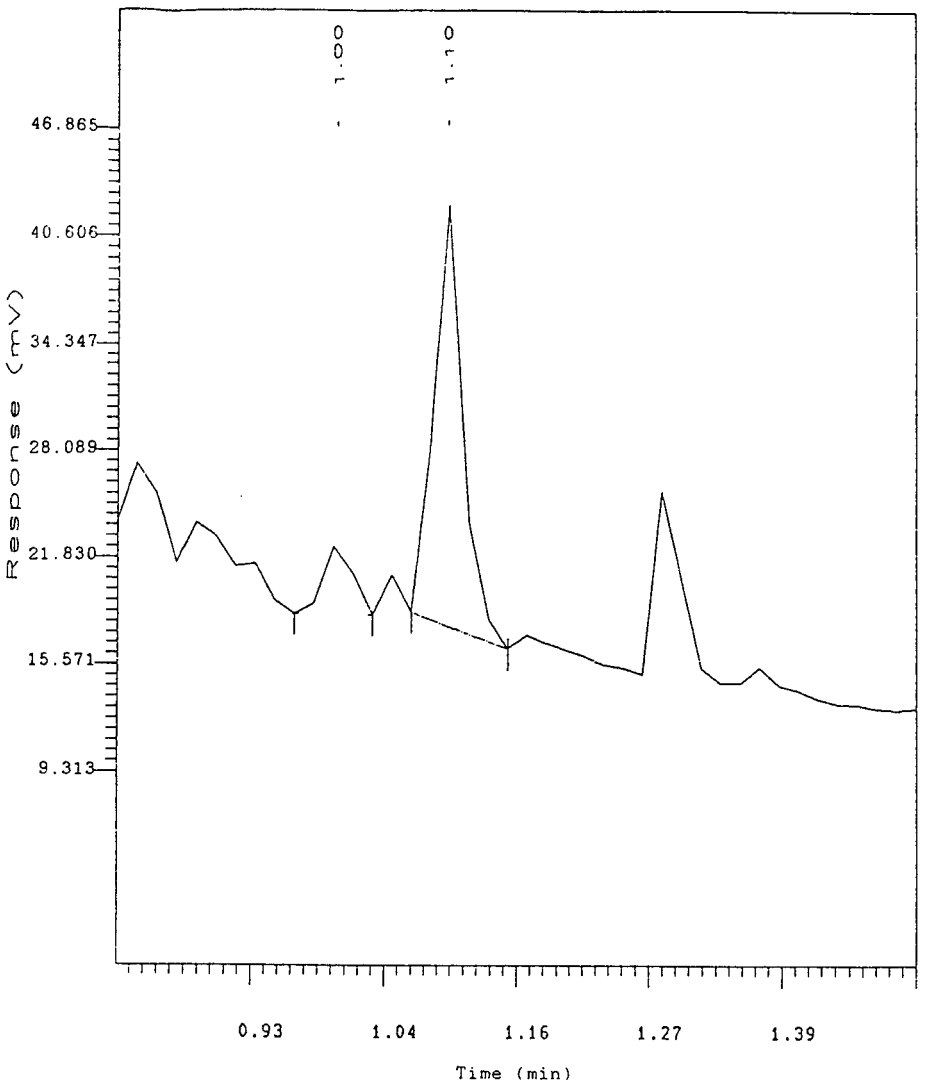

Fig. 3. Typical pyrogram of Tinuvin 662.

0.02 min for Tinuvin 622 and 2.36 ± 0.02 min for Sandostab P-EPQ. The relatively short retention times of these characteristic peaks permitted fast analysis and decreased interference.

Calibration solutions were injected into the pyrojector–GC system and calibration curves were obtained for each stabilizer by plotting concentration *versus* peak area of the characteristic peak. Solutions in toluene were made to obtain concentrations of 50–10 000 ppm. The calibration curves for Chimassorb 944, Tinuvin 622 and Sandostab P-EPQ are depicted in Fig. 6, 7 and 8, respectively.

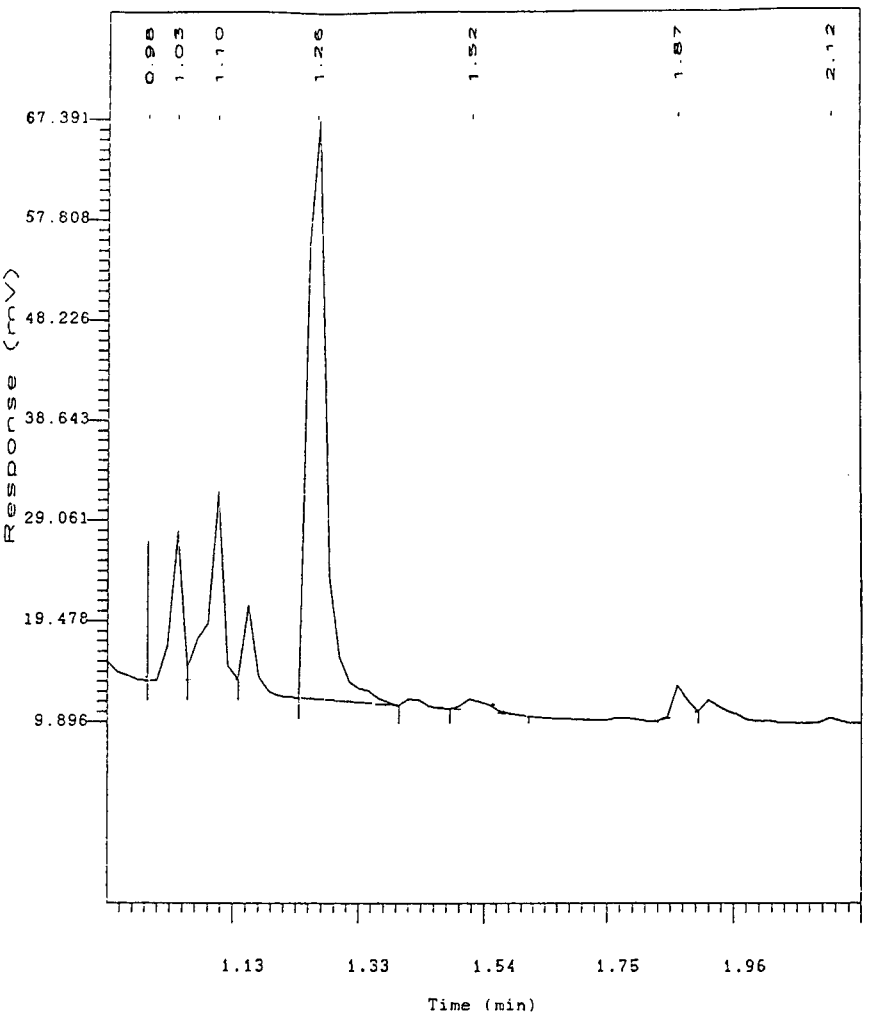

Fig. 4. Typical pyrogram of Chimassorb 944.

The polymer extraction samples, prepared as described in the Experimental section, were quantitized by the standard addition method. The results obtained for different amounts of samples are shown in Tables II, III and IV. Detection limits less than 50 ppm were achieved with this method. The method resulted in a wide dynamic range with no significant deviation observed from linearity up to 10 000 ppm. For concentrations higher than 10 000 ppm, dilutions of the final extract should be made to preserve the linearity.

The preliminary results reported here demonstrate the analytical power of combining capillary Py–GC with the selectivity of NPD for the quantitative and qualitative analysis of complex high-molecular-weight and polymeric stabilizers. This method has been successfully used for the analysis of unknown concentrations of

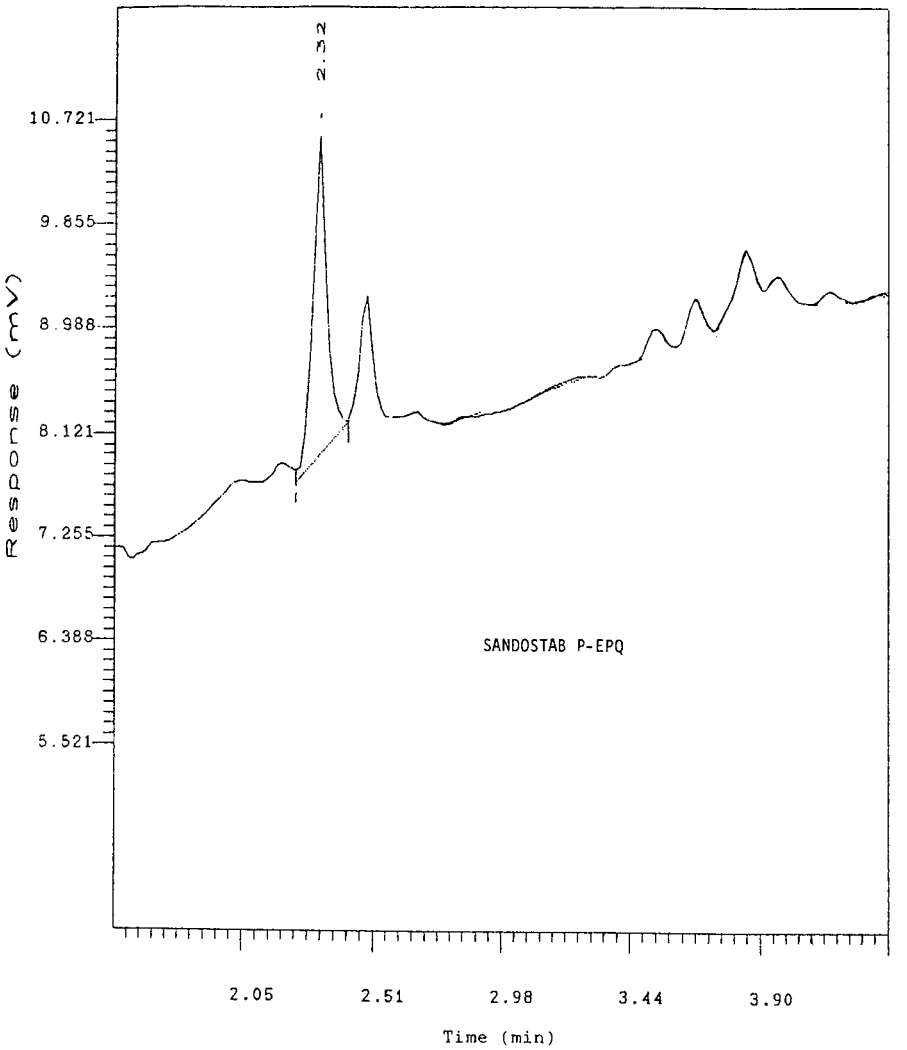

Fig. 5. Typical pyrogram of Sandostab P-EPQ.

TABLE II

RECOVERY OF TINUVIN 622 FROM POLYPROPYLENE

Target (ppm)	*Concentration found (ppm)*	*Recovery (%)*
10 230	8790	86.0
7350	7189	97.8
5500	5323	96.7
218	210	96.3

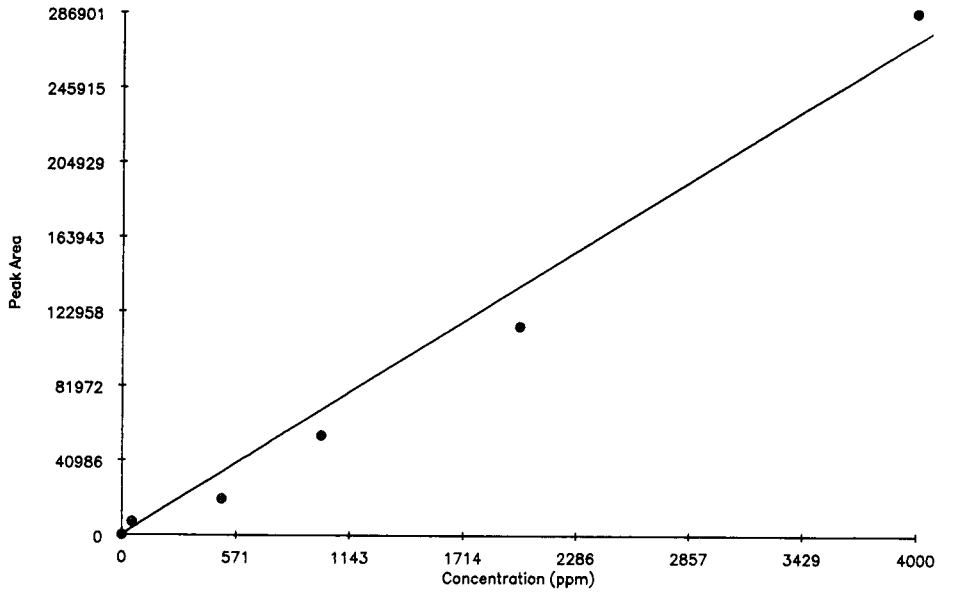

Fig. 6. Calibration curve for Chimassorb 944.

complex polymeric additives in polypropylene samples. This method should create significant industrial interest because of the simplified sample preparation requirements, the short analysis time and the good recovery rate. Further studies are necessary to determine the extent of interference of other complex stabilizers.

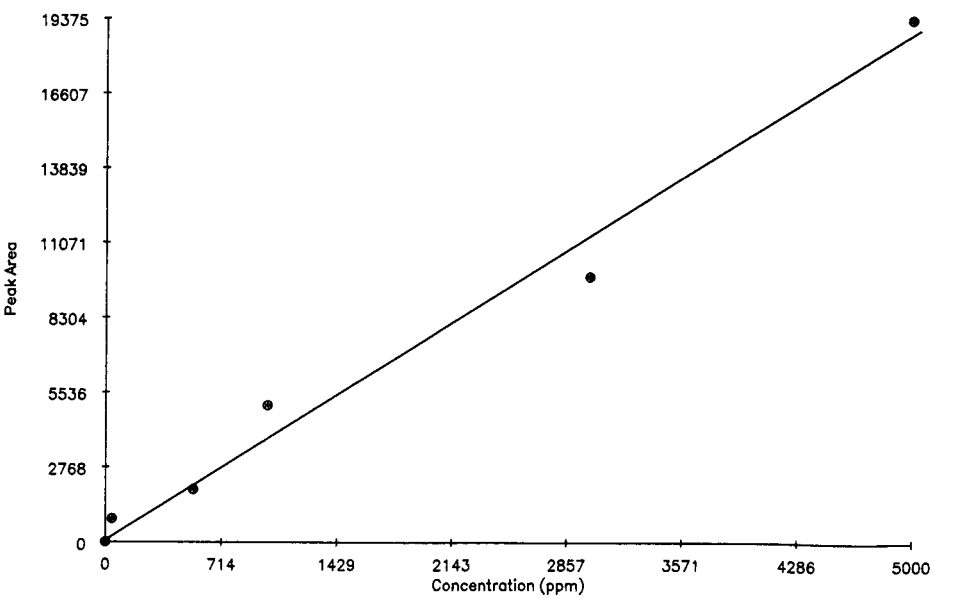

Fig. 7. Calibration curve for Tinuvin 622.

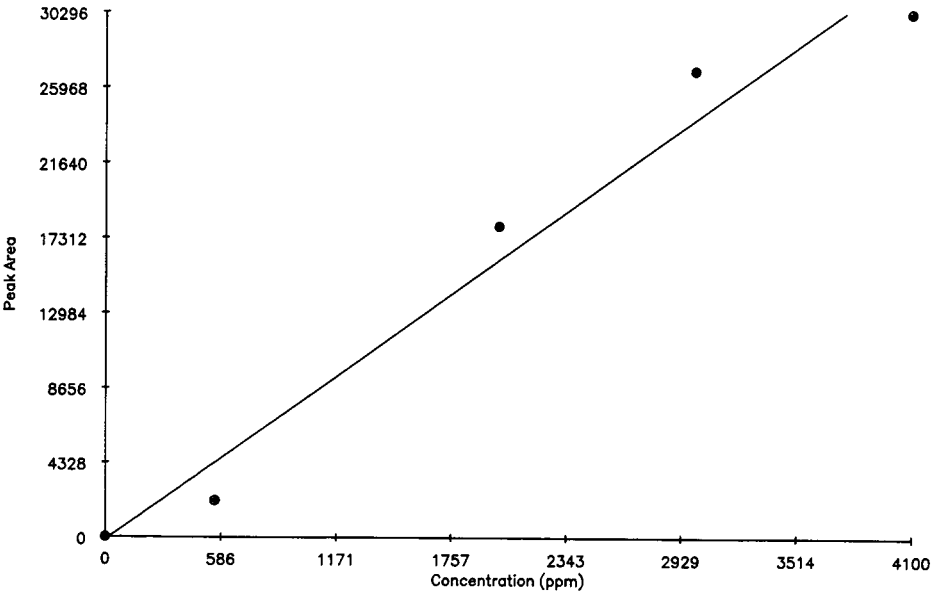

Fig. 8. Calibration curve for Sandostab P-EPQ.

TABLE III

RECOVERY OF CHIMASSORB 944 FROM POLYPROPYLENE

Different dilutions of 8000 and 550 ppm were analyzed.

Target (ppm)	*Concentration found (ppm)*	*Recovery (%)*
8000	7947	99.9
8000	8214	102.7
550	530	96.4
550	528	96.0
50	46	92.0

TABLE IV

RECOVERY OF SANDOSTAB P-EPQ® FROM POLYPROPYLENE

Target (ppm)	*Concentration found (ppm)*	*Recovery (%)*
10 280	9230	89.8
9030	8831	97.9
1300	1298	99.8
1180	1122	95.0

REFERENCES

1 P. Orme and P. Perlstein, *J. Chromatogr.*, 325 (1985) 87–93.
2 M. W. Raynor, K. Bartle, I. Davies, A. Williams, A. Clifford, J. Chalmers and B. Cook, *Anal. Chem.*, 60 (1988) 427–433.
3 M. Dexter, in H. F. Maek (Editor), *Encyclopedia of Polymer Science and Engineering*, Vol. 2, Wiley, New York, 1985, pp. 371–420.
4 G. R. Lappin, *Encyclopedia of Polymer Science and Technology*, Vol. 14, Interscience, New York, 1971, pp. 125–147.
5 B. N. Norbert (Editor), *Encyclopedia of Polymer Science and Technology*, Vol. 12, Interscience, New York, 1970, 725–737.
6 *Kirk–Othmer Encyclopedia of Chemical Technology*, Vol. 23, 1983, Wiley, New York, 615–627.
7 A. Hoff and S. Jacobsson, *J. Appl. Polym. Sci.*, 29 (1984) 465–480.
8 R. Juvet, J. Smith and K. Li, *Anal. Chem.*, 44 (1971) 49–56.
9 W. Blum and L. Damascemol, *J. High Resolut. Chromatogr. Chromatogr. Commun.*, 10 (1987) 472–476.
10 M. Krull, A. Kogerman, O. Kirret, J. Plogan, A. V. Yudin and A. S. Schevchenk, *Eesti NSV Tead. Akad. Toim. Recm.* 27 (3) (1978) 171–175.
11 C. Vogt and S. Kapila, *J. Chromatogr. Sci.* 17 (1979) 546–550.
12 Y. Gurvich, E. L. Styskin and A. A. Grinberg, *Kauch. Rezina*, 30 (1971) 53–54.
13 P. Perlstein, *Anal. Chim. Acta*, (1983) 155–173.
14 R. Basher, K. Chakbraborty and G. Scott *Polym. Degradation Stab.*, 4 (1982) 1.
15 N. S. Allen and A. Parkinson, *Polym. Degradation Stab.*, 4 (1982) 161.
16 N. S. Allen, A. Parkinson J. L. Gardet and J. Lemaire, *Polym. Degradation Stab.*, 5 (1983) 35.
17 W. Freitag, *Anal. Chem.*, 316 (1983) 495–501.
18 P. A. D. T. Vimalasiri, J. K. Haken and R. P. Burford, *J. Chromatogr.*, 300 (1984) 303–355.
19 D. Munteanu, A. IsFan, C. IsFan and I. Tincul, *Chromatographia*, 23 (1987) 7–14.
20 M. A. Holney and W. A. Dark, *J. Chromatogr. Sci.*, 18 (1980) 655–659.
21 F. Sevini and B. Marcato, *J. Chromatogr. Sci.*, 260 (1983) 507–512.
22 Santyo, *Brit. Pat.*, 1 196 224 (Jap. priority 22.61967).

Journal of Chromatography, 505 (1990) 385–394
Elsevier Science Publishers B.V., Amsterdam — Printed in The Netherlands

CHROM. 22 267

Multivariate optimization of a gas–liquid chromatographic analysis of fatty acid methyl esters of blackcurrant seed oil

URBAN OLSSON*, PETER KAUFMANN and BENGT G. HERSLÖF
*Department of Analytical Chemistry, University of Stockholm and *LipidTeknik, P.O. Box 15200, S-104 65 Stockholm (Sweden)*
(Received October 16th, 1989)

SUMMARY

A method was investigated and optimized for the analysis of fatty acid methyl esters using blackcurrant (*Ribes nigrum*) seed oil as a model. This was done with a total of eight runs, utilizing experimental design to explore the experimental domain, a multivariate ranking function to rank the chromatograms and response-surface methods to locate an optimum.

INTRODUCTION

As a part of our general programme on the analysis of natural lipid mixtures, we wanted to investigate the multivariate optimization of various types of lipid analyses. The objective of this particular study was to use this approach in the routine analysis of fatty acid methyl esters (FAMEs) from vegetable oils by gas–liquid chromatography (GLC).

Numerous reports on the analysis of FAMEs by GLC have appeared[1–4] and there is a wide selection of suitable commercially available capillary columns with different types of stationary phases. Owing to the many options and applications, a systematic approach to find the best performance in a specific case was needed. In order to investigate optimization based on multivariate analysis, we wanted a model system containing naturally occurring fatty acids and some unusual isomers, and blackcurrant (*Ribes nigrum*) seed oil was selected for this purpose. This oil has a relatively high content (12–20%)[5] of γ-linolenic acid [18:3 (n − 6)], which is an isomer of the common α-linolenic acid [18:3 (n − 3)].

Sample introduction

The use of an on-column injection technique in FAME analysis places high demands on sample purity, as particles or by-products from the derivatization of the acylglycerols may be deposited on the column inlet and in time cause degradation of the bonded phase. By installing a precolumn, *i.e.*, a retention gap, between the injector and the column inlet, these problems can be overcome.

0021-9673/90/$03.50

Precolumns

The retention gap is a deactivated and uncoated section of fused silica, which causes little or no retention of the solute molecules. The uncoated precolumn should be deactivated with a reagent that promotes good wettability of the inner column surface by the injected solvent, otherwise droplets containing solute molecules may form, causing peak broadening and split peaks[6–10]. The length of the retention gap is determined by the maximum length of the flooded zone reached by the solvent when injected below its boiling point. The length of the flooded zone is determined by the volume and type of solvent injected. Involatile sample impurities will be adsorbed on the column wall within the flooded zone of the retention gap, which in time might cause an increase in retention of the precolumn[11]. Eventually, the involatile components will migrate onto the analytical column if the retention gap is not exchanged or shortened periodically.

The connection between the retention gap and the analytical column is a critical part of the installation. By use of a conical glass seat, a so-called press-fit connector[12], a seal is established between the connector and the polyimide sheath of the fused-silica tubing. The connection will grow stronger with time and for most applications it may be considered as an integrated part of the column.

Experimental design

Factorial design allows for a very effective coverage of the experimental domain in comparatively few experiments. By varying all of the experimental factors simultaneously, according to a predetermined plan, the main effects of the variables and their interactions can be determined. Many different types of experimental design have been described, differing mainly in the type or accuracy of information wanted. Fractional factorials at two levels are very economical in the initial step for screening large numbers of potentially important factors. When the important factors have been determined as described above, full factorials at three levels or a central composite design can be used to optimize the experimental conditions[13,14].

The multivariate ranking function

The above approach implies the need for an objective measure of experimental behaviour, *i.e.*, a means of ranking the resulting chromatograms quantitatively, and for this a multivariate chromatographic ranking function was used. In this study the "chromatographic resolution statistic" (*CRS*) was applied[15]. This function is devised to take resolution, peak distribution and total analysis time into account and thus provides an objective and quantitative criterion for the ranking of chromatograms.

Optimization

Response-surface methods can be used to obtain a graphical representation of the response (optimization parameter) over the experimental domain. A model can be developed that relates the design variables to a measure of experimental behaviour. This can be done by using regression methods, either linear or non-linear, depending on the nature of the inherent relationship. In the case where the effects of more than one experimental variable are being considered, multivariate regression methods must be used. We have used multiple linear regression to model the experimental data and to generate the response surface in the optimization step[16].

EXPERIMENTAL

Study design

A two-level full factorial design in three variables was used in this study. This design allows one to see main and first-order effects in eight (2^3) experiments.

The variables chosen in this study were injector temperature, oven programming rate and injection volume. The design matrix and experimental domain are shown in Table I.

Each row in the design matrix describes an individual run, these runs being executed in random order to avoid any time-dependent trends in systematic variation. This experimental design was applied to the analysis of the standard mixture and the blackcurrant seed oil.

TABLE I

CHROMATOGRAPHIC VARIABLES AND *CRS* VALUES

Injection temperature (°C)	*Rate (°C/min)*	*Injection volume (µl)*	*Design*	*CRS values*	
				Standard[a]	*Sample*[b]
130	3	1.5	+ + +	8.66	7.25
130	3	0.5	+ + −	9.35	6.84
80	3	1.5	− + +	15.24	12.38
130	1	1.5	+ − +	16.14	12.52
80	3	0.5	− + −	16.67	13.08
130	1	0.5	+ − −	17.54	13.28
80	1	1.5	− − +	30.12	−[c]
80	1	0.5	− − −	40.20	39.04

[a] Reference mixture ME 32.
[b] Blackcurrant seed oil, methyl esters.
[c] Missing value: see text.

Chromatographic resolution statistic

We used the chromatographic resolution statistic (*CRS*) to rank the chromatograms objectively and quantitatively in this study:

$$CRS = \{\sum[(R_i - R_{opt})^2/R_i(R_i - R_{min})^2] + \sum(R_i)^2/a\bar{R}^2\} (T_f/n)$$

where R_i = resolution element for the ith peak pair, R_{opt} = chosen value of optimum resolution, R_{min} = chosen value of minimum resolution, $\bar{R}^2$ = square of mean resolution, a = total number of resolution elements, T_f = retention time of final peak and n = total number of peaks.

The *CRS* function was initially applied to a standard mixture of methyl esters in equal amounts, in order to obtain a uniform peak height for subsequent resolution measurements.

Materials

Cold-pressed blackcurrant seed oil was obtained from Bio Lipid (Falköping,

Sweden). The blackcurrants had been grown in Sweden. A standard mixture of methyl esters (ME 32) containing methyl palmitate (16:0), methyl stearate (18:0), methyl oleate (18:1), methyl linoleate (18:2) and methyl linolenate (18:3) in equal amounts was purchased from Larodan (Malmö, Sweden). The concentration of the mixture injected was 1.0 mg/ml. Dimethyl carbonate, isooctane, hexane and methanol were all of analytical-reagent grade from Merck (Darmstadt, F.R.G.).

Derivatization procedure

The conversion of acylglycerols to methyl esters by alcoholysis is widely employed[17]. In this reaction, which is suitable for materials low in free fatty acids (<3%), an alkali methanolysis procedure is used. It requires the use of two

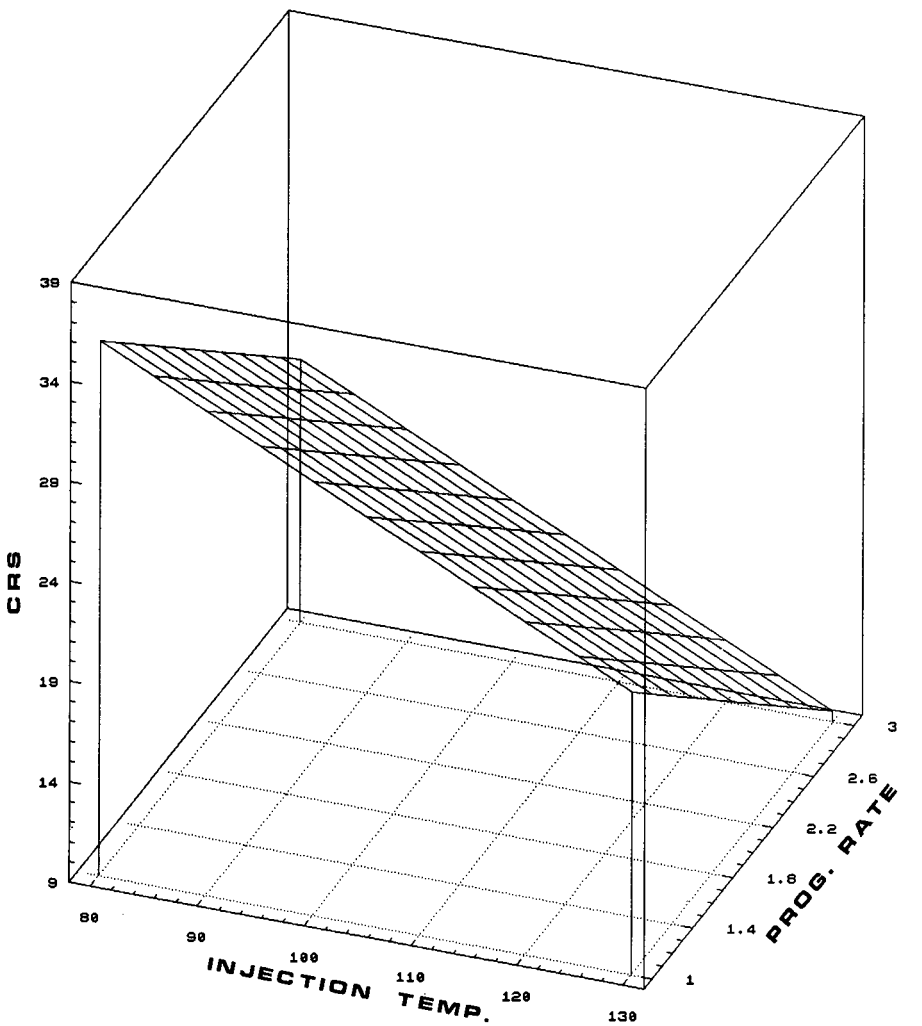

Fig. 1. Response surface of the design variables injection temperature and temperature programming rate plotted against the *CRS* values.

pre-prepared stock solutions: solution A, dimethyl carbonate–isooctane (1:1, v/v); and solution B, 2.3 g of sodium, cut clean under hexane, added in small pieces to 200 ml of methanol. Solution B was stable for several weeks at room temperature.

A 10-mg amount of oil was placed in a test-tube with a PTFE-lined screw-cap. The oil was dissolved in 2 ml of solution A, then 1 ml of solution B was added. The test-tube was sealed and shaken vigorously for 30 s, then left for 15 min to ensure complete methylation of the acylglycerols. After addition of 3 ml of water, the tube was shaken vigorously for 5 s and thereafter centrifuged at 2 *g* for 1 min. The organic (upper) layer containing the methyl esters was recovered and diluted 1:4 with isooctane for analysis by GLC.

Gas–liquid chromatography

The analysis of the methyl esters was conducted on a Varian (Walnut Creek, CA, U.S.A.) Model 3500 capillary gas chromatograph, equipped with a Varian temperature-programmable on-column injector and a capillary flame ionization detector.

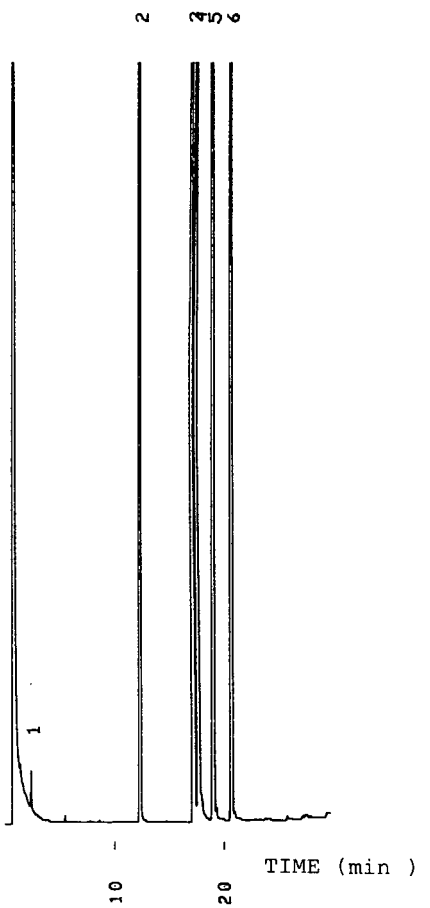

Fig. 2. Gas chromatogram of a five-component mixture of methyl esters. Design: (+ + +). Conditions as in Table I. Peaks, from left ro right: 16:0, 18:0, 18:1, 18:2, 18:3.

A DB-WAX fused-silica capillary column (30 m × 0.32 mm I.D.) coated with polyethylene glycol with film thickness 0.25 μm (J&W Scientific, Folsom, CA, U.S.A.) was used.

Between the injector body and the analytical column a precolumn, *i.e.*, retention gap (1.5 m × 0.32 mm I.D.), deactivated with diphenyltetramethyldisilyl (DPTMS), purchased from MEGA Capillary Columns Laboratory (Legnano, Italy), was installed. The two sections of fused silica were joined together with a press-fit connector (Mikro Kemi, Uppsala, Sweden).

Temperature programming was started at either 80 or 130°C, the latter representing hot on-column injection[18–20]. The temperature programming rate was set at 1 or 3°C/min and the volume injected was either 0.5 or 1.5 μl (Table I). The carrier gas was helium and the flow-rate was 3.0 ml/min throughout the investigation.

The temperature of the detector was 250°C. The detector signals were recorded with a C-R3A electronic integrator (Shimadzu, Kyoto, Japan).

RESULTS AND DISCUSSION

The overall objective of this study was to develop an optimum GLC method for the analysis of the fatty acid methyl esters of lipid materials of various origin, *e.g.*, blackcurrant seed oil. To this end the utility of experimental design in method

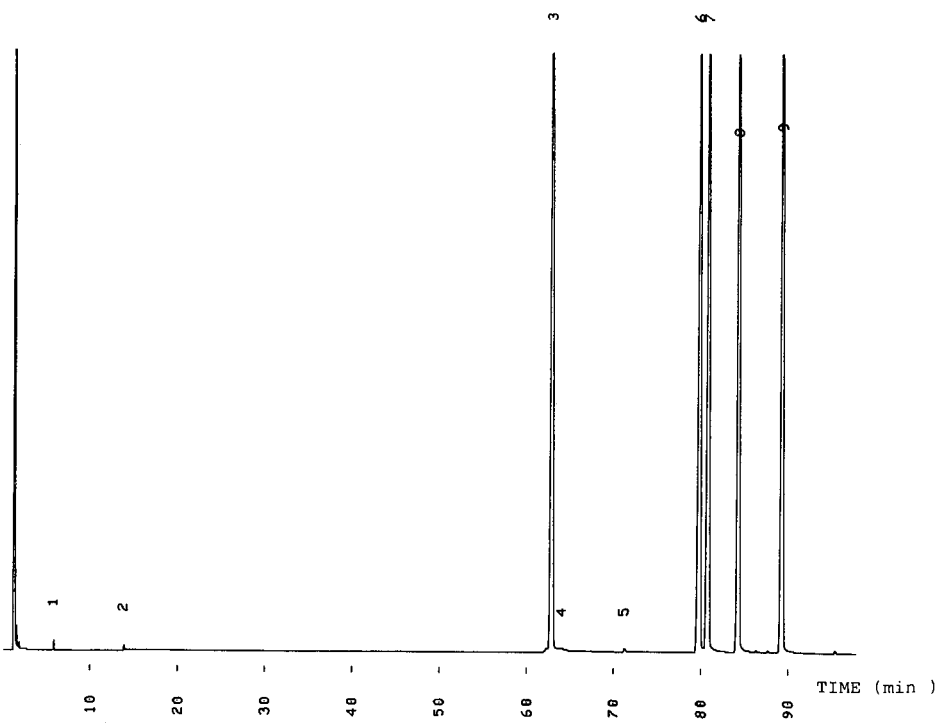

Fig. 3. Gas chromatogram of a five-component mixture of methyl esters. Design: (– – –). Conditions as in Table I. Peaks, from left to right: 16:0, 18:0, 18:1, 18:2, 18:3.

development was explored by employing a two-level full factorial experimental design in three variables to elucidate the effect of the selected experimental variables on the chromatography.

The results of this study can be summed up in the response surface plot (Fig. 1), where the *CRS* values for each individual chromatographic run are plotted against two

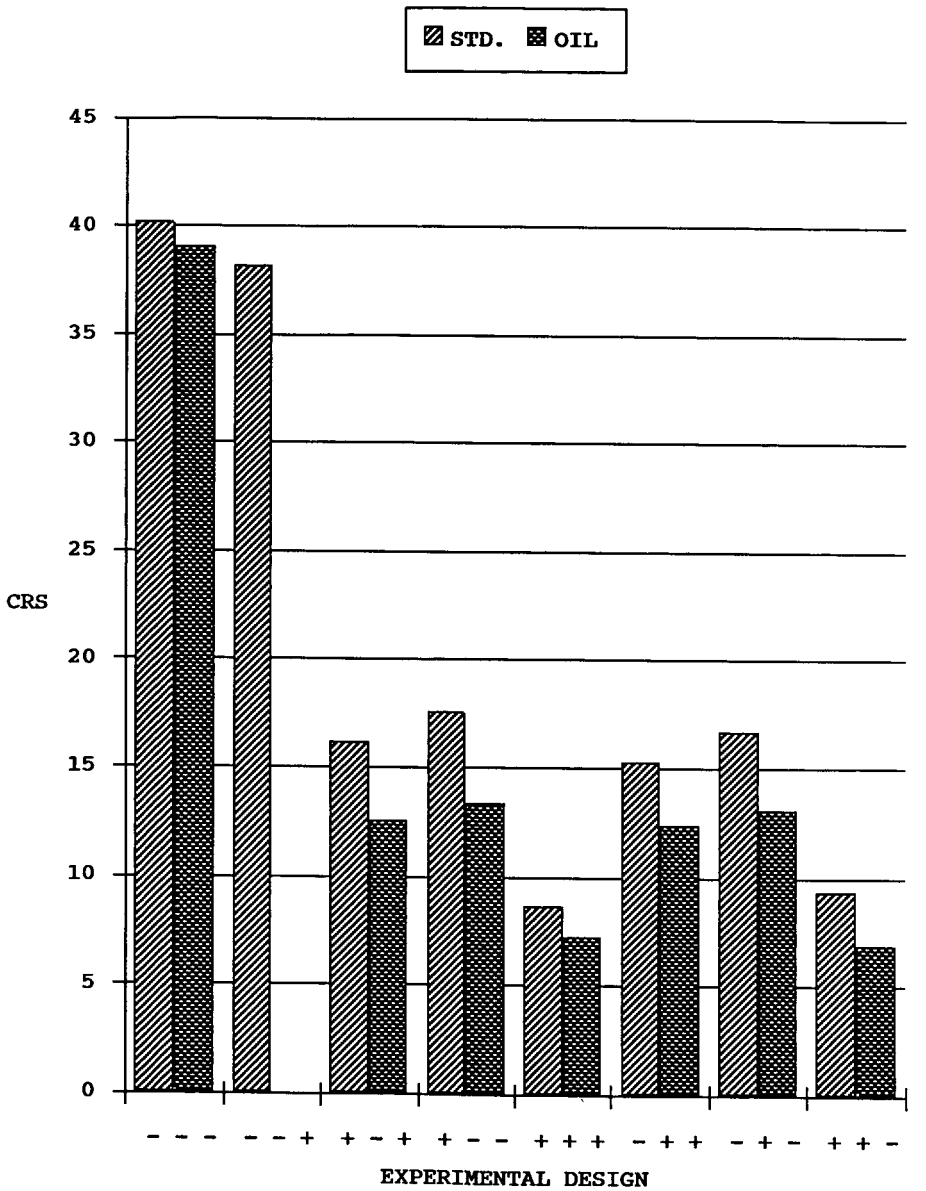

Fig. 4. Histogram over the *CRS* values of all runs from the standard mixture and blackcurrant seed oil. Missing value: see text.

of the design variables, injection temperature and temperature programming rate. The independent variables (Table I) are related to the dependent variable (*CRS* values) by a multiple linear regression model. This model explained 80% of the total variance present in the data.

The chromatograms at the extreme points of the experimental design in the standard runs are shown in Fig. 2 (design: + + +) and Fig. 3 (design: − − −). The *CRS* function as it is described, penalizes lengthy analysis times which account for the high *CRS* value (40.20) of run (− − −) in Fig. 3. However, this can be compensated for by adjusting the $1/T_f$ term, *i.e.*, total analysis time. The results of the *CRS* function for all the chromatographic runs are shown graphically in Fig. 4. The missing value for the oil sample in this figure (design: − − +) where the oleic acid isomers[18:1 (n − 9) and 18:1 (n − 7)] were only partially resolved, is due to the fact that the *CRS* function is not defined as R_i approaches R_{min}.

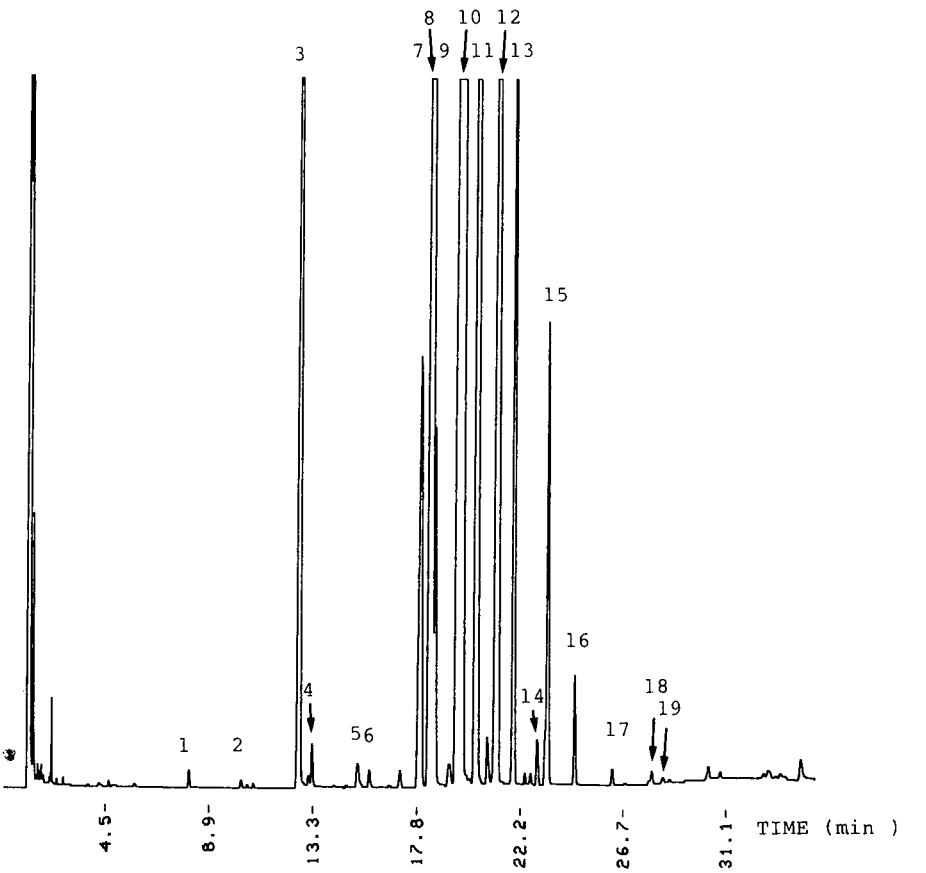

Fig. 5. Gas chromatogram of the methyl esters of blackcurrant seed oil. Design: (− + +). Conditions as in Table I. Peaks: 1 = 14:0; 2 = 15:0; 3 = 16:0; 4 = 16:1 (n − 7); 5 = 17:0; 6 = 17:1; 7 = 18:0; 8 = 18:1 (n − 9); 9 = 18:1 (n − 7); 10 = 18:2 (n − 6); 11 = 18:3 (n − 6); 12 = 18:3 (n − 3); 13 = 18:4 (n − 3); 14 = 20:0; 15 = 20:1 (n − 9); 16 = 20:2 (n − 6); 17 = 20:4 (n − 6); 18 = 22:0; 19 = 22:1.

According to the definition of the *CRS* function, the best chromatographic performance is attained when the function shows a minimum. The minimum in this experimental domain is at the maximum of the two design variables, *i.e.*, injection temperature and temperature programming rate 130°C and 3°C/min, respectively (Fig. 1). The chromatogram at this optimum point (design: + + −) for blackcurrant seed oil clearly reflects this behaviour (Fig. 5). All peaks are well resolved with adequate separation for the oleic acid isomers [18:1 (n − 9) and 18:1 (n − 7)], in a total analysis time of 32 min.

Optimum conditions are obtained for the oil sample with an injected volume of 0.5 μl, programming rate 3°C/min and initial column and injector temperature 130°C. The injection volume was found to be the least important of the design variables, its only noticable contribution being in the blackcurrant seed oil optimization.

The experimental domain can easily be extended by including in the design other variables that are believed to pertain to the chromatographic problem. This will make the procedure more time consuming, however, because more runs are demanded as the number of runs required for a full factorial at k levels and n factors is runs = k^n.

In Table II the fatty acid composition of the cold-pressed blackcurrant seed oil is given and in Fig. 5 a chromatogram of this oil, run with the optimized method, with a retention gap installed, is shown. The level of 18:3 (n − 6) is lower than that reported

TABLE II

FATTY ACID COMPOSITION (%) OF BLACKCURRANT SEED OIL

Fatty acid	*Composition (%, w/w)*	*S.D. (n = 4)*	*Peak No.*
14:0	tr[a]		1
15:0	tr		2
16:0	5.3	0.02	3
17:0	tr		5
18:0	1.5	0.01	7
20:0	0.1	0.00	14
22:0	tr		18
16:1 (n − 7)	tr		4
17:1[b]	0.2	0.04	6
18:1 (n − 9)	14.7	0.02	8
18:1 (n − 7)	0.7	0.01	9
20:1 (n − 9)	1.0	0.01	15
22:1[b]	tr		19
18:2 (n − 6)	47.0	0.09	10
20:2 (n − 6)	0.2	0.01	16
18:3 (n − 6)	12.2	0.02	11
18:3 (n − 3)	13.2	0.02	12
18:4 (n − 3)	2.7	0.01	13
20:4 (n − 6)	tr		17
Unidentified	0.9	0.29	

[a] tr = Trace (<0.10%).
[b] Positions not determined.

by other workers[5]. This might be due to climatological factors affecting the growth of the blackcurrants used.

CONCLUSIONS

By utilizing experimental design, a multivariate evaluation procedure such as the *CRS* function and response surface methods, a limited number of experiments are needed to reach at least a local optimum. This is a very efficient and time-saving approach in method development or in the validation of already established analytical procedures.

ACKNOWLEDGEMENTS

This work was supported by the Karlshamns Research Foundation. The authors express their gratitude to Professor Rolf Carlson, University of Umeå, for helpful discussions.

REFERENCES

1 W. W. Christie, *Gas Chromatography*, Oily Press, Ayr, 1989.
2 H. T. Badings and C. De Jong, *J. Chromatogr.*, 279 (1983) 493.
3 C. D. Bannon, J. D. Craske and A. E. Hilliker, *J. Am. Oil Chem. Soc.*, 62 (1985) 1501.
4 J. D. Craske and C. D. Bannon, *J. Am. Oil Chem. Soc.*, 64 (1987) 1413.
5 H. Traitler, H. J. Willie and A. Studer, *J. Am. Oil Chem. Soc.*, 65 (1988) 755.
6 K. Grob and B. Schilling, *J. Chromatogr.*, 391 (1987) 3.
7 K. Grob, Jr., *J. Chromatogr.*, 328 (1985) 55.
8 K. Grob, Jr. and H. P. Neukom, *J. Chromatogr.*, 323 (1985) 237.
9 K. Grob, Jr. and R. Müller, *J. Chromatogr.*, 244 (1982) 185.
10 S. Adam, *J. High Resolut. Chromatogr. Chromatogr. Commun.*, 6 (1983) 36.
11 K. Grob, Jr., H. P. Neukom and M.-L. Riekkola, *J. High Resolut. Chromatogr. Chromatogr. Commun.*, 7 (1984) 319.
12 E. R. Rohwer, V. Pretorius and P. J. Apps, *J. High Resolut. Chromatogr. Chromatogr. Commun.*, 9 (1986) 295.
13 S. N. Deming and S. L. Morgan, *Experimental Design: a Chemometric Approach*, Elsevier, Amsterdam, 1987.
14 G. E. P. Box, W. G. Hunter and J. S. Hunter, *Statistics for Experimenters*, Wiley, New York, 1978.
15 T. D. Schlabach and J. L. Excoffier, *J. Chromatogr.*, 439 (1988) 173.
16 D. L. Massart, B. G. M. Vandeginste, S. N. Deming, Y. Michotte and L. Kaufman, *Chemometrics: a Textbook*, Elsevier, Amsterdam, 1988.
17 F. D. Gunstone and F. A. Norris, *Lipids in Foods, Chemistry, Biochemistry and Technology*, Pergamon Press, Oxford, 1983, pp. 76–81.
18 R. F. Lang, *Anal. Chem.*, 58 (1986) 1259.
19 F.-S. Wang, H. Shanfield and A. Zlatkis, *J. High Resolut. Chromatogr. Chromatogr. Commun.*, 6 (1983) 471.
20 R. P. Snell, J. W. Danielson and G. S. Oxborrow, *J. Chromatogr. Sci.*, 25 (1987) 225.

Journal of Chromatography, 505 (1990) 395–401
Elsevier Science Publishers B.V., Amsterdam — Printed in The Netherlands

CHROM. 22 304

Characterization of the thermal decomposition products of the sulfonylurea herbicide chlorsulfuron

AUSTIN R. LONG, BAHRAM CHARKHIAN, LILY C. HSIEH, CHARLES R. SHORT and STEVEN A. BARKER*

Department of Veterinary Physiology, Pharmacology and Toxicology, School of Veterinary Medicine, Louisiana State University, Baton Rouge, LA 70803 (U.S.A.)

(First received September 7th, 1989; revised manuscript received January 19th, 1990)

SUMMARY

Gas chromatographic injection port thermal decomposition of chlorsulfuron resulted in two volatile decomposition products (2-amino-4-methoxy-6-methyl-1,3,5-triazine and 2-chlorobenzenesulfonamide) which were characterized by gas chromatography and gas chromatography–mass spectrometry. Quantitation of chlorsulfuron as its volatile thermal decomposition product 2-amino-4-methoxy-6-methyl-1,3,5-triazine was accomplished by gas chromatography–nitrogen–phosphorus detection analysis and the linearity of standard curves so obtained was independent of injection volume (0.5–3 μl) and injection port temperature (230–270°C) for the concentration range examined (62.5–1000 ng/ml).

INTRODUCTION

Chlorsulfuron {2-chloro-N-[[(4-methoxy-6-methyl-1,3,5-triazin-2-yl)amino]-carbonyl]benzenesulfonamide} is the active ingredient in DuPont's pre- and post-emergence herbicide. It is a member of the sulfonylurea class of compounds and finds application in wheat, oat and barley production[1]. The toxicological aspects of chlorsulfuron have been published[1].

Biological extracts containing sulfonylurea residues may be quantitated by analytical techniques such as high-performance liquid chromatography (HPLC)[2,3] utilizing photoconductivity detection or by gas chromatography (GC) of volatile methylated derivatives[4,5]. Chlorsulfuron has been analyzed by both approaches[6–8]. However, reaction conditions required to form volatile methylated chlorsulfuron derivatives necessary for GC analyses must be carefully controlled to avoid the formation of multiple derivative products or hydrolysis[4], both of which can make quantitative determinations difficult. The HPLC analyses of nanogram (ng/ml) levels of chlorsulfuron utilizing ultraviolet (UV) detection in the low UV range (210–230 nm) may be accomplished, provided the sample is free from interfering chromophores[9].

GC can provide greater flexibility than HPLC with UV detection and is capable of achieving sensitivities in the picogram (pg on column) range, provided the

0021-9673/90/$03.50

compound is amenable to GC and responds to a detector capable of attaining such levels of detection. Furthermore, GC coupled with mass spectrometry (MS) can provide structural information which can be difficult to accomplish by HPLC–UV. A combined approach by GC and GC–MS offers the advantages of high-resolution capillary chromatography and sensitive, selective detection and confirmation of compounds of interest.

The purpose of this research was to characterize the thermal decomposition products of chlorsulfuron as a prelude to quantitative determinations of chlorsulfuron present in biological extracts. We report here the characterization of the chlorsulfuron decomposition products. A method for the quantitative determination of the volatile thermal decomposition product 2-amino-4-methoxy-6-methyl-1,3,5-triazine (AMMT) by GC with nitrogen–phosphorus detection (NPD), and its characterization by GC–MS, is also presented.

EXPERIMENTAL

Chemicals and expendable materials

Chlorsulfuron was obtained from DuPont (Wilmington, DE, U.S.A.). Solvents (HPLC grade) were obtained from commercial sources and used without further purification. Stock chlorsulfuron standard solutions (1 mg/ml) were prepared by dissolving pure chlorsulfuron in dichloromethane and then serially diluting with dichloromethane to the desired concentration (62.5, 125, 250, 500 and 1000 ng/ml).

GC and GC–MS

GC analysis was conducted on a Varian (Palo Alto, CA, U.S.A.) Vista 6000 (column; 25 m × 0.25 mm I.D. fused silica, 0.25-μm coating, DB-5, J & W Scientific, splitless injection with the purge function being activated at 0.75 min post injection with a temperature program of 90°C for 1 min, increasing 20°C/min to 280°C and holding for 1 min). NPD was accomplished using a detector maintained at 300°C and 8 mV at a sensitivity of $32 \cdot 10^{-12}$. The injection port temperature (230, 240, 250, 260 and 270°C) and injection volume (0.5, 1.0, 2.0 and 3.0 μl) were varied according to the experimental design (Table I). Eluted peaks were integrated utilizing a Varian (Model

TABLE I

QUANTITATIVE RESULTS FOR THE GC–NPD ANALYSIS OF 2-AMINO-4-METHOXY-6-METHYL-1,3,5-TRIAZINE THERMAL DECOMPOSITION PRODUCT OF CHLORSULFURON

Correlation coefficients (r; mean of 5 standard curves ± standard deviation, S.D.) determined for chlorsulfuron at increasing concentrations (62.5, 125, 250, 500 and 1000 ng/ml). IV = Injection volume; IP = injection port temperature; n = number of samples.

	r (mean ± S.D.)		*n*
Interassay variability		11.6 ± 7.5%	25
Intraassay variability		6.2%	5
IV 2 μl, IP 250°C	0.992 ± 0.004		
IV 2 μl, IP = 230, 240, 250, 260 and 270°C	0.997 ± 0.003		
IP 250°C, IV = 0.5, 1, 2 and 3 μl	0.989 ± 0.001		

4290) integrator. Interassay variability was determined by calculating the mean and standard deviation (S.D.) of five replicates for each concentration and specific treatment. The S.D. was devided by its respective mean which gave the coefficient of variation (C.V.). The C.V. values so obtained were averaged and defined as the interassay variability. Intraassay variability was determined by dividing the S.D. by the mean area of an identical sample analyzed five times ($n=5$) under identical conditions.

GC–MS analyses were performed on a Finnigan (Model 9611) gas chromatograph (San Jose, CA, U.S.A.), as described above for GC determinations, linked to a Finnigan triple stage quadrupole mass spectrometer (TSQ-4500), maintaining the transfer line at 300°C. A 70 eV potential with the electron multiplier voltage set at 2000 and a 2 s/mass decade scan were utilized. Data were recorded and processed utilizing a Data General (Nova 4) data processing system.

Preparation of standard AMMT and 2-chlorobenzenesulfonamide (CB)

Standard AMMT and CB were prepared by acid hydrolysis of pure chlorsulfuron. Chlorsulfuron hydrolysis was carried out by acidifying 10 ml of a chlorsulfuron solution (1 mg/ml methanol) with one drop of 1 *M* hydrochloric acid and heating the acidified solution at 50°C for 4 h or until complete hydrolysis of chlorsulfuron had occurred. The formation of hydrolytic products was monitored at 1-h intervals by analyzing a portion of the reaction mixture by HPLC–UV (230 nm for AMMT and 270 nm for CB) until complete hydrolysis was obtained. The HPLC analysis was conducted utilizing a Hewlett-Packard HP1090 HPLC (HP79994A HPLC Chemstation) equipped with a photodiode array detector (UV; bandwidth 20 nm, spectrum range 200–350 nm and reference spectrum of 450 nm) and reversed-phase octadecylsilyl (ODS) derivatized silica column (Varian MCH-10, 10 μm, 30 cm × 4 mm) maintained at 40°C. The HPLC mobile phase was 0.017 *M* aqueous orthophosphoric acid–acetonitrile (35:65, v/v), at an isocratic flow-rate of 1 ml/min.

The identity of the hydrolytic products was confirmed by GC–MS as described under *GC and GC–MS*.

RESULTS AND DISCUSSION

Existing HPLC and GC methods for chlorsulfuron analysis lack sensitiviy in the pg range (HPLC) and/or require inexact derivatization methods to form volatile chlorsulfuron derivatives (GC). The HPLC methods utilizing photoconductivity or UV detection provide sufficient sensitivity at the maximal permissible level (300 ng/g) allowed by law in foods[10] but methods for detecting low levels (pg on column range) of chlorsulfuron are difficult without resorting to residue enrichment procedures such as solvent extractions and/or concentrating samples by column chromatography or solid phase extraction techniques. These procedures can be time and labor intensive. This led us to develop a detection method for a thermal decomposition product of chlorsulfuron which is sensitive, selective and precise enough for quantitative determinations in the low ng/ml (pg on column) range, as well as allowing for the characterization and confirmation of volatile thermal decomposition products of chlorsulfuron by GC–MS.

When standard chlorsulfuron solutions were injected into the GC injection port

a volatile thermal decomposition product was produced which resulted in a characteristic GC chromatogram (Fig. 1) when utilizing NPD. Results (Table I) indicated the detector response for this volatile thermal decomposition product was linear over the concentration range examined (62.5–1000 ng/ml, 2 μl injection volume) with acceptable inter (11.6 $\pm$ 7.5%) and intraassay (6.2%) variabilities, and was independent of injection port temperatures (230–270°C) and injection volumes (0.5–3 μl) tested. Blank sample controls, containing no chlorsulfuron, gave no indication of any peaks which might interfere with such analyses.

Characterization of the volatile thermal decomposition products of chlorsulfuron was conducted by GC–MS. Mass spectral data of the volatile thermal decomposition products indicated a thermal decomposition fragmentation pattern (Fig. 2A) occurred which produced two major volatile compounds which had molecular weights of 140 (Fig. 2B) and 191 (Fig. 2C). The nitrogen–phosphorus detectable fragment had a molecular weight of 140 (AMMT) which represents that part of the molecule which contained four nitrogen atoms (Fig. 2A). The 191 fragment was not a good NPD responder, at the concentrations examined, but the mass spectrum indicated a characteristic chlorine isotope cluster corresponding to a CB fragment.

Apparently the thermal decomposition process involves a unimolecular decomposition with minimal secondary bimolecular reactions, terminating with the formation of a minimal number of volatile fragments as a result of the extrusion of carbon monoxide, independent of the variables examined. There was no indication of intact chlorsulfuron being present when analyzed by GC–NPD or GC–MS, indicating that equilibrium temperature for primary bond fission was achieved under the specified GC operating conditions. The mass spectra generated for these two thermal decomposition products support this hypothesis and were identical to mass spectra of standard AMMT and CB generated by acid hydrolysis of chlorsulfuron. The mass spectrometry fragmentation ions generated for AMMT (Table II) and CB (Table III) are consistent

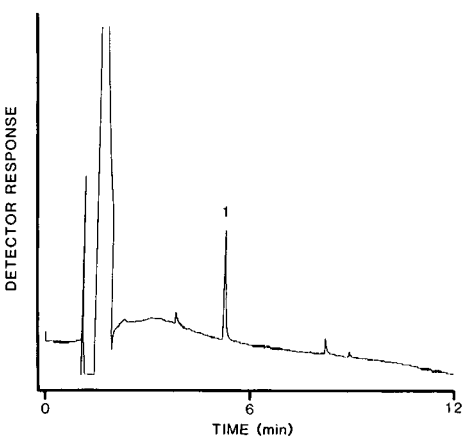

Fig. 1. Representative GC chromatogram of a nitrogen–phosphorus detectable volatile thermal decomposition product (2-amino-4-methoxy-6-methyl-1,3,5-triazine) of chlorsulfuron (peak 1). Peak 1 was not present in a solvent blank.

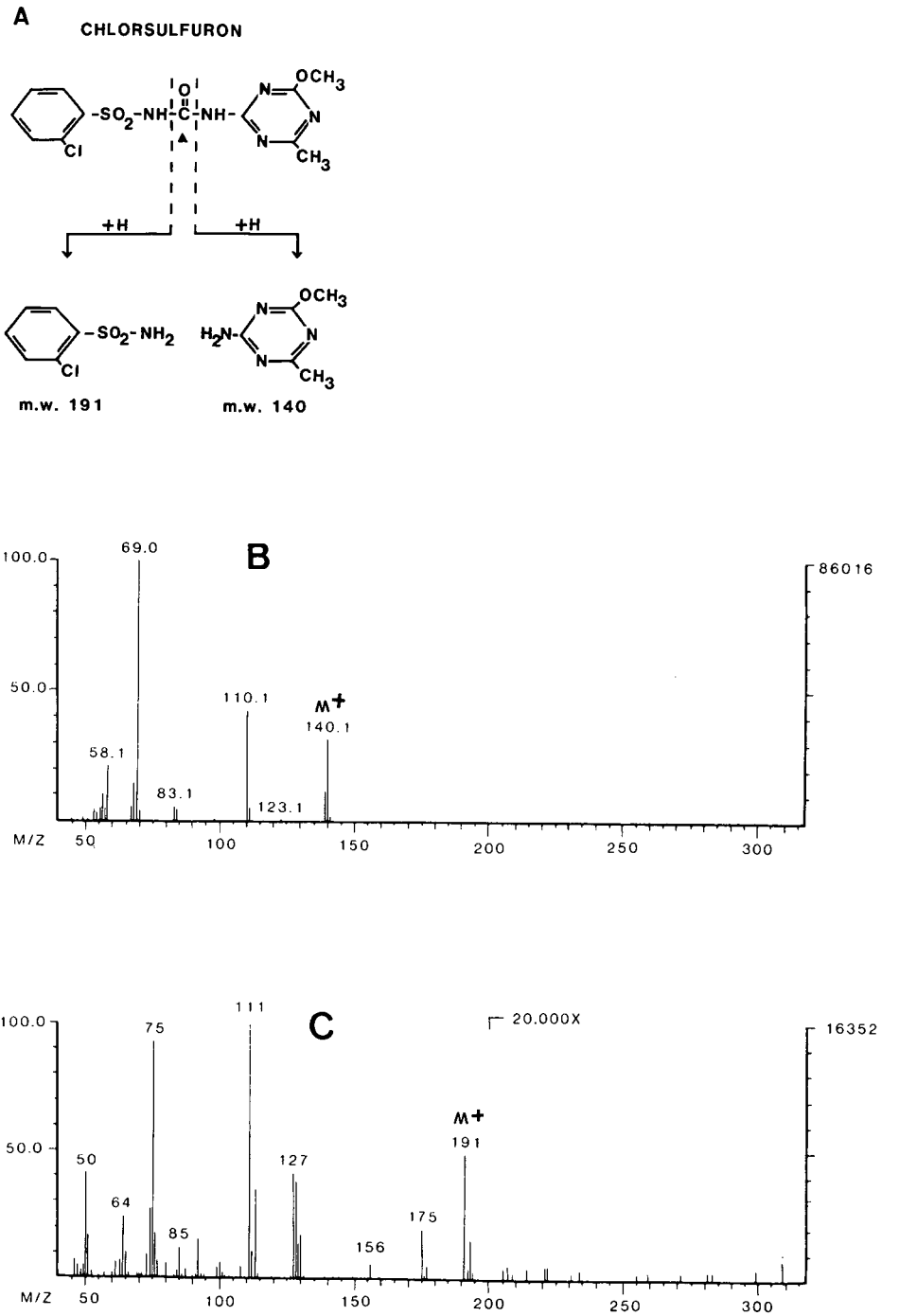

Fig. 2. Proposed thermal decomposition pattern (A) of chlorsulfuron and the positive ion, electron impact mass spectrum of fragments 1 [AMMT (B)] and 2 [CB (C)]. m.w. = Molecular weight.

TABLE II

RELATIVE ABUNDANCE OF MS FRAGMENTATION IONS FOR 2-CHLOROBENZENESULFONAMIDE THERMAL DECOMPOSITION PRODUCT OF CHLORSULFURON

Ion (isotope)	*Fragmentation*	*Relative abundance (%)*
191 (193)	M (molecular ion)	48 (15)
175 (177)	M − 16 (NH_2)	19 (5)
156	M − 35 (Cl)	5
128 (130)	M − 64 ($SONH_2$) + 1 (H)	38 (16)
127 (129)	M − 64 ($SONH_2$)	41 (13)
111 (113)	156 − SO_2NH	100 (33)
93	128 − 35 (Cl)	14
75	C_6H_3 (from benzene)	93
64	SO_2 or H_2NSO	24

TABLE III

RELATIVE ABUNDANCE OF MS FRAGMENTATION IONS FOR 2-AMINO-4-METHOXY-6-METHYL-1,3,5-TRIAZINE THERMAL DECOMPOSITION PRODUCT OF CHLORSULFURON

Ion	*Fragmentation*	*Relative abundance (%)*
140	M (molecular ion)	31
139	M − 1 (H)	11
111	M − 30 (formaldehyde) + 1 (H)	5
110	M − 30 (formaldehyde)	42
69	111 − 42 (CH_2N_2)	100
58	83 − 15 (methyl)	21

with the fragmentation pattern of other 1,3,5-triazines[11] and chlorobenzenesulfonamides[12,13].

Standard AMMT and CB were generated by acid hydrolysis of chlorsulfuron. The isolated hydrolytic products were characterized by HPLC–UV, GC–NPD and GC–MS and the mass spectra of isolated AMMT and CB were identical to the mass spectra of the thermal decomposition products of chlorsulfuron. The generation of AMMT and CB from chlorsulfuron by both acid hydrolysis and thermal decomposition, coupled to the almost identical spectra of CB to that of 4-chlorobenzenesulfonamide[13], indicates that the thermal decomposition of chlorsulfuron takes place as described. Additionally, structures of degradative products of chlorsulfuron[14] are consistent with results presented here. The unequivocal mechanistic details of AMMT and CB formation from chlorsulfuron by thermal decomposition will require additional MS characterization of isotopically labelled chlorsulfuron.

The method presented allows for the separation, characterization and quantitative determination of a volatile nitrogen–phosphorus detectable thermal decomposition product (2-amino-4-methoxy-6-methyl-1,3,5-triazine) of chlorsulfuron down to 125 pg on column. This, coupled with GC–MS allows for structural confirmations of chlorsulfuron decomposition products as well. Thus, quantitation and confirmation of chlorsulfuron as AMMT in the low ng/g range can be accomplished by thermal decomposition GC.

ACKNOWLEDGEMENTS

This research was supported by Cooperative Agreements 5V01-FD-01-319 and FD-V-000235 with the United States Food and Drug Administration. The laboratory assistance of Ms. Wendy Looney is greatly appreciated.

REFERENCES

1 M. B. Levitt, H. L. Ploeg, R. C. Weigel, Jr. and D. J. Fitzgerald, *J. Agric. Food Chem.*, 29 (2) (1981) 416–418.
2 E. Wahlin-Boll and A. Melander, *J. Chromatogr.*, 164 (1979) 541–546.
3 M. Uehlein and N. Sistorasis, *J. Chromatogr.*, 227 (1982) 93–101.
4 P. Hartvig, C. Fagerlund and O. Gyllenhaal, *J. Chromatogr.*, 181 (1980) 17–24.
5 T. Maeda, T. Yamaguchi and M. Hasimoto, *J. Chromatogr.*, 223 (1981) 357–363.
6 E. W. Zahnow, *J. Agric. Food Chem.*, 30 (5) (1982) 854–857.
7 R. V. Slates, *J. Agric. Food Chem.*, 31 (1) (1983) 113–117.
8 I. Ahmad, *J. Assoc. Off. Anal. Chem.*, 70 (4) (1987) 745–748.
9 M. J. M. Wells and J. L. Michael, *J. Chromatogr. Sci.*, 25 (1987) 345–350.
10 *Code of Federal Regulations*, 40CFR (1988) 180.405.
11 Q. N. Porter, in E. C. Taylor and A. Weissbergen (Editors), *Mass Spectrometry of Heterocyclic Compounds*, Wiley, New York, 1985, Ch. 18, pp. 811–825.
12 H. Budzikiewicz, C. Djerassi and D. H. Williams, *Mass Spectrometry of Organic Compounds*, Holden-Day, San Francisco, CA, 1967, Ch. 19, pp. 558–561.
13 *Hewlett-Packard Mass Spectral Library (Part No. 59868A)*, National Bureau of Standards NBS/Wiley registry of mass spectral data, Palo Alto, CA, 1987.
14 M. M. Kelley, E. W. Zahnow, W. C. Petersen and S. T. Toy, *J. Agric. Food Chem.*, 33 (5) (1985) 962–965.

Journal of Chromatography, 505 (1990) 402–407
Elsevier Science Publishers B.V., Amsterdam — Printed in The Netherlands

CHROM. 22 276

Note

Analysis of decomposition products of alkyl nitronic acids by reversed-phase high-performance liquid chromatography

A. J. SHAW and A. GESCHER*

Mechanisms of Drug Toxicity Research Group, Pharmaceutical Sciences Institute, Aston University, Aston Triangle, Birmingham B4 7ET (U.K.)

(First received November 3rd, 1989; revised manuscript received January 11th, 1990)

Nitroalkanes (I), such as 2-nitropropane, are important industrial solvents with hepatotoxic and mutagenic properties[1]. The interpretation of their pharmacological and biochemical properties is complicated by the fact that they exist in tautomeric equilibrium with their respective nitronates (II) and nitronic acids (III).

$$\underset{\text{I}}{R^1R^2CHNO_2} + B \rightleftharpoons \underset{\text{II}}{R^1R^2C{=}NO_2^-} + BH^+ \rightleftharpoons \underset{\text{III}}{R^1R^2C{=}NOOH} + B \qquad (1)$$

The kinetics of equilibrium 1 have been extensively studied [for a review, see ref. 2]. Nitronic acids (III) resemble carboxylic acids in strength (pK_a 2–6). Their isomerisation to the nitroalkane tautomer proceeds essentially to completion for most simple nitronic acids, because of the relatively weaker acidity of a nitroalkane compared to its corresponding nitronic acid. The mechanism of the reaction III→II requires hydrogen abstraction and reaction II→I involves C-protonation on the intermediate anion II. Consequently, the tautomerisation rate is accelerated in neutral to slightly basic solution and inhibited in acidic solution[3]. Strong acid usually favours decomposition of III by hydrolysis, the so called Nef reaction (reaction 2). The Nef reaction is a convenient preparative route to the carbonyl compound IV, aldehydes in the case of primary nitronic acids or ketones in the case of secondary nitronic acids. Two further reactions 3 and 4 invariably accompany the Nef reaction. The redox reaction 3 yields the alkyl oxime V and the nitrosation reaction 4 leads to the pseudonitrole VI:

$$R^1R^2C{=}NOOH + H_3O^+ \rightarrow \underset{\text{IV}}{R^1R^2C{=}O} + H^+ + HNO + H_2O \qquad (2)$$

$$R^1R^2C{=}NOOH + HNO \rightarrow \underset{\text{V}}{R^1R^2C{=}NOH} + HNO_2 \qquad (3)$$

$$R^1R^2C{=}NO_2^- + HNO_2 + H^+ \rightarrow \underset{\text{VI}}{R^1R^2C(NO)NO_2} + H_2O \qquad (4)$$

0021-9673/90/$03.50

The blue colouration that often accompanies these reactions is due to the formation of nitronitroso (VI) and hydroxynitroso [$R^1R^2C(OH)NO_2$] derivatives[4,5]. In the case of primary nitroalkanes the colouration often disappears rapidly as these derivatives rearrange to form the more stable, colourless nitrooximes $RC=NOH(NO_2)$ (VII)[5]. Ultimately the structure of the nitronic acid determines its rate of tautomerisation and decomposition. For example, highly ionised nitronic acids, *e.g.* $XCH=NO_2H$ (X = Cl, Br), tautomerise rapidly even at low pH without undergoing the Nef reaction[5]. Conversely branching at the nitronate α-carbon can greatly hinder both tautomerisation and the Nef reaction[6,7].

As part of an investigation into the role of metabolism in the toxicity of nitroalkanes and their anionic tautomers we have developed a simple reversed-phase high-performance liquid chromatography (RP-HPLC) programme to detect and quantitate potential metabolites with a range of hydrophilic and hydrophobic properties. We show here how this procedure can be used to determine the extent of equilibriation between nitro and nitronate forms and to quantitate the decomposition products of nitronic acids.

EXPERIMENTAL

Materials

All chemicals were purchased from Aldrich (Gillingham, U.K.) with the following exceptions; 1-nitropropane and 2-nitropropane were obtained from Fluka (Glossop, U.K.) and were redistilled until they were > 98% pure. Glutathione and N-acetylcysteine were purchased from Sigma (Poole, U.K.). Nitronates were prepared by dissolving nitroalkanes in 1 *M* aqueous potassium hydroxide in equimolar proportions[8]. These solutions were adjusted to the desired pH and used within 2 h of preparation. 2-Nitro-2-nitrosopropane (propylpseudonitrole) was synthesised by reacting propyl-2-nitronate slowly on ice with concentrated hydrochloric acid according to Nygaard[9]. The cream-coloured precipitate produced, the dimeric form of the compound, was reverted to the blue monomeric state by dissolution in acetic acid. S-Nitrosoglutathione was synthesised by reacting HNO_2 with reduced glutathione as described by Hart[10]. S-Nitroso-N-acetylcysteine was prepared by reacting HNO_2 with N-acetylcysteine in a similar fashion.

RP-HPLC

The chromatographic equipment consisted of a Waters (Milford, MA, U.S.A.) 600E multi solvent delivery system equipped with a Waters 480 UV detector. The detector signals were recorded on a Waters 745B data handling system capable of baseline subtraction. The column was a Waters reversed-phase Nova-Pak C_{18} radial column (4 μm particle size; 10 cm × 5 mm) contained within a Waters RCM compression module. Injections (10 μl) were made using a Waters 700 Satellite automatic sample processor. Mobile phase: solvent A was 0.15% acetic acid (FSA Laboratory Supplies, Loughborough, U.K.) in HPLC-grade water (BDH, Poole, U.K.); solvent B was HPLC-grade methanol (BDH). Both solvents were passed through a 0.2-μm Millipore filter and degassed before use. Solvents were sparged with helium during use. The solvent programme commenced with 95% solvent A in B for 5 min followed by a linear transition to 20% A in B over 10 min. The solvent mixture

was reversed (convex curve) to its original proportions over a 5-min period and left to establish the initial conditions for 15 min. The flow-rate was 1.0 ml/min and the column effluent was monitored at 220 nm.

RESULTS AND DISCUSSION

The RP-HPLC retention times of the simple nitroalkanes studied increased with chain length, and, predictably, they were greater for primary nitroalkanes than for the respective isomeric secondary ones (Table I). Calibration graphs for the nitroalkanes in the concentration range 1–25 m*M* showed good linearity with correlation coefficients $\geqslant 0.998$. All nitroalkanes under study except the tertiary derivative 2-methyl-2-nitropropane tautomerised completely to the nitronates on addition of equimolar sodium hydroxide. The resolution of the neutral and ionic tautomers was good except in the case of the highly hydrophilic (nitromethane) or hydrophobic (1-nitropentane and 1-nitrohexane) nitroalkanes (Table I and Fig. 1A and B). Regeneration of the nitroalkane from the nitronate was >99% when the pH was gradually adjusted to pH 5.5 using Tris–HCl buffer. Calibration graphs of the well-resolved nitronates within the concentration range 0.5–10 m*M* displayed good linearity with correlation coefficients $\geqslant 0.997$. The limit of detection for nitroalkanes and nitronates was 50 μM using 220 nm as detection wavelength. In studies of the equilibrium I→III or the enzymatic oxidation of II nitronates have hitherto been quantified spectrophotometrically[8] using their UV absorption between 220 and 235 nm. Compared to the UV-spectrophotometric analysis the HPLC method described here should allow greater versatility and better specificity.

Addition of strong acid, *e.g.* hydrochloric acid, to nitronates generates the

TABLE I

RETENTION TIMES OF NITROALKANES, THEIR NITRONATES AND PRODUCTS OF NITRONIC ACID DEGRADATION

Retention times are the mean of five determinations made on separate days. The standard deviation was <2% of the mean in all cases.

Nitroalkane	*Retention times (min)*[a]				
	Nitro form (I)	*Nitronate (II)*	*Alkyl oxime (V)*	*Nitrooxime (VII)*	*Pseudonitrole (VI)*
Nitromethane	2.0	1.9	–	–	–
Nitroethane	3.8	1.9	2.4	2.0	–
1-Nitropropane	10.6	3.6	5.1	–	–
1-Nitropentane	19.7	19.6	18.4	17.8	–
1-Nitrohexane	21.1	21.0	20.1	19.7	–
2-Nitropropane	10.4	3.0	4.8	–	16.0
Nitrocyclopentane	18.0	9.0	14.5	–	19.5
Nitrocyclohexane	19.8	15.7	17.2	–	20.9
2-Methyl-2-nitropropane	16.9	–	–	–	–

[a] Assignment of retention times by comparison with reference compounds in the case of V and VI, speculative for VII.

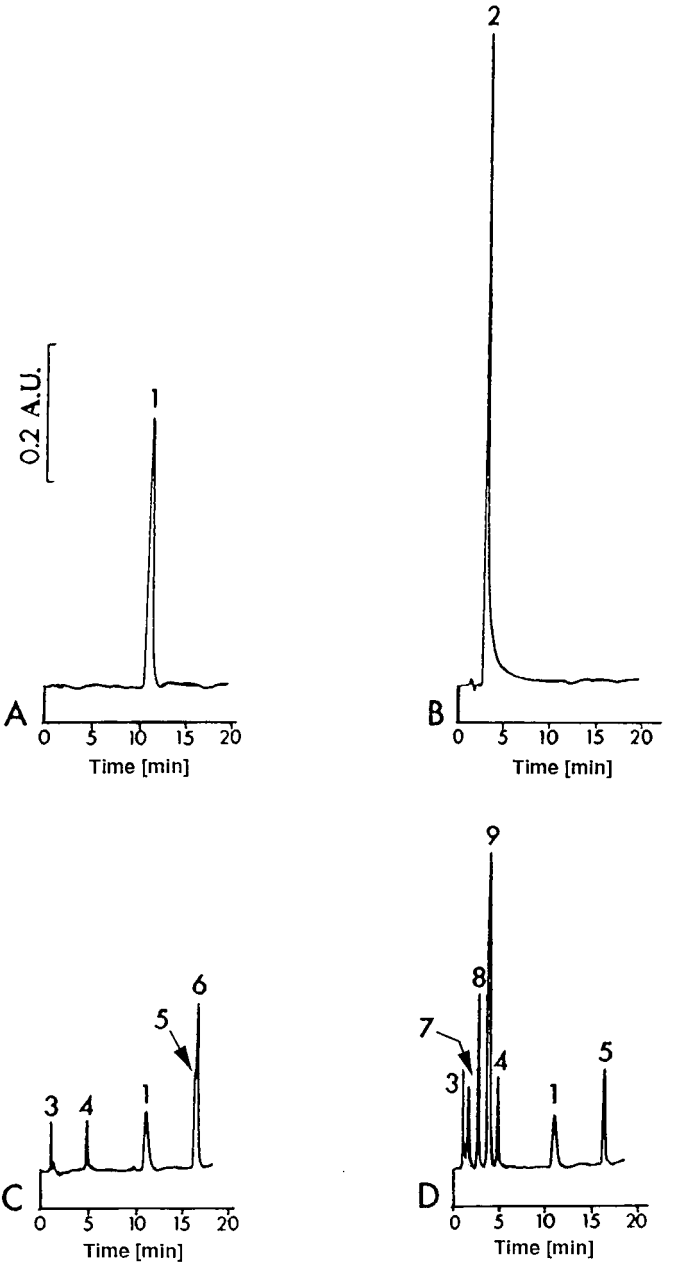

Fig. 1. RP-HPLC chromatograms of (A) 2-nitropropane (25 m*M*) in water, (B) propyl-2-nitronate (10 m*M*), (C) products of tautomerisation and degradation of propyl-2-nitronate 20 min after rapid adjustment to pH 3 using hydrochloric acid, and (D) products of propyl-2-nitronate 20 min after rapid adjustment to pH 3 and 10 min after addition of reduced glutathione (10 m*M*). For chromatographic conditions see Experimental. The eluent was monitored at 220 nm. The chromatograms were obtained after subtraction of the background recorded in solvent controls. Peaks (tentatively assigned by comparison with reference compounds, or by speculation in the case of peak 5): 1 = 2-nitropropane; 2 = propyl-2-nitronate; 3 = nitrous acid; 4 = acetone oxime; 5 = 2-hydroxy-2-nitrosopropane; 6 = propylpseudonitrole; 7 = glutathione (GSH); 8 = glutathione disulfide (GSSG); 9 = S-nitrosoglutathione.

corresponding nitronic acids which, due to the acidic environment, undergo rapid hydrolysis and further reactions (reactions 2–4, Fig. 1C). Aldehydes and ketones generated by the Nef reaction were undetectable by RP-HPLC. Other products were tentatively identified by cochromatography with authentic material as alkyl oximes (V) and pseudonitroles (VI). These decomposition products were well resolved as they were eluted before and after the precursor nitroalkanes, respectively (Table I). Calibration graphs of the oximes at 220 nm and of the pseudonitroles at either 220 or 290 nm showed good linearity with correlation coefficients $\geqslant 0.997$.

We have utilised the RP-HPLC programme described here to investigate the reaction of nitroalkane derivatives with biological thiols such as glutathione and N-acetylcysteine. The blue pseudonitroles VI generated from secondary nitroalkanes, for example propyl-2-pseudonitrole (VI with $R^1,R^2=CH_3$), reacted with glutathione to produce a red coloured conjugate with a retention time of 3.8 min (Fig. 1D). The conjugate was identified as S-nitrosoglutathione (VIII, R = glutathionyl, see reaction 5) by fast atom bombardment mass spectroscopy and high-field ^1H NMR spectroscopy[11].

$$\underset{}{RSH} + \underset{VI}{R^1R^2C(NO)NO_2} \rightarrow \underset{VIII}{RSNO} + \underset{III}{R^1R^2C{=}NO_2H} \qquad (5)$$

S-Nitrosglutathione decomposed slowly to form glutathione disulfide (retention time: 2.8 min). Similarly N-acetylcysteine reacted with secondary alkyl pseudonitroles to form S-nitroso-N-acetylcysteine (retention time: 5.4 min) which degraded slowly to N-acetylcystine (retention time: 4.5 min). Production of S-nitroso conjugates, monitored at 220 or 336 nm, was accompanied by further generation of alkyl oxime V. In the light of reaction 5 V is presumably generated by acidic decomposition of the nitronic acid III formed via denitrosation of VI.

CONCLUSIONS

The RP-HPLC method described here can be used to (i) determine the concentration of nitroalkanes in aqueous and non-aqueous solutions, (ii) detect and measure the nitronate tautomers of nitroalkanes and (iii) detect products of the decomposition of nitronic acids. The procedure should be applicable to most nitroalkanes except those which are strongly hydrophobic. A disadvantage of the technique is its inability to detect aldehydes or ketones as nitronic acid degradation products, their measurement requires different chromatographic conditions.

ACKNOWLEDGEMENT

This research was supported by a generous grant from the Health and Safety Executive of Great Britain.

REFERENCES

1 IARC (International Agency for Research on Cancer), in *Monographs on the Evaluation of Carcinogenic Risk of Chemicals to Man*, Vol. 29, WHO, Lyon, 1982, p. 331.
2 A. T. Nielson, in H. Feuer (Editor), *The Chemistry of the Nitro and Nitroso Groups*, Part 1, Interscience, New York, 1969, p. 349.

3 H. Feuer and A. T. Nielson, *Tetrahedron*, 19 (Suppl. 1) (1963) 65.
4 M. F. Hawthorne, *J Am. Chem. Soc.*, 79 (1957) 2510.
5 J. Armand, *Bull. Soc. Chim. Fr.*, (1965) 3246.
6 E. E. Van Tamelen and R. J. Thiede, *J. Am. Chem. Soc.*, 74 (1952) 2615.
7 R. A. Smiley and W. A. Pritchett, *J. Chem. Eng. Data*, 11 (1966) 617.
8 D. J. T. Porter and H. J. Bright, *J. Biol. Chem.*, 258 (1983) 9913.
9 E. M. Nygaard, *U.S. Pat.*, 2 401 267 (1946); *C.A.* 40 (1946) 6092.
10 T. W. Hart, *Tetrahedron Lett.*, 26 (1985) 2013.
11 A. J. Shaw, A. Gescher, D. Tooth, I. Linhart and P. B. Farmer, *Chem. Res. Toxicol.*, in press.

Journal of Chromatography, 505 (1990) 408–412
Elsevier Science Publishers B.V., Amsterdam — Printed in The Netherlands

CHROM. 22 278

Note

Normal-phase high-performance liquid chromatographic analysis of polyhydroxysteroids using non-polar bonded silica columns

NAGUIB KAOUADJI and RENÉ LAFONT*

École Normale Supérieure, Département de Biologie, CNRS URA 686 "Biochimie et Physiologie du Développement", 46 Rue d'Ulm, F-75230 Paris Cedex 05 (France)

(First received May 25th, 1989; revised manuscript received December 29th, 1989)

Ecdysteroids represent a class of polyhydroxylated steroids widely represented among invertebrates and plants[1–3]. Their high-performance liquid chromatographic (HPLC) analysis can be performed using various techniques[4,5]. However, the use of normal-phase systems has so far been restricted to medium-polarity ecdysteroids, and polar compounds are analysed by either reversed-phase or ion-exchange HPLC. It would nevertheless be of interest to use normal-phase systems in the latter instance, either as a means of ascertaining compound identity by co-migration with reference compounds or for the final step in the purification of polar ecdysteroids prior to spectrometric analyses.

Up to now, normal-phase HPLC separations of ecdysteroids have been performed by using either silica or polar-bonded silica columns, *e.g.*, aminopropylsilane (APS)[4,6] or diol-bonded[4,7] silicas. Polar bonded phases can provide interesting results, *e.g.*, for the separation of $3\alpha/3\beta$ pairs[6] or the separation of compounds over a wide range of polarity[7].

This paper results from an experimental mistake in which an ODS-bonded column was used instead of a silica column and unexpectedly gave a fairly efficient separation. This induced us to undertake a more extensive analysis of the possible use of polar bonded columns for normal-phase HPLC. The results appear promising and are reported here.

EXPERIMENTAL

Chemicals

Reference ecdysteroids (Fig. 1) were obtained from various sources. Ecdysone and makisterone A were purchased from Simes (Milan, Italy). Ponasterone A, 2-deoxyecdysone and 2-deoxy-20-hydroxyecdysone were gifts from Dr. D. H. S. Horn (Acheron, Australia). 20-Hydroxyecdysone, integristerone A, 20,26-dihydroxyecdysone and 20-hydroxyecdysone glucosides were purified from various plant sources[8]. 25-Deoxyecdysone was synthesized from ecdysone according to Heinrich[9].

0021-9673/90/$03.50

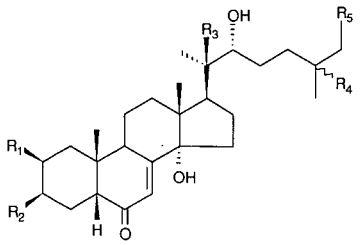

COMPOUND	R_1	R_2	R_3	R_4	R_5
25-Deoxyecdysone	OH	OH	H	H	H
Ponasterone	OH	OH	OH	H	H
2-Deoxyecdysone	H	OH	H	OH	H
2-Deoxy-20-hydroxyecdysone	H	OH	OH	OH	H
Ecdysone	OH	OH	H	OH	H
20-Hydroxyecdysone	OH	OH	OH	OH	H
20,26-Dihydroxyecdysone	OH	OH	OH	OH	OH
20-Hydroxyecdysone 25-glucoside	OH	OH	OH	OGlu	H
20-Hydroxyecdysone 3-glucoside	OH	OGlu	OH	OH	H

Fig. 1. Structures of the ecdysteroids.

Solvents (HPLC grade) were obtained from Prolabo (dichloromethane) or Carlo Erba (methanol, isopropanol). High-purity water was obtained with a Milli-Q system (Millipore).

HPLC equipment

All experiments were performed with a DuPont Model 8800 instrument equipped with a two-solvent gradient system, a fixed-wavelength UV detector (Model 850) and a Rheodyne 7125 injector. Several types of analytical columns were used: Zorbax-Sil (250 × 4.6 mm I.D.), Zorbax-TMS (150 × 4.6 mm I.D.), Zorbax-ODS (250 × 4.6 mm I.D.), Spherisorb 5-ODS-2 (250 × 4.6 mm I.D.), LiChrosorb Diol (250 x 4.0 mm I.D.) ad Nucleosil-NH_2 (150 × 4.6 mm I.D.). All the columns were run isocratically with dichloromethane–isopropanol–water mixtures[10]. Some experiments were carried out using the gradient mode, with methanol as secondary solvent.

RESULTS AND DISCUSSION

A typical separation of ecdysone and 20-hydroxyecdysone obtained on three different columns from the same manufacturer is shown in Fig. 2. The retention times of ecdysone and 20-hydroxyecdysone on the different columns are given in Table I (values are the means of three separate assays and the fluctuations did not exceed ±3%, provided that the ambient temperature was kept constant). It is obvious from these data that TMS- and amino-bonded columns give results close to those with non-bonded silica, and that ODS-bonded columns give much reduced although significant retention times. The latter result was surprising, as it was expected that ecdysteroids would elute with the solvent front, as they do when using pure methanol. The result seems understandable, however, when it is considered that a significant percentage of silanol groups remain free in such columns, which would be responsible for the chromatographic process. This idea is supported by the fact that when using two ODS columns from the same manufacturer, the new column gave lower retention times than the older column (data not shown). The TMS-bonded column appeared of

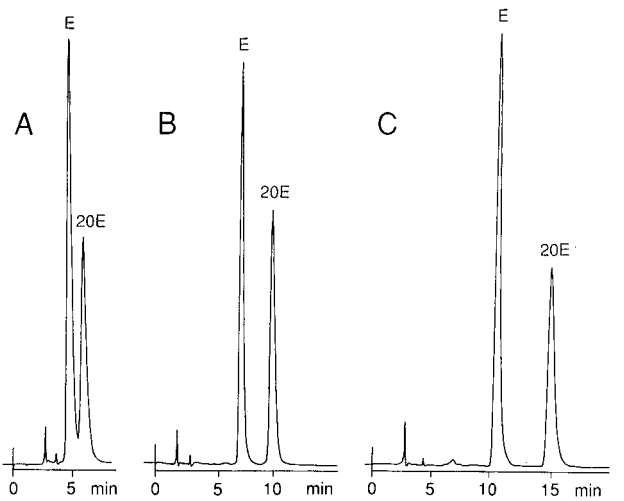

Fig. 2. Separation of an ecdysone (E)–20-hydroxyecdysone (20E) mixture using three different HPLC columns. Solvent system: dichloromethane–isopropanol–water (125:40:3); flow-rate, 1 ml min^{-1}. A, Zorbax-ODS (25 cm); B, Zorbax-TMS (15 cm); C, Zorbax-SIL (25 cm).

interest because the eluted peaks were perfectly symmetrical, whereas in the other instances there was always some tailing. For that reason, we carried out a more extensive study of this particular type of column.

TMS packings have good efficiency and are particularly interesting for polar compounds, which elute within reasonable times. Such columns can be used not only in the isocratic mode, but also in the gradient mode, in order to optimize separations of compounds over a wide range of polarity. This was checked by using a slow linear gradient of methanol (0–20% in 45 min) in the primary solvent (dichloromethane–

TABLE I

COMPARISON OF THE RETENTION TIMES OF ECDYSONE (E) AND 20-HYDROXYECDYSONE (20E) USING DIFFERENT COLUMNS AND TWO DIFFERENT SOLVENT SYSTEMS

Column	*Solvent system 1*[a]			*Solvent system 2*[a]		
	$t_R(E)$[b]	$t_R(20E)$[b]	N/m[c]	$t_R(E)$[b]	$t_R(20E)$[b]	N/m[c]
Zorbax-SIL	44.8	78.9	34 400	13.0	18.8	15 600
Zorbax-TMS	46.0	76.3	25 200	14.3	20.3	17 200
Zorbax-ODS	13.7	22.3	8 000	5.6	6.6	–
Spherisorb ODS-2	4.6	6	–	2.8	3.1	–
Lichrosorb DIOL	17.7	27.1	–	6.4	7.9	–
Nucleosil-NH_2	32.5	62.3	–	13.2	17.7	–

[a] Solvents: dichloromethane–isopropanol–water: system 1 125:20:1.5 (v/v/v); system 2, 100:30:2 (v/v/v).

[b] t_R = Retention time in minutes; values standardized for a 25 cm × 4.6 mm I.D. column; flow-rate, 1 ml min^{-1}

[c] N/m = Number of plates per metre column length.

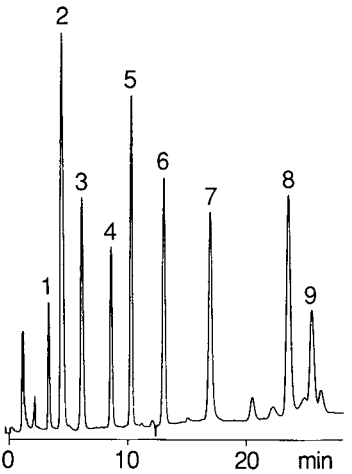

Fig. 3. Separation of an ecdysteroid mixture on a Zorbax-TMS column (15 cm × 0.46 cm I.D.). Operating conditions: flow-rate, 2 ml min^{-1}; primary solvent, dichloromethane–isopropanol–water (125:20:1.5, v/v/v); secondary solvent, methanol, gradient from 0 to 20% methanol in 45 min. Peaks: 1 = 25-deoxyecdysone; 2 = ponasterone A; 3 = 2-deoxyecdysone; 4 = 2-deoxy-20-hydroxyecdysone; 5 = ecdysone; 6 = 20-hydroxyecdysone; 7 = 20,26-dihydroxyecdysone; 8 = 20-hydroxyecdysone 25-glucoside; 9 = 20-hydroxyecdysone 3-glucoside.

isopropanol–water, 125:20:1.5), and this allowed us to separate within 20 min a mixture of compounds bearing between four and nine hydroxyl groups (Fig. 3). Column re-equilibration after such a gradient required no more than 10 min (at 2 ml/min) in order to obtain reproducible analyses. This type of solvent system therefore appeared well suited for metabolic studies.

In conclusion, the use of TMS columns for the normal-phase analysis of polar steroids seems very promising, and such systems might be of more general use. A parallel of the present data can be made with the columns used for supercritical fluid chromatography (SFC), which was recently applied to ecdysteroids[11,12] with either silica[11] or non-polar bonded phases[12]. Supercritical carbon dioxide acts as a non-polar mobile phase that is modified by adding a small percentage of methanol[12]. In SFC, non-polar bonded columns provide reduced retention times in comparison with silica and this seems to have a similar explanation to that proposed here. It is therefore suggested that TMS columns could perhaps also be successfully used for the SFC analysis of polar compounds.

REFERENCES

1 C. Hêtru and D. H. S. Horn, in J. A. Hoffmann (Editor), *Progress in Ecdysone Research*, Elsevier, Amsterdam, 1980, p. 13.
2 R. Lafont and D. H. S. Horn, in J. A. Koolman (Editor), *Ecdysone*, Georg Thieme, Stuttgart, 1989, p. 39.
3 H. H. Rees, in J. A. Koolman (Editor), *Ecdysone*, Georg Thieme, Stuttgart, 1989, p. 28.
4 R. Lafont, P. Beydon, B. Mauchamp, G. Sommé-Martin, M. Andrianjafintrimo and P. Krien, in F. Sehnal, A. Zabza and B. Cymborowski (Editors), *Regulation of Insect Development and Behaviour*, Technical University of Wrocław Press, Wrocław, 1981, p. 199.

5 R. Lafont, in H. Kalasz and E. S. Ettre (Editors), *Chromatography '87*, Akadémiai Kiádo, Budapest, 1988, p. 1.
6 L. N. Dinan, P. L. Donnahey, H. H. Rees and T. W. Goodwin, *J. Chromatogr.*, 205 (1981) 139.
7 B. Fournier and D. Radallah *Arch. Insect Biochem. Physiol.*, 7 (1988) 211.
8 J.-P. Girault, M. Bathori, E. Varga, K. Szendrei and R. Lafont, *J. Nat. Prod.*, (1990) in press.
9 G. Heinrich, *Dissertation*, Cologne, 1970.
10 R. Lafont, G.Sommé-Martin and J.C. Chambet, *J. Chromatogr.*, 170 (1979) 185.
11 E. D. Morgan, S. J. Murphy, D. Games and I. C. Mylchreest, *J. Chromatogr.*, 441 (1988) 165.
12 M. W. Raynor, J. P. Kithinji, I. K. Barker, K. D. Bartle and I. D. Wilson, *J. Chromatogr.*, 436 (1988) 497.

Journal of Chromatography, 505 (1990) 413–416
Elsevier Science Publishers B.V., Amsterdam — Printed in The Netherlands

CHROM. 22 272

Note

High-performance liquid chromatographic separation of cyromazine and its metabolite melamine

PAOLO CABRAS*, MARCO MELONI and LORENZO SPANEDDA
Istituto di Chimica Farmaceutica, Tossicologica ed Applicata, Viale A. Diaz 182, 09126 Cagliari (Italy)
(Received November 2nd, 1989)

Cyromazine (N-cyclopropyl-1,3,5-triazine-2,4,6-triamine) (I, Fig. 1) is an insect growth regulator with specific activity against dipterous larvae. It is used to control fly larvae on animals and is also recommended against leafminers of the *Liriomyza* genus. When used on ornamental plants and vegetables, cyromazine exhibits a systemic action, with a strong translaminar effect when applied to the leaves; applied to the soil it is taken up by roots and translocated acropetally[1].

In both plants and animals, cyromazine undergoes degradation, the cyclopropyl group being eliminated to form melamine (1,3,5-triazine-2,4,6-triamine) (II, Fig. 1). This metabolite is of great importance owing to its potential carcinogenicity[2] even though at high dosages; therefore, in pesticide tolerances for cyromazine, the residue limits are established as the sum of the active ingredient (a.i.) and its metabolite.

Gas chromatographic[3,4] and liquid chromatographic[5–7] methods have been developed for the determination, in different matrices, of melamine, which also originates from the degradation of *s*-triazine herbicides and is also employed in the manufacture of thermosetting plastics for houseware.

For the determination of cyromazine and melamine residues, gas chromatographic methods have recently been reported[8,9], and also a high-performance liquid chromatographic (HPLC) method[10].

In this paper, the HPLC separation of cyromazine from melamine by means of columns with different mechanisms is reported.

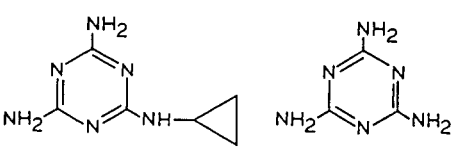

CYROMAZINE I MELAMINE II

Fig. 1. Cyromazine (I) and its major metabolite melamine (II).

0021-9673/90/$03.50

EXPERIMENTAL

Apparatus

A Varian (Palo Alto, CA, U.S.A.) Model 5020 liquid chromatograph was used, fitted with a UV-100 variable-wavelength UV–VIS detector and a Rehodyne injection valve (50-μl loop), connected to an HP 3390 A reporting integrator (Hewlett-Packard, Avondale, PA, U.S.A.).

Chromatography

Hibar RP-8 and RP-18 (250 mm × 4.0 mm I.D.; 10 μm) (Merck, Darmstadt, F.R.G.) and Whatman (Clifton, NJ, U.S.A.) Partisil 10 SAX (250 mm × 4.6 mm I.D.; 10 μm) columns were used. The mobile phase was acetonitrile–$0.5 \cdot 10^{-3}$ *M* sulphuric acid (in different ratios) for the RP columns and phosphate buffer (at different pH values) for the SAX column. The flow-rate was 1 ml/min for the RP columns and 0.8 ml/min for the SAX column; the detector was always operated at 214 nm.

Chemicals and materials

Acetonitrile was of HPLC grade (Carlo Erba, Milan, Italy) and potassium dihydrogen phosphate, phosphoric acid, sodium hydroxide and sulphuric acid were of analytical-reagent grade (Carlo Erba). Water was distilled twice and filtered through a Milli-Q apparatus (Millipore, Molsheim, France) before use. The pH of the buffer solution, (10^{-2} M KH_2PO_4) was adjusted to the required value with H_3PO_4 or NaOH. The analytical standard of cyromazine (99.3%) was obtained from Ciba Geigy (Milan, Italy); melamine (99.5%) was purchased from Carlo Erba.

RESULTS AND DISCUSSION

In the FDA method[10], the separation of cyromazine from melamine was achieved with a normal-phase (amino-bonded) column and acetonitrile–water (95:5, v/v) as the mobile phase; on the reversed-phase columns this mobile phase did not allow, in any ratio, the separation of the two compounds. By replacing the water in the mobile phase with a $0.5 \cdot 10^{-3}$ M sulphuric acid, the separation of cyromazine from melamine was achieved (Table I). On reducing the percentage of sulphuric acid in the mobile phase, the retention times of I and II increased (more on the RP-8 than on the RP-18 column). Analogous results were achieved with methanol–sulphuric acid as eluent, but the peak sharpness was poorer than with acetonitrile. The best resolution was achieved with the RP-8 column by using acetonitrile–sulphuric acid (50:50, v/v) as the mobile phase (Fig. 2). Under these conditions, the detection limits for cyromazine and melamine were 0.02 and 0.01 ppm, respectively; the calibration graphs were constructed by plotting peak height *vs.* concentration; good linearity was achieved in the range 0–2 ppm with correlation coefficients of 0.9997 and 0.9998 for I and II, respectively.

With the SAX column, at a mobile phase pH of 3, cyromazine and melamine were hardly retained and their separation was impossible. On increasing the pH, the retention times of I and II also increased (Table I); at pH 4.5 a good separation was achieved (Fig. 2). A further increase in pH did not result in a better separation, and the peak sharpness, especially with regard to cyromazine, became poorer. The detection

TABLE I

RETENTION TIMES OF CYROMAZINE AND ITS METABOLITE MELAMINE WITH DIFFERENT COLUMNS AND ELUENTS

Column	*Mobile phase*	*Flow-rate (ml/min)*	*Retention time (min)*	
			Melamine (II)	*Cyromazine (I)*
	Acetonitrile–sulphuric acid:			
RP-8	40:60	1.0	4.34	5.63
	50:50	1.0	5.39	6.89
	60:40	1.0	6.31	8.00
RP-18	50:50	1.0	4.26	5.44
	60:40	1.0	6.33	8.03
	70:30	1.0	8.08	10.19
	Buffer:			
SAX	pH 3.0	0.8	3.30	3.67
	pH 4.5	0.8	4.64	6.64
	pH 5.5	0.8	7.26	10.02

limits at pH 4.5 were similar to those obtained with RP-8 and reported above.

The possibility of achieving the separation of cyromazine from melamine by means of columns with different mechanisms may be useful in residue determinations, either as a confirmatory assay or to overcome the problem of interfering compounds in different samples.

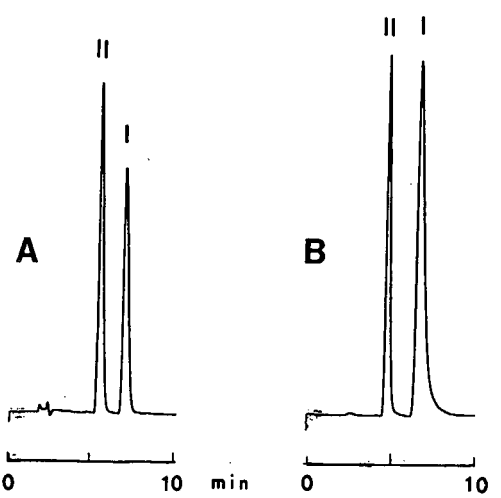

Fig. 2. Chromatography of cyromazine (I) and melamine (II). (A) RP-8 column; mobile phase, acetonitrile–0.5 · 10^{-3} M sulphuric acid (50:50, v/v); flow-rate, 1 ml/min; detection, UV at 214 nm. (B) SAX column; mobile phase, phosphate buffer (pH = 4.5); flow-rate, 0.8 ml/min; detection, UV at 214 nm.

ACKNOWLEDGEMENTS

This work was supported by grants from the Ministero dell'Agricoltura e Foreste, P.F. "Lotta Biologica ed Integrata par la Difesa delle Piante Agrarie e Forestali", Gruppo Residui.

REFERENCES

1 *The Agrochemicals Handbook*, Royal Society of Chemistry, Nottingham, 2nd ed., 1988.
2 R. L. Melnick, G. A. Boorman, J. K. Haseman, R. J. Montali and J. Huff, *Toxicol. Appl. Pharmacol.*, 72 (1984) 292.
3 P. G. Stocks and A. W. Schwartz, *J. Chromatogr.*, 168 (1979) 455.
4 H. Ishiwata, T. Inoue and A. Tanimura, *Food Addit. Contam.*, 3 1986) 63.
5 T. Inoue, H. Ishiwata, K. Yoshihira and A. Tanimura, *J. Chromatogr.*, 346 (1985) 450.
6 H. Ishiwata, T. Inoue, T. Yamazaki and K. Yoshihira, *J. Assoc. Off. Anal. Chem.*, 70 (1987) 457.
7 R. Bisaz and A. Kummer, *Mitt. Geb. Lebensmittelunters. Hyg.*, 74 (1983) 74.
8 P. C. Bardalaye, W. B. Wheeler and C. W. White, *J. Assoc. Off. Anal. Chem.*, 70 (1987) 455.
9 J. P. Toth and P. C. Bardalaye, *J. Chromatogr.*, 408 (1987) 335.
10 *Pesticide Analytical Manual*, Vol. II, Food and Drug Administration, Washington, DC, 1988, Sec. 180.414.

Journal of Chromatography, 505 (1990) 417–423
Elsevier Science Publishers B.V., Amsterdam — Printed in The Netherlands

CHROM. 22 281

Note

Dünnschichtchromatographie von Guajanoliden des Unterstammes Centaureinae

GERARD NOWAK

Chair and Department of Medicinal Plants, Academy of Medicine, Mazowiecka 33, 60-623 Poznań (Poland)

(Eingegangen am 24. August 1989; geänderte Fassung am 30. November 1989)

Guajanolide gehören zu den häufigsten Sesquiterpenlaktonen der Pflanzen des Unterstammes Centaureinae, Familiae Compositae. Diese Inhaltsstoffe haben wesentliche Bedeutung bei Bestimmung der richtigen Pflanzenverwandschaften und beweisen eine breite biologische Wirksamkeit.

Eine Vorbestimmung der Sesquiterpenlaktonen wird mittels Dünnschichtchromatographie am Kieselgel durchgeführt. Als Nachweisreagens wird am häufigsten Schwefelsäure verwendet. Es wurde beobachtet, dass verschiedene Farben der Guajanolide von manchen strukturellen Einzelheiten abhängig sind. Diese Beobachtung bezieht sich auf 20 verschiedene Verbindungen von diesem Typ, u.a. aus *Centaurea bella* Trautv.[1,2], *Psephellus leucophyllus* MB.[3], *Chartolepis pterocaula* (Trautv.) Czer.[4] und *Leuzea carthamoides* DC[5].

MATERIAL UND METHODEN

Das Untersuchungsmaterial bildeten Guajanolide, die vorher aus Pflanzen des Unterstammes Centaureinae isoliert wurden. Die Isolierungsmethoden sind in der Literatur zu finden[1–5]. 15-Desoxyrepin und Linichlorin B stammten aus *Psephellus leucophyllus*[3], Cynaropikrin aus *Leuzea carthamoides*[5], Grossheimin und Pterocaulin aus *Chartolepis pterocaula*[4], Centaurepensin, Repin, Chlorojanerin, Acroptilin, Janerin, Repdiolid, Cebellinen A, B, D[a], E, F, G, H, I, J aus *Centaurea bella*[1,2]. Die genannten Sesquiterpenlaktone (Tabelle I) wurden mit chromatographischen, physikalischen (Schmelztemperatur) und spektralen (IR, MS, ^{1}H NMR) Methoden identifiziert[1–5].

Die chromatographischen Analysen wurden bei der Zimmertemperatur ($\approx$20°C) an 20 × 20 cm DC-Plastikfolien Kieselgel 60/Merck, Darmstadt, B.R.D.) geführt.

Die Guajanolide wurden in der Menge von 10–15 μg auf Folien aufgetragen. Bei geringerer Menge (6–8 μg) wurden die Fleckenfarben unbestimmbar.

[a] Guajanolid früher als 8-Desacetylcentaurepensin-8-O(4-hydroxy)tiglinat beschrieben[6].

0021-9673/90/$03.50

Die Folien wurden in ungesättigen Kamern entwickelt. Folgende Fliessmittel wurden verwendet:

(A) Chloroform–Hexan–Ethylacetat (1:1:1, v/v/v) für die Trennung von Sesquiterpenlaktonen aus *Psephellus leucophyllus* und *Leuzea carthamoides*;

(B) Hexan–Ethylacetat (1:3, v/v) für die Trennung von Guajanoliden aus *Chartolepsis pterocaula*;

(C) Hexan–Chloroform–Benzen–Ethylacetat (2:2:1:7, v/v) für die Trennung von Verbindungen aus *Centaurea bella.*

Die entwickelten und getrockneten Chromatogramme wurden mit konzentrierter H_2SO_4 besprüht und bei einer Temperatur von 100°C binnen 1–2 min erhitzt. Die Fleckenfarben wurden in 15 min nach Besprühen des Chromatogramms bestimmt.

Die Ergebnisse der chromatographischen Kontrolle wurden in Tabelle I dargestellt.

ERGEBNISSE UND DISKUSSION

Die Flecken der analysierten Guajanolide (Tabelle II) wurden vorwiegend grün (Centaurepensin, Chlorojanerin, Cebellin D, E, I, J und Pterocaulin), dunkelblau (15-Desoxyrepin, Linichlorin B, Cynaropikrin und Cebellin F), braun (Repin, Acroptilin und Janerin) und schwarz (Cebellin A, B und Repdiolid) gefärbt.

TABELLE I

AUFGABEN ÜBER AUFTRETEN UND CHROMATOGRAPHIE DER ANALYSIERTEN GUAJANOLIDE

Guajanolid	*Gewonnen aus*	*Fliessmittel*	R_F	*Farbe in konzentrierter* H_2SO_4
15-Desoxyrepin	*Psephellus leucophyllus*	A	0.71	Dunkelblau
Linichlorin B			0.60	Dunkelblau
Cynaropikrin	*Leuzea carthamoides*	A	0.43	Dunkelblau
Grossheimin	*Chartolepis pterocaula*	B	0.68	Orange
Pterocaulin			0.33	Grün
Centaurepensin	*Centaurea bella*		0.74	Grün
Cebellin A			0.67	Schwarz
Repin			0.63	Braun
Cebellin B			0.61	Schwarz
Chlorojanerin			0.57	Grün
Acroptilin			0.54	Braun
Cebellin D		C	0.51	Grün
Cebellin E			0.44	Grün
Janerin			0.41	Braun
Cebellin F			0.38	Dunkelblau
Cebellin G			0.28	Grau
Repdiolid			0.26	Schwarz
Cebellin H			0.24	Grau
Cebellin I			0.17	Grün
Cebellin J			0.08	Grün

TABELLE II

AUFTEILUNG VON MANCHEN GUAJANOLIDEN AUS DEM UNTERSTAMM CENTAUREINAE NACH IHRER FLEBKENFARBE IN H_2SO_4

Guajanolid	*Strukturformel*[a]	*Farbenbestimmende Substituente*
	Braun	
Repin	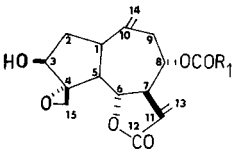	
Acroptilin	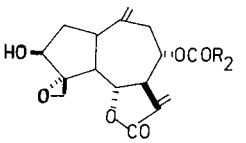	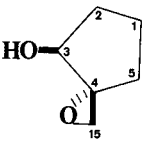
Janerin	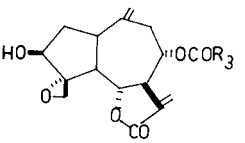	
	Dunkelblau	
15-Desoxyrepin	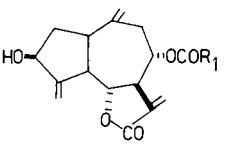	
Linichlorin B	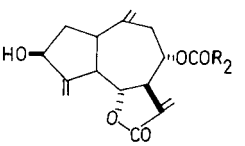	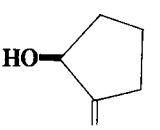
Cynaropikrin	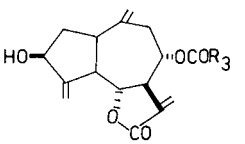	
Cebellin F	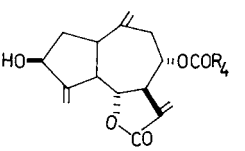	

(*Fortsetzung S. 420*)

TABELLE II (*Fortsetzung*)

Guajanolid	*Strukturformel*[a]	*Farbenbestimmende Substituente*
	Schwarz	
Cebellin A	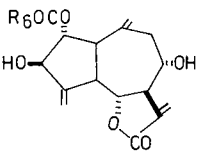	
Cebellin B	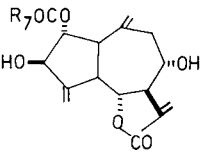	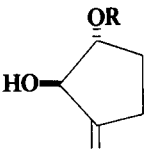
Repdiolid	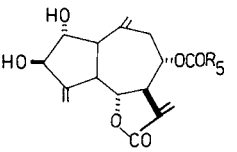	
	Grün	
Centaurepensin	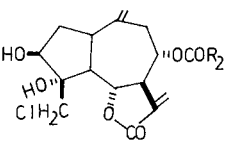	
Chlorojanerin	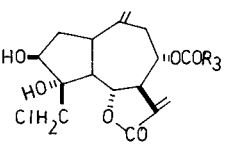	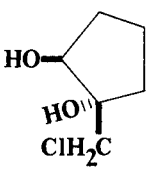
Cebellin D	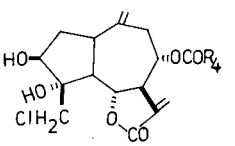	
Cebellin E	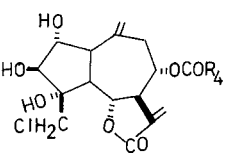	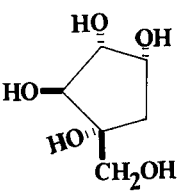
Cebellin I	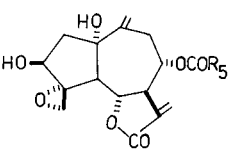	

TABELLE II (*Fortsetzung*)

Guajanolid	*Strukturformel*[a]	*Farbenbestimmende Substituente*
Pterocaulin	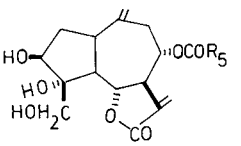	
Cebellin J	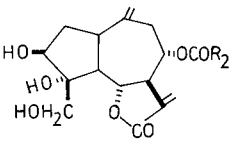	
	Grau	
Cebellin G	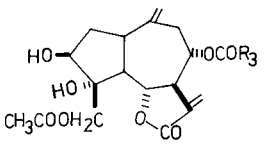	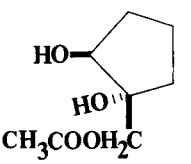
Cebellin H	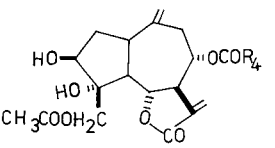	
	Orange	
Grossheimin	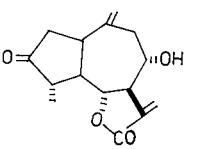	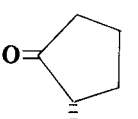

[a] R_1  ; R_2  ; R_3 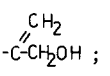 ;

R_4 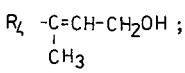 ; R_5 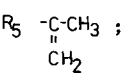 ;

R_6 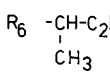 ; R_7 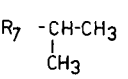

Für die Farbveränderungen sind Substituente am fünfgliedrigen Guajanolidring verantwortlich. Das erweist sich aus dem Strukturvergleich z.B. von Linichlorin B, Acroptilin und Centaurepensin, die sich in der Farbe und nur mit Substituenten an C-4 voneinander unterscheiden (Tabelle II).

Es scheint, dass die braune Farbe des Guajanolidfleckens vom Epoxid an C-4 und von der OH-Gruppe an C-3 bedingt ist. An C-15 fehlt hingegen der Sauerstoff —beim Übergang des Epoxids in Exomethylen werden also die Flecken dunkelblau gefärbt. Demnach ergibt Repin auf Chromatogrammen braune und 15-Desoxyrepin dunkelblau Farbe. Analog wird Acroptilin braun und Linichlorin B (15-Desoxy-acroptilin) dunkelblau. Derselbe Zusammenhang tritt bei Janerin und Cynaropikrin (15-Desoxyjanerin) auf.

Zusätzlichen Sauerstoffgruppen an C-2, im Bereich des kleinen Guajanringes 15-Desoxyrepins und ähnlichen Verbindungen, verursachen schwarze Fleckenfarbe, wie es bei Cebellin A, B und Repdiolid der Fall ist.

Bei Strukturanalyse der grüngefärbten Guajanolide ist die Anwesenheit von mehreren Sauerstoffverbindungen und Chlor bemerkenswert. Bei jeder dieser Verbindungen erscheinen an C-15 Sauerstoff (Cebellin I), Hydroxyl (Pterocaulin, Cebellin J) oder Chlor (Centaurepensin, Chlorojanerin, Cebellin D, Cebellin E). Die meisten haben auch eine Hydroxylgruppe an C-4, Cebellin E und I enthalten das zusätzliche Hydroxyl an C-2 und C-1, was den beiden Verbindungen eine grössere Polarität verleiht, ähnlich wie die Hydroxylgruppe an C-15 anstelle von Chlors.

Die Blockierung der Hydroxylgruppe an C-15 verursacht, dass Flecken des Cebellins G und H (bei Erhaltung derselben chromatographischen Konzentration) auf dem mit H_2SO_4 entwickelten Chromatogramm wenig sichtbar sind und graue Farben detegierten.

Alle bisher analysierten Verbindungen enthalten eine Hydroxylgruppe an C-3, in dieser Hinsicht ist Grossheimin abweichend und ergibt eine orange Farbe.

TABELLE III

SUBSTITUENTE DER GUAJANOLIDE DES UNTERSTAMMS CENTAUREINAE NACH DER STEIGERNDEN POLARITÄT

C-4	*C-8*
	
	
	
	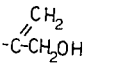
	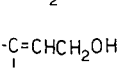

Wie bereits erwähnt, haben die Substituente an C-8, die bei den meisten Guajanoliden des Unterstammes Centaureinae auftreten, keinen Einfluss auf ihre Farbe mit H_2SO_4. Manche Schlussfolgerungen betreffend Esterbindungen an C-8 sind jedoch aus ihrer Polarität zu ziehen, was in Tabelle III illustriert wird.

Angaben aus den Tabellen II und III können zur Voridentifizierung der isolierten Sesquiterpenlaktone dienen.

Die Untersuchungen der Beziehungen zwischen Guajanolidstrukturen und -farben auf Chromatogrammen mit H_2SO_4 werden fortgesetzt, weil sie auch für andere Sorten Sesquiterpenlaktone interessant sind.

DANKSAGUNG

Die Arbeit wurde aus dem Zwischeressort-Problem CPBP 01.13 20 finanziert.

LITERATUR

1 G. Nowak, B. Drożdż, M. Holub, M. Buděšínský und D. Šaman, *Acta Soc. Bot. Pol.*, 55 (1986) 227.
2 G. Nowak, M. Holub und M. Buděšínský, *Acta Soc. Bot. Pol.*, 58 (1989) 97.
3 G. Nowak, B. Drożdż, M. Holub und A. Łagodzińska, *Acta Soc. Bot. Pol.*, 55 (1986) 629.
4 G. Nowak, B. Drożdż und M. Holub, *Acta Soc. Bot. Pol.*, 55 (1986) 233.
5 G. Nowak, M. Holub und M. Buděšínský, *Acta Soc. Bot. Pol.*, 57 (1988) 156.
6 A. Rustaiyan, Z. Sharif, A. Tajarodi, J. Ziesche und F. Bohlmann, *Planta Med.*, 2 (1984) 193.

Journal of Chromatography, 505 (1990) 424–428
Elsevier Science Publishers B.V., Amsterdam — Printed in The Netherlands

CHROM. 22 285

Note

Determination of vasicine and related alkaloids by gas chromatography–mass spectrometry

INTO LAAKSO*
Pharmacognosy Division, Department of Pharmacy, University of Helsinki, Fabianinkatu 35, SF-00170 Helsinki (Finland)
and
PERTTU VIRKAJÄRVI, HELENA AIRAKSINEN and EERO VARIS
Department of Crop Husbandry, University of Helsinki, SF-00710 Helsinki (Finland)
(Received October 31st, 1989)

Goat's rue, *Galega orientalis* Lam., is a promising perennial forage legume for Finnish climatic conditions[1]. However, its fodder value is thought to be impaired by the bitter-tasting quinazoline alkaloid vasicine[2]. Plants containing vasicine have long been used in folk medicine, and a number of pharmacological activities have been described[3]. In addition to effects on the respiratory system, vasicine has ben reported to have oxytocic, abortifacient and even insecticidal properties[4,5]. Its acute toxicity is 290 mg/kg (LD_{50}, oral, mouse)[6].

Thin-layer chromatography has traditionally been used for the determination of alkaloids in *Galega* species[2,7]. Recently, a high-performance liquid chromatographic method was developed to determine vasicine and vasicinone levels in *Adhatoda vasica* leaves[8].

As only traces of vasicine could be found in our preliminary tests on goat's rue samples, the need arose for a sensitive and rapid technique. This paper reports a gas chromatographic–mass spectrometric (GC–MS) method for the determination of vasicine in *Galega* species.

EXPERIMENTAL

Most of the *G. orientalis* used for experiments in Finland originates from goat's rue populations cultivated in the Estonian SSR[1,9]. The following amounts of material were used for the preparation of a single sample: 4 g of seeds of *G. orientalis* and dried herbs at different stages of development grown both in the field and in greenhouses; 1 g of seeds of wild *Galega officinalis* L. plants collected from Manawatu River Valley, New Zealand (by Dr. K. Lindström), and dried herbs at different stages of development grown in greenhouses; 1 g of dried herbs of *Peganum harmala* L. from the Botanical Garden of Turku University; and 1 g of dried herbs of *Linaria vulgaris* L. collected from Southern Finland.

Alkaloid samples were prepared by modifying the method described earlier[8]. Alkaloids were extracted with 20 ml of 40% ethanol and 1 ml of scopolamine

0021-9673/90/$03.50

hydrobromide solution (1 mg/ml, scopolamine · HBr · $2.5H_2O$; Sigma, St. Louis, MO, U.S.A.) was added as an internal standard. Of this extract, 2.5 ml was made alkaline with 10% ammonia solution and extracted with 1 ml of chloroform (E. Merck, Darmstadt, F.R.G.). The chloroform extract was dried with anhydrous sodium sulphate and evaporated to 100 μl.

Mass spectrometric identification was performed on a Hewlett-Packard (HP) 5890 gas chromatograph coupled to an HP 5970 quadrupole mass-selective detector. The latter was operated at 70 eV with a scan rate of 1100 a.m.u./s, an electron multiplier voltage of 1800 V and an ion source temperature of 250°C. The mass spectrometer was controlled by an HP 9825B desktop computer with an HP 9134 disc memory for data storage. The samples were analysed on a fused-silica capillary column coated with NB-54 (15 m × 0.20 mm I.D.; Nordion, Finland). The oven temperature was 240°C and helium was used as the carrier gas at a flow-rate of 0.5 ml/min.

GC–MS identification was based on computer matching against library spectra built up from samples of pure vasicine, and on published MS data for vasicine, vasicinone, desoxyvasicine and desoxyvasicinone[8,10–12]. In quantitative analyses by selected ion monitoring (SIM), the fragment ions were of *m/z* 187 (vasicine), 146 (vasicinone), 171 (desoxyvasicine), 185 (desoxyvasicinone) and 94 (scopolamine). When analysing vasicine levels in *G. orientalis*, the fragment ion of *m/z* 188 was also used (Fig. 2).

RESULTS AND DISCUSSION

The ten most abundant fragments of the four quinazoline alkaloids are presented in Table I. The concentrations of vasicine found in *P. harmala*, *G. officinalis* and *L. vulgaris* were high enough to obtain a reliable spectral comparison with an

TABLE I

FRAGMENTATION AND NORMALIZED ABUNDANCES OF VASICINE AND ITS DERIVATIVES

Desoxyvasicine (1)[a]		*Vasicine (2)*[a]		*Desoxyvasicinone (3)*[a]		*Vasicinone (4)*[a]	
m/z	*Abundance (%)*	*m/z*	*Abundance (%)*	*m/z*	*Abundance (%)*	*m/z*	*Abundance (%)*
171	100	187	100	185	100	146	100
172[b]	42	188[b]	50	186[b]	79	202[b]	79
116	8	131	26	130	12	119	58
68	8	159	23	76	10	145	24
129	6	77	12	102	10	118	24
77	6	104	8	187	9	130	17
51	6	89	8	129	9	147	16
41	6	169	7	50	9	129	15
143	5	189	6	103	8	187	11
85	5	171	5	77	7	203	11

[a] Elution order on NB-54 column: *cf.*, Fig. 2.
[b] $[M]^+$, electron impact mode.

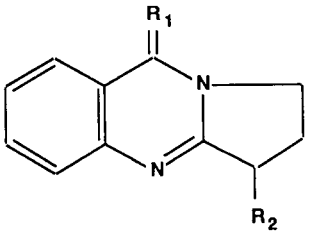

Vasicine	$R_1 = H_2$, $R_2 = OH$
Vasicinone	$R_1 = O$, $R_2 = OH$
Desoxyvasicine	$R_1 = H_2$, $R_2 = H$
Desoxyvasicinone	$R_1 = O$, $R_2 = H$

Fig. 1. Structures of vasicine and related alkaloids.

authentic sample. The spectra of desoxyvasicine, vasicinone and desoxyvasicinone, corresponding to the data presented in the literature[8,10,11], were obtained from analyses of *P. harmala* and were used as the basis for comparison in the remaining experiments.

Vasicine is the major alkaloid in *G. officinalis*[7,13] accompanied by its oxidation product vasicinone (Fig. 1). In order to avoid further oxidation of vasicine during extraction, ethanol (40%) was used as the solvent according to an earlier report[8]. Galegine, a guanidine alkaloid which is another poisonous compound in this plant[13,14], could not be confirmed by means of the present analyses, probably because of thermal decomposition in the GC–MS system. No significant amounts of galegine have been found in *G. orientalis*[15].

The reproducibility of the GC–MS–SIM method is shown in Table II. The mean relative standard deviations (R.S.D.) for vasicine and vasicinone contents were 3.5% and 3.4%, respectively, in the analyses of *G. officinalis* samples. With *G. orientalis*, the SIM analyses were unreliable when the fragment ion of *m/z* 187 was used for vasicine (R.S.D. = 13.1%). However, the reproducibility was considerably improved by selecting the ion of *m/z* 188 (R.S.D. = 6.9%) (Table II).

TABLE II

REPRODUCIBILITY OF QUANTITATIVE ANALYSES OF VASICINE AND VASICINONE BY GC–MS–SIM TECHNIQUE (n = 6)

Compound	*G. officinalis*		*G. orientalis*			
	Mean (μg/g)	*R.S.D. (%)*	*Mean (μg/g)*	*R.S.D. (%)*	*Mean (μg/g)*	*R.S.D. (%)*
Vasicine	3470[a]	3.5	1.4[a]	13.1	1.6[c]	6.9
Vasicinone	258[b]	3.4	–	–	–	–

[a] Fragment of *m/z* 187.
[b] Fragment of *m/z* 146.
[c] Fragment of *m/z* 188.

TABLE III

CONTENT OF QUINAZOLINE ALKALOIDS IN DRIED PLANT MATERIALS

Plant material	*Vasicine (%)*	*Vasicine (literature)*		*Vasicinone (%)*	*Desoxyvasicine (%)*	*Desoxyvasicinone (%)*
		%	*Ref.*			
G. orientalis herbs	$(1.4–1.6) \cdot 10^{-4}$	+	2			
G. officinalis herbs	0.1–0.35	0.0–0.3	13	0.03	$6.5 \cdot 10^{-4}$	$11.3 \cdot 10^{-4}$
G. officinalis seeds	0.03	+	2	$9.3 \cdot 10^{-4}$	$12.2 \cdot 10^{-4}$	$3.1 \cdot 10^{-4}$
P. harmala herbs	0.35	0.2–0.5	16	0.03	0.12	0.01
L. vulgaris herbs	0.03	0.5–0.8	17	$30.8 \cdot 10^{-4}$		

According to the GC–MS–SIM analyses, the content of vasicine varied between 0.1 and 0.35% in *G. officinalis* herbs of different development stages (Table III, Fig. 2). Recovery experiments, which were made by adding pure vasisine to a *G. officinalis* extract, gave a mean value of 96.7%. The quantitative results agree with the literature values[16] also in the case of *P. harmala*.

With respect of the presence of vasicine in *G orientalis*, no quantitative data have previously been presented. Its occurrence was verified by typical fragments (Table I, Fig. 2), the concentration remaining at ppm level in all the samples from this plant (Table III). It is obvious that such a low vasicine content cannot be responsible for lowering the fodder value of goat's rue. However, larger amounts of material need to be screened to evaluate the variations in alkaloid production and especially the proportion of the variations due to colder environmental conditions.

The results show that vasicine and its related alkaloids can be reliably determined using the GC–MS–SIM technique. The method is rapid and sensitive and therefore highly suitable for controlling the vasicine content in goat's rue.

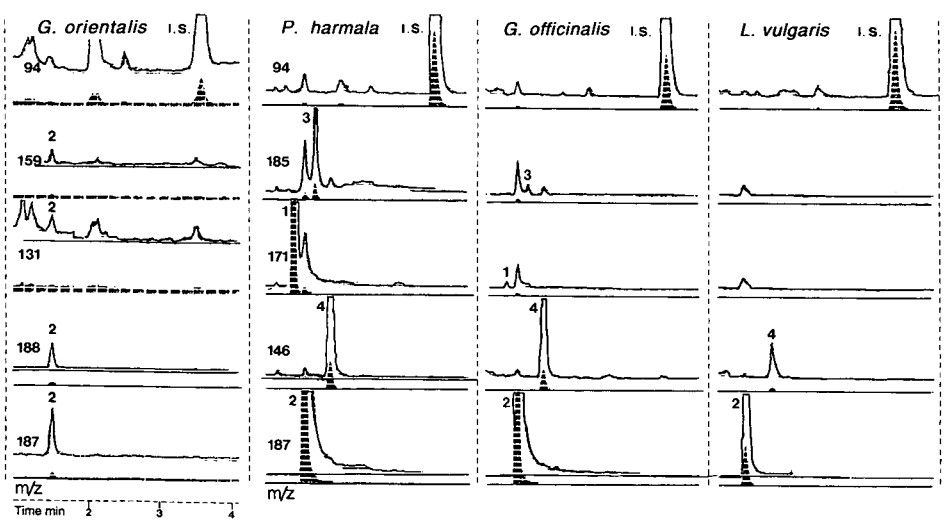

Fig. 2. GC–MS–SIM of quinazoline alkaloids. Peak numbers refer to constituents in Table I.

ACKNOWLEDGEMENTS

The authors are grateful to Dr. V. N. Gupta (Regional Research Laboratory, Jammu, India) for supplying a sample of pure vasicine, and to Dr. K. Lindström (Department of Microbiology, University of Helsinki, Finland) for supplying seed samples of *G. officinalis*.

REFERENCES

1 E. Varis, *J. Agric. Sci. Finl.*, 58 (1986) 83.
2 K. Schreiber, O. Aurich and K. Pufahl, *Arch. Pharm. (Weinheim, Ger.)*, 295 (1962) 271.
3 A. J. Duke, *CRC Handbook of Medicinal Herbs*, CRC Press, Boca Raton, 1987.
4 V. N. Gupta, M. P. Jain, C. K. Atal, V. B. Rao and B. G. Nagavi, *Indian Drugs*, 23 (1985) 32.
5 B. P. Saxena, K. Tikku, C. K. Atal and K. Opender, *Insect. Sci. Appl.*, 7 (1986) 489.
6 R. Engelhorn and S. Püschmann, *Arzneim.-Forsch.*, 13 (1963) 474.
7 K. Pufahl and K. Schreiber, *Züchter*, 33 (1963) 287.
8 K. R. Brain and B. B. Thapa, *J. Chromatogr.*, 258 (1983) 183.
9 H. Raig, *Söödagaleega Kasvatamise Kogemusi*, Kirjastus "Valgus", Tallinn, 1988.
10 K. Pandita, M. S. Bhat, R. K. Thappa, S. G. Agarwal, K. L. Dhar and C. K. Atal, *Planta Med.*, 48 (1983) 81.
11 A. Al-Shamma, S. Drake, D. L. Flynn, L. A. Mitscher, Y. H. Park, G. S. R. Rao, A. Simpson, J. K. Swayze, T. Veysoglu and S. S.-T. Wu, *J. Nat. Prod.*, 44 (1981) 745.
12 A. K. Bhatnagar and S. P. Popli, *Indian J. Chem.*, 4 (1966) 291.
13 J. Schäfer and M. Stein, *Biol. Zentralbl.*, 88 (1969) 755.
14 J. Petricic and Z. Kalodera, *Acta Pharm. Jugosl.*, 32 (1982) 119.
15 G. Reuter, *Flora*, 154 (1964) 136.
16 S. H. Hilal, M. Y. Haggag and S. A. El-Kashoyry, *Egypt. J. Pharm. Sci.*, 18 (1977) 9.
17 D. Gröger and S. Johne, *Planta Med.*, 13 (1965) 182.

Journal of Chromatography, 505 (1990) 429–434
Elsevier Science Publishers B.V., Amsterdam — Printed in The Netherlands

CHROM. 22 235

Note

Gas chromatographic–mass spectrometric analysis of major indole alkaloids of *Catharanthus roseus*

MARKKU YLINEN, PEKKA SUHONEN, TOIVO NAARANLAHTI, SEPPO P. LAPINJOKI* and AARRE HUHTIKANGAS

Department of Pharmaceutical Chemistry, University of Kuopio, P.O. Box 6, SF-70211 Kuopio (Finland)

(First received October 31st, 1989; revised manuscript received January 2nd, 1990)

During the 1980s, a considerable amount of research has been devoted to studies of the production of medicinally useful indolic alkaloids in cell and tissue cultures of *Catharanthus roseus*[1]. The principal targets of this research are vincristine and vinblastine, which are used in cancer chemotherapy and serve as precursors for some semisynthetic derivatives[2]. The above bisindole alkaloids are biosynthesized by combining catharanthine and vindoline (Fig. 1), which belong to the *Iboga* and *Aspidosperma* groups of monoterpene indole alkaloids, respectively. The third related alkaloid group abundant in *C. roseus* is the *Corynanthé* family, of which ajmalicine is the most abundant compound[3]. In the plant *Aspidosperma* alkaloids exist predominantly in the green parts, whereas the other types are also found in the roots[4], and it seems that only trace amounts of the end products of the *Aspidosperma* pathway are found in the cell and tissue cultures[5]. Consequently, screening of product yield from the different pathways is one of the basic routines included in these studies.

As the compounds are polar and not very volatile, high-performance liquid chromatographic (HPLC) methodology has predominated[6]. The regular target compounds catharanthine, vindoline and ajmalicine may be analysed simultaneously by using gradient elution and UV detection in HPLC[4]. However, this approach is not particularly sensitive and although electrochemical detection has improved sensitivity[7], it does not tolerate a true gradient elution and only a few alkaloids are properly

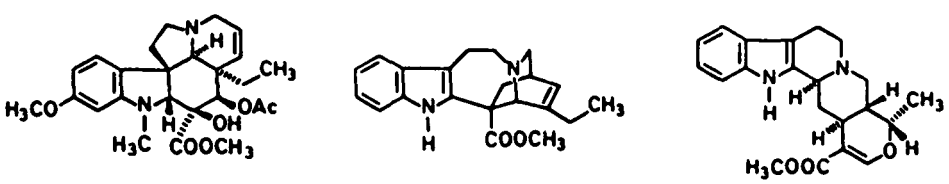

Fig. 1. Structures of the major indole alkaloids of *Catharanthus roseus*.

0021-9673/90/$03.50

quantified per isocratic run. A special problem is the separation of vindoline from ajmalicine and some other compounds that tend to co-migrate.

The commercial availability of an extensive choice of stationary phases in fused-silica capillary gas chromatographic (GC) columns has greatly enhanced the scope of the GC analysis of a variety of drugs and natural compounds, including amines and alkaloids[6,8,9]. This, and the observation that vindoline appeared to be analysable also by using packed-column GC[10], led us recently to try to detect it by capillary GC. We were able to identify it from a plant cell sample using GC–mass spectrometry (MS) after careful purification[5]. This prompted us to develop a GC–MS method for the simultaneous direct detection of vindoline and ajmalicine and for the detection of catharanthine as a pentafuoropropionate derivative from *C. roseus* cells after a simple purification procedure.

EXPERIMENTAL

Preliminary GC experiments with fused-silica capillary columns (OV-1, 15 and 25 m × 0.32 mm I.D., 0.1-μm coating; Nordion Instruments, Helsinki, Finland) were carried out with a Hewlett-Packard HP 5790A instrument with flame-ionization detection (FID). The final GC–MS was performed using the longer of the columns and an HP 5790A–Jeol JMS 300 integrated system. Splitless (60 s) injection was used, and the oven temperature was programmed from the initial 130°C (2 min) to 280°C at 10°C/min with injector and detector temperatures of 250 and 300°C, respectively. The MS results were processed with the JMA 2000 data analysis system included in the instrument.

Trials on the silylation and acylation of catharanthine were performed under a wide range of reaction conditions using the following reagents: N-methyl-N-(*tert.*-butyldimethylsilyl)trifluoroacetamide, N,O-bis(trimethylsilyl) trifluoroacetamide, N-methyl-N-trimethylsilyl trifluoroacetamide, N-trimethylsilylimidazole, pentafluoropropionic anhydride (PFPA), methyl chloroformate, heptafluorobutyric anhydride and trifluoroacetic anhydride. The final reproducible acylation used was achieved when a sample was dissolved in 500 μl of toluene and 50 μl of pyridine and 50 μl of PFPA were added. The reaction mixture was then maintained at 60°C for 30 min and washed with 1 ml of 5 M ammonia solution. A 2-μl volume of the organic solution was used directly for GC–MS, which was performed with a combination of HP 5890 and VG Trio-2 instruments, but the conditions for the analysis were as described above for the underivatized alkaloids.

The *C. roseus* cell material used and the procedures for alkaloid purification have been described previously[11]. Analytical-reagent grade chemicals were obtained from the usual commercial sources and the alkaloid standards were those described earlier[4].

RESULTS AND DISCUSSION

Preliminary GC experimentation with standard samples of ajmalicine, vindoline and catharanthine using FID indicated that the first two are volatile and detectable under the conditions specified above (data not shown), but catharanthine gave no analytically useful signal under any conditions. Subsequently, ajmalicine and vin-

doline standards were subjected to GC–MS to obtain the mass spectra (not shown) that were utilized in analysing the plant cell samples.

It was essential to use a thin (0.1-μm) stationary phase film in order to keep these relatively involatile analytes moving in the column at reasonable temperatures and to achieve comparatively good separations and peak shapes. The use of helium instead of nitrogen as the carrier gas was also beneficial, as the poorer diffusibility of the latter required strict control of the gas stream.

Fig. 2 shows a typical semipreparative HPLC trace when alkaloids are isolated from cultured *C. roseus* cells using the previously described method[11]. When a narrow middle fraction of eluate from the peak with a retention time of 17 min was analysed by GC–MS, in essence a single total ion current (TIC) peak was observed at 17 min 40 s (Fig. 3) and its mass spectrum (Fig. 4A) was almost identical with that obtained for a standard sample of ajmalicine. There was no distinct HPLC peak at 16 min, where vindoline should appear (Fig. 2), but when the eluate of the zone indicated in Fig. 2 was collected and the existence of the molecular ion for vindoline (*m/z* 456) was monitored, it could be seen in the gas chromatogram at 16 min 15 s (Fig. 3), and the mass spectrum (Fig. 4B) corresponded to that of standard material[5]. As would be expected from the wide sampling range used for vindoline and from the high baseline of the HPLC trace (Fig. 2), the sample contained various other compounds, including ajmalicine, as indicated by the TIC graph (Fig. 3).

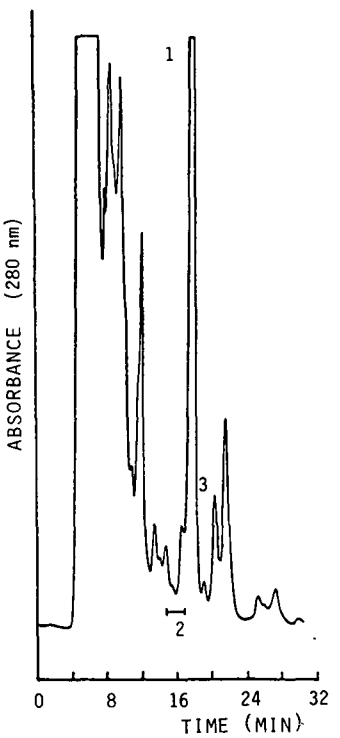

Fig. 2. Semi-preparative HPLC of *C. roseus* cell culture extract. The eluate constituents used for GC–MS analysis of ajmalicine (1), vindoline (2) and catharanthine (3) are indicated.

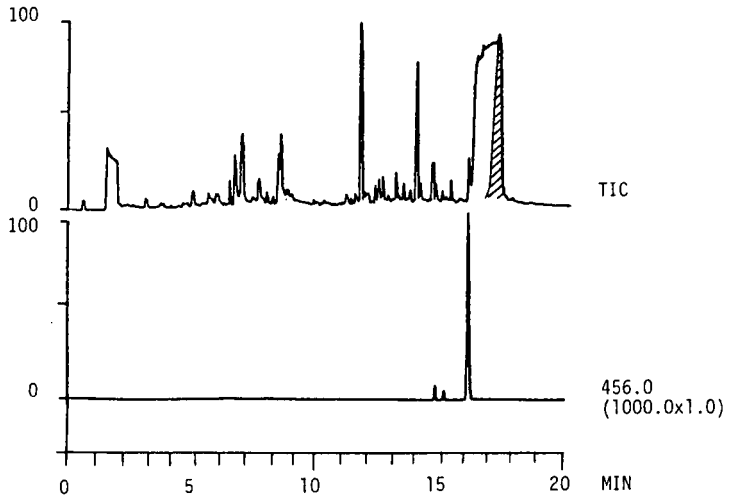

Fig. 3. Top: superimposed TIC GC–MS traces from ajmalicine (shaded area) and vindoline zones of the HPLC trace in Fig. 2. Bottom: ion monitoring trace indicating the existence of vindoline molecular ions (*m/z* 456) in the vindoline zone of Fig. 2.

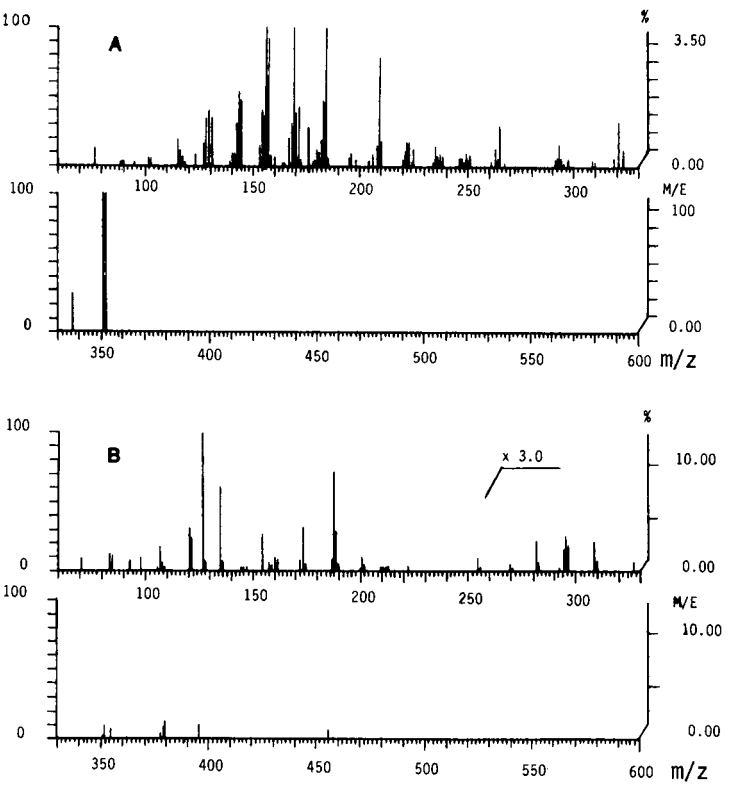

Fig. 4. Mass spectra of (A) the ajmalicine and (B) the vindoline peaks indicated in Fig. 3.

As the direct GC analysis of catharanthine was unsuccessful, a method for preparing a volatile derivative was developed as described under Experimental. When an aliquot of sample eluate from the HPLC (peak at 21 min (Fig. 2) was processed accordingly, all the TIC peaks present in previous standard runs were present (Fig. 5A). Peak 1 at 12 min 40 s represents the main PFP derivative, for which the mass spectrum is given in Fig. 5B. The smaller peak 2 preceding the main one at 12 min 10 s in Fig. 5A is obviously due to a stereoisomeric PFP derivative, as it gives a mass spectrum identical with that in Fig. 5B. The other TIC peaks in Fig. 5A were also seen in standard graphs, and their mass spectra suggest that they are related to the derivatization reagents.

As indicated by the complexity of the TIC graph in Fig. 3, a vast number of compounds could be resolved by GC from a relatively narrow zone of the HPLC eluate. Comparable complexity was also observed for other eluate portions when they were screened by GC. The mass spectra of many of the TIC peaks in Fig. 3 and in the

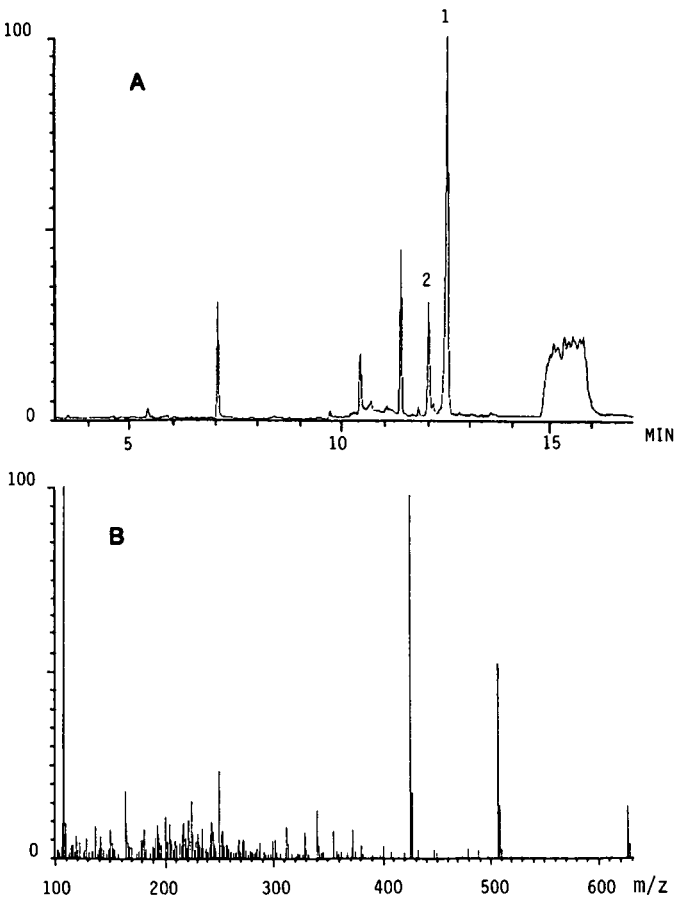

Fig. 5. (A) TIC GC–MS trace after PFP derivatization of the catharanthine zone in Fig. 2 and (B) the common mass spectrum obtained for peaks 1 and 2.

graphs from other eluate portions suggested them to be related to the target alkaloids, but the lack of reference compounds prevented their further identification.

Although the example of catharanthine revealed that direct GC–MS may not be considered a universal method for analysing indole alkaloids, we conclude that according to the present results many such alkaloids may be added to the list of amines and alkaloids[6,8,9] that can be analysed by modern capillary GC techniques.

ACKNOWLEDGEMENTS

The work was financially supported by the Technology Development Centre (Helsinki, Finland), the Research Foundation of Kemira Oy (Helsinki, Finland) and the Savo Foundation for Advanced Technology (Kuopio, Finland).

REFERENCES

1 P. Morris, *Planta Med.*, 52 (1986) 121.
2 R. A. Bender, in B. A. Chabner and H. M. Pinedo (Editors), *The Cancer Pharmacology Annual*, Vol. 4, Elsevier, Amsterdam, 1986, p. 91.
3 W. I. Taylor and N. R. Farnsworth, *The Catharanthus Alkaloids: Botany, Chemistry, Pharmacology and Clinical Use*, Marcel Dekker, New York, 1975.
4 T. Naaranlahti, M. Nordström, M. Lounasmaa and A. Huhtikangas, *J. Chromatogr.*, 410 (1987) 488.
5 T. Naaranlahti, S. P. Lapinjoki, A. Huhtikangas, L. Toivonen, U. Kurtén, V. Kauppinen and M. Lounasmaa, *Planta Med.*, 55 (1989) 155.
6 R. Verpoorte and A. Baerheim Svendsen, *Chromatography of Alkaloids, Part. B: Gas–Liquid Chromatography and High-Performance Liquid Chromatography*, Elsevier, Amsterdam, 1984.
7 T. Naaranlahti, V.-P. Ranta, P. Jarho, M. Nordström and S. P. Lapinjoki, *Analyst (London)*, 114 (1989) 1229.
8 H.-O. Hoppen, R. Heuer and G. Seidel, *Biomed. Mass Spectrom.*, 5 (1978) 133.
9 M. Polgár and L. Vereczkey, *J. Chromatogr.*, 241 (1982) 29.
10 H. Lastra, R. Perez, A. Pena and M.G. del Risco, *Rev. Cubana Farm.*, 18 (1984) 289.
11 T. Naaranlahti, M. Nordström, S. Lapinjoki, A. Huhtikangas and M. Lounasmaa, *J. Chromatogr. Sci.*, (1990) in press.

Journal of Chromatography, 505 (1990) 435–437
Elsevier Science Publishers B.V., Amsterdam — Printed in The Netherlands

CHROM. 22 266

Note

Rapid determination of caffeine in green tea by gas–liquid chromatography with nitrogen–phosphorus-selective detection

BINGYING GUO and HAIBIN WAN
Tea Research Institute, Chinese Academy of Agricultural Science, Hangzhou (China)
(Received November 15th, 1989)

Caffeine is an important component of tea, comprising 3–5% of the total weight. Many methods for determining caffeine in tea have been reported, including high-performance liquid chromatography[1–4], spectrophotometry[5,6] and gas–liquid chromatography (GLC)[7,8]. In these methods, a tea sample is extracted with boiling water and the extract is cleaned up prior to the determination. The clean-up procedure usually involves such operations as partitioning (several times), concentration, acid–base treatment and precipitation. This paper describes a simpler and quicker method, based on the sensitive response of a nitrogen–phosphorus detector to caffeine and the difference in solubility between caffeine and other polar compounds in green tea.

EXPERIMENTAL

Materials and apparatus

Analytical-reagent grade toluene, anhydrous sodium sulphate, 4.5 *M* sulphuric acid, 0.01 *M* hydrochloric acid and saturated basic lead acetate solution were used.

A Hewlett-Packard HP-5790A gas–liquid chromatograph equipped with a nitrogen–phosphorus-selective detector and a glass column (1.2 m × 2 mm I.D.) packed with 6% OV-101 on Chromosorb W (80–100 mesh) was used, and also a Shimadzu UV-265 FW spectrophotometer.

Proposed GLC method

Ground tea (1.000 g) was extracted with boiling water (200 ml) for 20 min in a 250-ml erlenmeyer flask. The extract was filtered and an aliquot (0.1 ml) of the filtrate was transferred to a 10-ml volumetric flask. Toluene (9.9 ml) and anhydrous sodium sulphate (*ca.* 1 g) were added. The flask was shaken vigorously for 0.5 min prior to GLC determination.

The operating conditions of the instrument were as follows: oven temperature, 205°C; injector temperature, 230°C; detector temperature, 240°C; carrier gas (nitrogen) flow-rate, 50 ml/min; hydrogen flow-rate, 1.5 ml/min; air flow-rate, 80 ml/min; injection volume, 5 μl.

Under the above conditions, the retention time of caffeine was 1.9 min and the

0021-9673/90/$03.50

detection limit was 0.04%. Quantification was carried out by comparing the peak heights of a standard and the samples.

National standard method

To assess the GLC method, the national standard method was used as a reference. This method was developed by the Tea Research Institute, Chinese Academy of Agricultural Sciences, and was recently approved as a national standard method by the National Standard Bureau (China).

Ground tea (3.000 g) was extracted with boiling water (450 ml) for 45 min and the extract was filtered. An aliquot of the filtrate (20 ml) was mixed with 0.01 *M* hydrochloric acid (10 ml) and saturated basic lead acetate solution (2 ml); the mixture was then diluted to 250 ml with water. The flask was shaken vigorously for 1 min and was allowed to stand for 10 min, after which the solution was filtered. An aliquot of the filtrate (50 ml) was mixed with 4.5 *M* sulphuric acid solution (0.2 ml) in a 100-ml volumetric flask and diluted to 100 ml with water. The flask was shaken vigorously for 1 min, then the solution was filtered. The filtrate was analysed using a UV spectrophotometer at 274 nm.

RESULTS AND DISCUSSION

Selection of extraction time

Tea samples were extracted with boiling water for 10, 20, 30 and 45 min and the caffeine content was determined by the GLC method and by the standard method. The results are given in Table I.

The results suggest that the efficiency of the 10-min extraction is as good as that of a 45-min extraction. Therefore, 20-min extraction was adopted.

Application of the method

Five tea samples were analysed by the GLC method with four replicates for each sample. The coefficients of variation were 1.20, 0.95, 1.42, 0.90 and 3.18%. Three tea samples were analysed by the standard method, with four replicates for each

TABLE I

INFLUENCE OF EXTRACTION TIME ON THE EXTRACTION EFFICIENCY

Sample	*Method*	*Extraction time (min)*	*Caffeine content*[a] *(%)*
A	GLC	10	2.19 ± 0.026
	GLC	20	2.20 ± 0.021
	GLC	45	2.16 ± 0.031
	Standard	20	2.18 ± 0.061
	Standard	45	2.18 ± 0.099
B	GLC	30	3.23 ± 0.029
	GLC	45	3.37 ± 0.107
	Standard	30	3.32 ± 0.212
	Standard	45	3.36 ± 0.086

[a] Mean of four replicates ± standard deviation.

sample, and an average coefficient of variation of 3.67% was obtained. The data in Table I suggest that the results obtained by the GLC method are the same as those obtained by the standard method.

An advantage of the GLC method is its simplicity, which not only saves considerable amounts of reagents and time, but also reduces the possibility of errors.

Prior to GLC analysis, sample clean-up procedures are usually needed to remove impurities which may affect accurate quantification. This simplified GLC method is based on the selective response of the instrument to caffeine and the difference in solubility of caffeine and the coextractives. Tea contains about 30% of water-extractable components, mainly polyphenols (80%) and caffeine (10%). When caffeine is injected into a gas chromatograph in the nanogram range, the amount of impurities introduced into the instrument should be in the same range, even if no clean-up treatment is used. Polyphenols are very soluble in water and almost insoluble in toluene. Therefore, when toluene is used to extract caffeine from water, the percentage of polyphenols and other polar impurities entering the toluene phase should be much less than that of caffeine. During analysis with this GLC method, the baseline and the response remained steady after over 100 injections, and no other peaks were observed in the chromatogram, suggesting that the samples were sufficiently clean.

REFERENCES

1 S. J. Reid and T. J. Good, *J. Agric Food Chem.*, 30 (1982) 775.
2 J. L. Blunch and S. M. Tarka, Jr., *J. Food Sci.*, 48 (1983) 745.
3 S. H. Ashoor, G. J. Seperich, W. C. Monte and J. Welty, *J. Assoc. Off. Anal. Chem.*, 66 (1983) 606.
4 M. Dulitzky, E. de la Teja and H. F. Lewis, *J. Chromatogr.*, 317 (1984) 403.
5 M. S. Karawya, A. M. Diab and N. Z. Swelem, *Anal. Lett.*, 17 (1984) 77.
6 Y. Ruan and M. Li, *Experimental Handbook of Physiology and Biochemistry of Tea*, Agriculture Press, Beijing, 1983.
7 Weerasinghe, *Tea Q.*, 51 (1982) 175.
8 J. Chen, *Sepu*, 5 (1987) 367.

Author Index

Erratum

J. Chromatogr., 503 (1990) 237–243
Page 239, Fig. 1, *x*-axis, "mV" should read "V".
Page 240, 10th text line, "Fe^{III}" should read "Fe^{II}".
Page 241, Table I, 3rd line, "iron(II)" should read "iron(III)".
Page 242, 8th text line, "8-hydroxyquinoline" should read "8-quinolinol".

Request for manuscripts

R. Majors, F. Regnier and K. Unger will edit a special, thematic issue of the *Journal of Chromatography* entitled **"LC Column Packings"**. Both reviews and research articles will be included.

Topics such as the following will be covered:

- organic packings
- inorganic packings
- non-porous particles
- macroporous particles
- restricted access media
- functionalized membranes
- solid-phase extraction materials
- commercially available packings
- physical-chemical characterization
- relative performance of packings
- packing procedures and hardware
- column care.

Only minor coverage of topics such as affinity chromatography and chiral separations is planned since these will be the topics of other thematic issues.

Potential authors of reviews should contact Roger Giese, Editor, prior to any submission. Address: 110 Mugar Building, Northeastern University, Boston, MA 02115, U.S.A.; tel.: (617) 437-3227; fax: (617) 437-2855.

The deadline for receipt of submissions is **June 1, 1990**. Manuscripts submitted after this date can still be published in the Journal, but then there is no guarantee that an accepted article will appear in this special, thematic issue. **Five** copies of the manuscript should be submitted to R. Giese. All manuscripts will be reviewed and acceptance will be based on the usual criteria for publishing in the *Journal of Chromatography*.

PUBLICATION SCHEDULE FOR 1990

Journal of Chromatography and Journal of Chromatography, Biomedical Applications

MONTH	J	F	M	A	M	J	
Journal of Chromatography	498/1 498/2 499	500 502/1	502/2 503/1 503/2 504/1	504/2 505/1	505/2 506 507 508/1	508/2 509/1 509/2 510	The publication schedule for further issues will be published later
Cumulative Indexes, Vols. 451–500		501					
Bibliography Section		524/1		524/2		524/3	
Biomedical Applications	525/1	525/2	526/1	526/2 527/1	527/2	528/1 528/2	

INFORMATION FOR AUTHORS

(Detailed *Instructions to Authors* were published in Vol. 478, pp. 453–456. A free reprint can be obtained by application to the publisher, Elsevier Science Publishers B.V., P.O. Box 330, 1000 AH Amsterdam, The Netherlands.)

Types of Contributions. The following types of papers are published in the *Journal of Chromatography* and the section on *Biomedical Applications:* Regular research papers (Full-length papers), Notes, Review articles and Letters to the Editor. Notes are usually descriptions of short investigations and reflect the same quality of research as Full-length papers, but should preferably not exceed six printed pages. Letters to the Editor can comment on (parts of) previously published articles, or they can report minor technical improvements of previously published procedures; they should preferably not exceed two printed pages. For review articles, see inside front cover under Submission of Papers.

Submission. Every paper must be accompanied by a letter from the senior author, stating that he is submitting the paper for publication in the *Journal of Chromatography*. Please do not send a letter signed by the director of the institute or the professor unless he is one of the authors.

Manuscripts. Manuscripts should be typed in double spacing on consecutively numbered pages of uniform size. The manuscript should be preceded by a sheet of manuscript paper carrying the title of the paper and the name and full postal address of the person to whom the proofs are to be sent. Authors of papers in French or German are requested to supply an English translation of the title of the paper. As a rule, papers should be divided into sections, headed by a caption (*e.g.*, Summary, Introduction, Experimental, Results, Discussion, etc.). All illustrations, photographs, tables, etc., should be on separate sheets.

Introduction. Every paper must have a concise introduction mentioning what has been done before on the topic described, and stating clearly what is new in the paper now submitted.

Summary. Full-length papers and Review articles should have a summary of 50–100 words which clearly and briefly indicates what is new, different and significant. In the case of French or German articles an additional summary in English, headed by an English translation of the title, should also be provided. (Notes and Letters to the Editor are published without a summary.)

Illustrations. The figures should be submitted in a form suitable for reproduction, drawn in Indian ink on drawing or tracing paper. Each illustration should have a legend, all the *legends* being typed (with double spacing) together on a *separate sheet*. If structures are given in the text, the original drawings should be supplied. Coloured illustrations are reproduced at the author's expense, the cost being determined by the number of pages and by the number of colours needed. The written permission of the author and publisher must be obtained for the use of any figure already published. Its source must be indicated in the legend.

References. References should be numbered in the order in which they are cited in the text, and listed in numerical sequence on a separate sheet at the end of the article. Please check a recent issue for the layout of the reference list. Abbreviations for the titles of journals should follow the system used by *Chemical Abstracts*. Articles not yet published should be given as "in press" (journal should be specified), "submitted for publication" (journal should be specified), "in preparation" or "personal communication".

Dispatch. Before sending the manuscript to the Editor please check that the envelope contains three copies of the paper complete with references, legends and figures. One of the sets of figures must be the originals suitable for direct reproduction. Please also ensure that permission to publish has been obtained from your institute.

Proofs. One set of proofs will be sent to the author to be carefully checked for printer's errors. Corrections must be restricted to instances in which the proof is at variance with the manuscript. "Extra corrections" will be inserted at the author's expense.

Reprints. Fifty reprints of Full-length papers, Notes and Letters to the Editor will be supplied free of charge. Additional reprints can be ordered by the authors. An order form containing price quotations will be sent to the authors together with the proofs of their article.

Advertisements. Advertisement rates are available from the publisher on request. The Editors of the journal accept no responsibility for the contents of the advertisements.

ADVANCED SCIENTIFIC COMPUTING IN BASIC: with applications in chemistry, biology and pharmacology

P. VALKÓ, *Eötvös Loránd University, Budapest, Hungary, and*
S. VAJDA, *Mount Sinai School of Medicine, New York, NY, USA*

Data Handling in Science and Technology Volume 4

Advanced Scientific Computing in BASIC gives a practical introduction to numerical methods and presents BASIC subroutines for real-life computations in the areas of chemistry, biology, and pharmacology. The choice of BASIC as the programming language is motivated by its simplicity, its availability on all personal computers and by its power in data acquisition. While most of the scientific packages currently available in BASIC date back to the period of limited memory and speed, the subroutines presented here can handle a broad range of realistic problems with the power and sophistication needed by professionals and with simple, step-by-step instructions for students and beginners.

The book shows how to extract useful information from measurements via modelling, simulation, and statistical data evaluations. Efficient, robust numerical methods have been chosen to solve related problems in numerical algebra, nonlinear equations and optimization, parameter estimation, signal processing, and differential equations. For each class of routines an introduction to the relevant theory and techniques is given, so that the reader will recognise and use the appropriate method for solving his or her particular problem. Simple examples illustrate the use and applicability of each method.

1989 xvii + 322 pages; US$ 92.75 / Dfl. 190.00
ISBN 0-444-87270-1
5.25" Diskette: US$ 53.75 / Dfl. 110.00
ISBN 0-444-87271-X

ELSEVIER SCIENCE PUBLISHERS

P.O. Box 211, 1000 AE Amsterdam, The Netherlands
P.O. Box 882, Madison Square Station, New York, NY 10159, USA